Smart Hydrogel Engineering for Soft Robotics: Synthesis, Characterization, and Mechanical Properties of PNIPAM Hydrogel

Graduation thesis

Srinivas Ajit Sagaram Radhakrishna

Delft University of Technology

TU Delft

Smart Hydrogel Engineering for Soft Robotics: Synthesis, Characterization, and Mechanical Properties of PNIPAM Hydrogel

by

Srinivas Ajit Sagaram Radhakrishna

Student Name	Student Number
S. A. Sagaram Radhakrishna	5300622

Chair	Dr. J. Jovanova
Daily Supervisor:	Q. Chen (Aaron chen)
Faculty:	Faculty of Mechanical Engineering, Delft
Report number:	**2024.MME.8974**
Date:	30-08-2024.

TU Delft

Preface

Four years ago, I embarked on a journey that was as challenging as it was rewarding. This thesis is the final chapter of that journey, capturing the essence of my studies and the passion for engineering that has driven me. When I joined TU Delft in 2020, I stepped into the unknown, unaware of the challenges that awaited me both personally and professionally. The journey was not without its obstacles. I grappled with self-doubt and imposter syndrome in my academic pursuits, while also confronting a personal struggle with addiction. These challenges tested my resilience and determination in ways I never anticipated. Reaching this finishing line fills me with a profound sense of pride. Despite the difficulties, I persevered and have emerged stronger, having grown both as an engineer and as an individual.

I would like to express my deepest gratitude to those who supported and guided me on the academic front, helping me navigate through the challenges and self-doubt that arose during this journey. First and foremost, I am immensely grateful to my Chair, Dr. Jovana Jovanova, and my Supervisor, Ir.Q. (Aaron) Chen. Their unwavering support and encouragement kept me going, especially during moments of uncertainty. Their guidance was instrumental in shaping this thesis, and their belief in my abilities gave me the confidence to persevere. I would also like to extend my sincere thanks to Dr. Baris Kumru, whose expertise and assistance were invaluable in the chemical aspects of my research. His help in gaining access to the chemistry lab and getting started with the hydrogels was crucial to my work. Beyond the technical support, Mr. Kumru was a constant pillar of support, always available to discuss my findings and helping me reason through challenges with clarity.

A special mention goes to Dr. Georgy Filonenko, who was truly a godsend. Our paths crossed unexpectedly, but his impact on my research was profound. Dr. Filonenko's understanding of hydrogels provided me with the insights I needed to advance my work. Through him, I was also introduced to Ir. Anand Raja, whose expertise in the rheological studies of soft matter further enriched my research. Their combined support significantly contributed to the depth and quality of this thesis.

I would also like to extend my heartfelt appreciation to the technical support staff, whose daily assistance made this thesis possible. Their expertise and dedication helped me overcome numerous challenges along the way. A sincere thank you to Ms. Caitlin van den Hondel for her invaluable help with the chemistry aspects of my research. Her guidance was instrumental in navigating the complexities of this work. I am also deeply grateful to Mr. Raymond Dekker for his assistance with the indentation test setup, which was critical to the success of my experiments. I would like to express my gratitude to Mrs. Aleksandra Kondakova for her support with the rheological experiments, ensuring that I had the necessary tools and knowledge to conduct my research effectively. A special thank you to Mr. Vittorio Garofano and Mr. Bart Boogmans, who welcomed me into their lab with open arms. Their continuous support, friendliness, and the organization of a workspace for me have made a lasting impact, and I will dearly miss the environment they created.

On a personal front, I owe my deepest thanks to my parents, Mr. Radhakrishna Sagaram and Mrs. Padmaja Turup. Their unwavering support and belief in me made it possible for me to study at TU Delft, and without their continuous encouragement, I would not have made it this far. From the very beginning, they have been my pillars of strength, providing not just the means but also the motivation to pursue my dreams. They have worked tirelessly and have always been determined to provide me with opportunities and a life they themselves never had. Their love and guidance have been the foundation upon which I have built this entire journey, and for that, I am eternally grateful.

I am also sincerely grateful to my friends Pratyush, Akul, Kadi, Sampreeth, Revanth, Arun, Rathish, Trayana, Barshaleena, and Harsha. Your constant support, the safe space you provided, and your kind words have been invaluable to me throughout this journey. You have reflected both the best and worst in me, offering me the opportunity to recognize my strengths while also confronting my weaknesses. Your honesty and compassion have helped me to work on my flaws and grow not just as a student, but

as a person. Whether through late-night conversations, shared laughter, or simply being there when I needed someone to talk to, you all have played an integral role in my life during these years.

I am confident that each of you will go on to achieve great things in life, and I feel incredibly fortunate to have had you by my side. Your friendship has not only enriched my experience here at TU Delft but has also contributed to my personal development in profound ways. I am forever grateful for each of you, and I look forward to seeing the amazing paths you will all carve out for yourselves in the future.

Lastly, throughout my journey as a mechanical engineer, I explored a broad spectrum of engineering fields—ranging from wind energy to the manufacturing and production of automobiles, heavy-duty industrial magnets, and logistics, ultimately culminating in research that required significant chemical analysis. These diverse experiences have taught me that with dedication and a commitment to the process, success is achievable in any discipline. This exploration of multiple engineering avenues not only broadened my technical expertise but also reinforced the belief that perseverance and adaptability are key to overcoming challenges and achieving one's goals.

Srinivas Ajit Sagaram Radhakrishna
Delft, August 2024

Summary

In recent years, the development of smart materials has become a cornerstone for advancements in fields like soft robotics, where materials that can adapt to external stimuli are essential. Hydrogels, and specifically Poly(N-isopropylacrylamide) (PNIPAM) hydrogels, have garnered significant attention due to their unique ability to undergo reversible volume changes in response to temperature variations. This thermoresponsive behavior makes them particularly suitable for applications ranging from drug delivery systems to actuators in soft robotics, where material flexibility and adaptability are crucial.

This thesis focuses on the synthesis, characterization, and application potential of PNIPAM hydrogels, aiming to deepen the understanding of these materials to better facilitate their practical application across both small-scale experimental setups and large-scale industrial processes. The study is guided by the question of how varying synthesis parameters, particularly the concentrations of monomers and crosslinkers, influence the swelling ability and mechanical properties of these hydrogels. Understanding this relationship is critical for tailoring the hydrogels' properties to meet the specific demands of applications in soft robotics, where both responsiveness to environmental changes and mechanical robustness are required.

The research begins by detailing the synthesis process of PNIPAM hydrogels using free radical polymerization, a method that allows for precise control over the composition of the hydrogels. The study explores how different ratios of monomers to crosslinkers can be used to manipulate the hydrogels' stiffness, elasticity, and swelling behavior. A variety of experimental techniques, including rheometry, indentation tests, swelling-deswelling tests, and cyclic loading and unloading tests (fatigue tests), were employed to characterize the mechanical properties and thermoresponsive behavior of the hydrogels under various conditions. In addition to these experimental approaches, simulations using the Finite Element Method (FEM) were conducted to model the swelling behavior of the hydrogels. These simulations, implemented through the ABAQUS software package, aimed to replicate the experimental conditions and provided valuable insights into the hydrogel's response to temperature-induced swelling and shrinking. The results from these simulations were compared with experimental data to evaluate the accuracy of the models and identify any discrepancies, thereby enhancing the understanding of PNIPAM hydrogels' behavior and guiding further optimization for practical applications.

The findings reveal that the mechanical properties of PNIPAM hydrogels, such as stiffness and swelling ability, can be finely tuned by adjusting the synthesis parameters. The study also examines the feasibility of fabricating hydrogels in specific geometries, which is a critical factor for their application in soft robotics. However, the research highlights the challenges in accurately predicting the behavior of these hydrogels through simulations, particularly when it comes to maintaining the desired shape and mechanical integrity under operational conditions.

Furthermore, this research delves into the practical challenges associated with scaling up the production of PNIPAM hydrogels for large scale applications. The study identifies key areas where improvements in synthesis techniques and materials processing can lead to more consistent and reliable hydrogel performance. A potential application in soft robotics is also showcased, demonstrating how PNIPAM hydrogels can be effectively used for actuation and stiffness enhancement for a soft gripper, thereby highlighting their adaptability and functionality in advanced technological applications. By addressing these challenges, the research lays the groundwork for future innovations in the field of (smart)hydrogels, where the adaptability and resilience of PNIPAM hydrogels could be pivotal. The thesis concludes by recommending further exploration into advanced modeling techniques and experimental methodologies to enhance the understanding and utilization of these hydrogels, ultimately contributing to the evolution of soft robotics and other emerging technologies.

Contents

Nomenclature

Abbreviations

Abbreviation	Definition
NiPAAm	N-Isopropylacrylamide
MBA/BIS	N,N′-Methylenebis(acrylamide)
APS	Ammonium persulfate
KPS	Potassium persulfate
TEMED	N,N,N′,N′-Tetramethylethylenediamine
LCST	Lower critical solution temperature
UCST	Upper critical solution temperature
H_M1_C003	Hydrogel sample with 1g monomer and 0.03g crosslinker
H_M1_C005	Hydrogel sample with 1g monomer and 0.05g crosslinker
H_M1_C007	Hydrogel sample with 1g monomer and 0.07g crosslinker
H_M2_C003	Hydrogel sample with 2g monomer and 0.03g crosslinker
H_M2_C005	Hydrogel sample with 2g monomer and 0.05g crosslinker
H_M2_C007	Hydrogel sample with 2g monomer and 0.07g crosslinker
SMM	Shape Memory Material
SMA	Shape Memory Alloy
SMP	Shape Memory Polymer
MEMS	Micro Electromechanical Systems
PVA	Polyvinyl Alcohol
PAM	Poly Acrylamide
PEG	Polyethelene Glycol
DN	Double Network
IPN	Interpenetrating Network
EAP	Electroactive Polymer
DEA	Dielectric Elastomer Actuator
IPMC	Ionic Polymer-Metal Composites
PNIPAM	Poly(N-isopropylacrylamide)
PAAc	Poly(acrylic acid)
EGDMA	Ethyleneglycol Dimethacrylate
LVR	Linear Viscoelastic Region
FEM	Finite Element Method
DoE	Design of Experiments
PLA	Polylactic acid
PMMA	Poly(methyl methacrylate)

1

Introduction

In recent years, the fields of robotics and material science have witnessed significant advancements, specifically through the development of soft robotics and smart materials. Traditional robotics, which essentially focuses on creating rigid, metal-based machines designed to replace humans in monotonous, dangerous, or highly repetitive tasks, has been the foundation of industrial automation. These robots are effective in stable environments requiring precision, such as in automotive manufacturing and electronics assembly [1]. However, their rigid structure limits their adaptability and safety in applications where interaction with delicate objects or human tissues is required [2].

Soft robotics emerged as a response to these limitations, focusing on the creation of robots that are more flexible, adaptable, and capable of safe interaction with their environment [3]. Unlike the traditional robots, soft robots are constructed from compliant materials, such as elastomers and hydrogels. This allows them to perform complex and delicate tasks, such as handling fragile items in agriculture, logistics, or biomedical applications [3]. This shift has opened new avenues for innovation, specifically in sectors like healthcare, where soft robotic grippers can be used in minimally invasive surgeries or even as prosthetic devices that closely mimic natural human movement [4].

Central to the advancement of soft robotics is the development of smart materials, materials that can change their properties in response to external stimuli. Among the most promising smart materials are hydrogels, which are three-dimensional networks of hydrophilic polymers that can absorb and retain large amounts of water [2]. These materials are particularly valued for their bio-compatibility, flexibility, and ability to undergo significant volume changes in response to environmental triggers [2]. Hydrogels have been extensively studied for their applications in drug delivery, tissue engineering, and as actuators in soft robotics. Their capacity to respond to external stimuli such as temperature, pH, or electric fields makes them ideal candidates for creating responsive and adaptable systems [5].

This thesis focuses specifically on the synthesis and characterization of thermoresponsive hydrogels, with an emphasis on Poly(N-isopropylacrylamide) (PNIPAM) hydrogel. PNIPAM is a well-studied polymer that exhibits a lower critical solution temperature (LCST) around 32°C, making it capable of reversible swelling and shrinking in response to temperature changes. This thermoresponsive behavior is particularly useful in applications where controlled actuation is required, such as in soft robotic grippers or as part of drug delivery systems where release is triggered by body temperature [6].

Hydrogels like PNIPAM, while promising, present challenges in their synthesis and application. The mechanical properties of hydrogels, such as their elasticity and strength, are crucial for their performance in real-world applications. These properties are heavily influenced by the synthesis parameters such as, the concentrations of the monomer and crosslinker used during polymerization. Tailoring these parameters to achieve the desired balance between flexibility and mechanical robustness is essential for optimizing hydrogels for specific uses in soft robotics [7].

Testing the mechanical properties of hydrogels can be challenging due to their soft and delicate nature. Due to their delicate nature traditional testing methods and equipment often struggle to accurately mea-

sure the properties of such compliant materials. However, in this research, a straightforward approach to testing was employed to demonstrate that it is possible to evaluate hydrogel properties using simple methods. This approach not only makes the testing process more accessible but also shows that essential insights into the mechanical behavior of hydrogels can be obtained without the need for highly specialized equipment.

1.1. Research Objective

The primary objective of this research is to investigate the influence of monomer and crosslinker concentrations on the synthesis, characterization, and mechanical properties of PNIPAM hydrogels. By understanding these relationships, this study aims to contribute to the development of hydrogels that are not only responsive to temperature but also possess the necessary mechanical strength and durability required for their application in soft robotic systems.

1.1.1. Research Question

The main research question guiding this study is: **How can PNIPAM hydrogels be synthesized and characterized to optimize their mechanical properties and behavior for use in soft robotics?**

1.1.2. Sub-questions

To address the primary research question, the following sub-questions will be explored:

1. How can PNIPAM hydrogels be synthesized effectively?
2. What are the factors that affect hydrogel synthesis and its final properties?
3. What are the methods to characterize a hydrogel's behavior?
4. What are the methods to characterize hydrogel's mechanical properties?
5. How can hydrogels be fabricated in different shapes and sizes to be effectively used in soft robotics?

These sub-questions are designed to systematically guide the research towards answering the main research question by exploring the synthesis process, the factors influencing hydrogel properties, and the methods for their characterization.

In addressing these objectives, this thesis is structured as follows: Chapter 2 provides a comprehensive literature review, covering smart materials, the various types of hydrogels, and the specific focus on PNIPAM hydrogels. Chapter 3 details the methodology used in the synthesis and characterization of the hydrogels, while Chapter 4 presents the materials and experimental setups used. Finally, Chapter 5 discusses the results of the experiments and through analysis and interpretation of the data.

By systematically exploring these aspects, this research aims to contribute to the broader understanding and application of thermoresponsive hydrogels in innovative fields like soft robotics, potentially paving the way for new, adaptable technologies in various industries.

2

Literature review

In this chapter, a comprehensive literature review done on smart materials, soft grippers, hydrogel (both synthesis and testing) is presented. Robotics is the science of building machines with desired abilities of movement, perception, cognition, which make robots, machines that are intended to perform tasks in the service of human beings [1]. Robotic grippers were machines, oirginally made of rigid joints and rigid body parts which was a revolution by itself, but as the time progressed the use of rigid parts and joints experienced limitations in their application and use. These limitations were overcome by the new field of Soft robotics where robotic grippers were built using softer materials which allowed their application in delicate environments such as the medical industry [1]. Hard robotics excel in tasks such as large-scale production but struggle with precise control due to their need for high precision. They operate efficiently in stable environments where little adaptation is necessary, making them less adaptable in unpredictable settings. Conversely, soft grippers, despite their lower rigidity stemming from the use of flexible materials, demonstrate greater efficiency and safety in complex and uncertain environments. In essence, any gripper, regardless of type, requires an actuator to generate a reaction force for effective work delivery; without this, the gripper lacks the necessary firmness to handle objects.

Hydrogels represent a class of smart materials known for their unique ability to absorb and retain significant amounts of water while maintaining their structural integrity [6]. These materials have garnered significant attention in various fields, particularly in soft robotics, due to their remarkable flexibility and responsiveness to environmental stimuli. In the field of soft robotic grippers, hydrogels play a vital role in mimicking the dexterity and adaptability of natural biological systems. Utilizing hydrogels in soft robotic grippers involves integrating them into the gripper's structure or as part of its actuation [3]. By exploiting the swelling and deswelling properties of hydrogels in response to changes in environmental conditions such as pH, temperature, or humidity, these grippers can adjust their shape, size, and stiffness accordingly. This dynamic behavior enables soft robotic grippers to delicately grasp and manipulate objects with precision, making them ideal for applications in handling fragile or irregularly shaped objects. Furthermore, the inherent biocompatibility of hydrogels opens up possibilities for use in biomedical and biotechnological applications, showcasing their versatility and potential impact in the field of soft robotics.

2.1. Classification of smart materials

Thousands of years in the past, humans utilized various materials for diverse purposes, leading to advancements in their quality of life. This utilization also marked the division of civilizations, with significant periods like the Stone Age denoting the earliest stages [8]. However, the Bronze Age emerged as a pivotal era due to the discovery of bronze, a material renowned for its enhanced durability and hardness. This discovery heralded a new chapter in metallurgy, subsequently leading to the unveiling of numerous other materials [8]. Over the last couple of decades, significant strides have been made in science and technology, particularly in the synthesis of novel materials. These materials can be broadly categorized into polymers, ceramics, metals, and smart materials [9]. Notably, smart materials are gaining popularity owing to their versatile applications compared to conventional materials. These

extraordinary materials possess the ability to alter their properties, such as changing shape upon exposure to heat or instantly transitioning phases near a magnet. Following are a few examples of smart materials which have been used as sensors and also as actuators (see Table 2.1 and Table 2.2), it can be seen that some of the materials can be used both as sensors and actuators and it's use depends on the application. Also, each material has its own advantages and disadvantages

Table 2.1: Examples of smart materials used as actuators [10, 11].

Actuators		
Material class	**Stimulus**	**Response**
Piezoelectric	Electric current	Mechanical strain
Electrostrictors	Electric current	Mechanical strain
Electroactive polymers	Electric current	Mechanical strain
Electrorheological fluids	Electric current	Viscosity change
Magnetostrictors	Magnetic field	Mechanical strain
Magnetorheological fluids	Magnetic field	Viscosity change
Shape memory alloys	Temperature change	Mechanical strain

Table 2.2: Examples of smart materials used as sensors [10, 11].

Sensors		
Material class	**Stimulus**	**Response**
Piezoelectric	Mechanical strain	Electric polarization
Electrostrictors	Mechanical strain	Electric polarization
Electroactive polymers	Mechanical strain	Electric polarization
Electroluminescent	Electric field	Light emission
Magnetostrictors	Mechanical strain	Change in magnetic field
Photoluminescent	Incident light	Light emission
Pyroelectrics	Temperature change	Electric polarization

2.1.1. Shape memory alloys

Shape memory alloys, a subset of smart materials known as shape memory materials (SMMs), represent a significant breakthrough in material science due to their remarkable ability to retain a specific shape and revert to the original when exposed to external stimuli, typically thermomechanical changes due to temperature fluctuations. Discovered initially in 1932 by Arne Olander [12], these materials gained prominence after Frederick Wang's demonstration of the shape memory effect in Nitinol (NiTi) in 1962 [13, 14]. Since then, shape memory alloys (SMAs), particularly Nitinol, have seen growing demand in various industries such as aerospace, automotive, microelectromechanical systems (MEMS), robotics (including soft robotics), and biomedical applications.

SMAs exhibit a unique property of transitioning between two phases and three distinct crystal structures (Figure 2.1): twinned martensite, detwinned martensite, and austenite [8]. The stable structure at higher temperatures is austenite, while martensite becomes stable at lower temperatures. During heating, SMAs tend to transform from martensite to austenite structures, with specific temperature thresholds known as austenite start and finish temperatures [3]. Conversely, during cooling, martensite start and finish temperatures dictate the reversal of this transformation. Additionally, there exists a critical temperature beyond which martensite cannot be stress-induced, leading to permanent deformation similar to conventional metals. This phenomenon, known as the shape memory effect or pseudoelasticity, can be categorized into one-way shape memory effect and two-way shape memory effect, depending on the behavior of the material upon deformation and subsequent heating [3, 8].

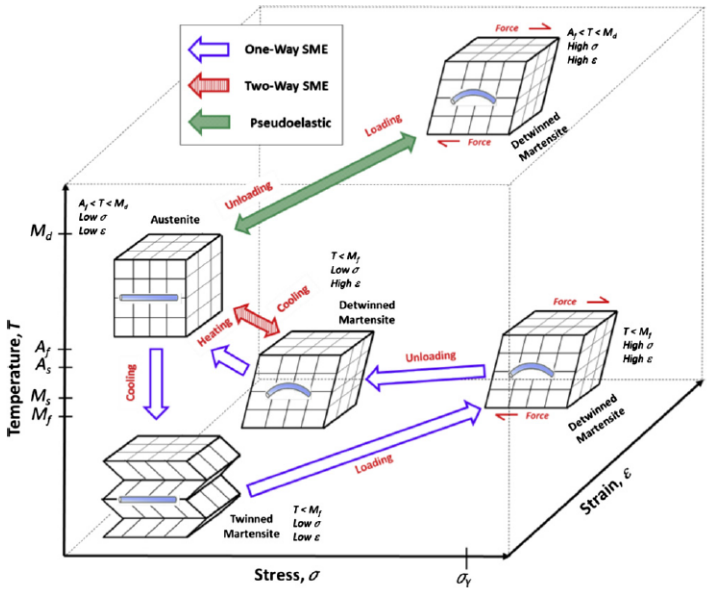

Figure 2.1: SMA phases and crystal structures [8].

2.1.2. Shape memory polymers

Shape memory polymers (SMPs) exhibit principles akin to shape memory alloys (SMAs) but with some distinctions. In their cool state, typically below a specific transition temperature, SMPs maintain a rigid shape and resist deformation. However, upon heating to a temperature above this transition point, they become pliable and can be reshaped by external forces [15]. Upon cooling while maintaining the deformation, the SMPs stiffen again, retaining the altered shape. Reheating above the transition temperature allows the material to return to its original, undeformed state [15]. Unlike SMAs, which require only one heating cycle for shape restoration, SMPs may undergo multiple cycles of heating and cooling to modify their properties through phase changes such as crystallization-melting or vitrification-glass transitions [15]. Moreover, SMPs exhibit a broader range of stimuli for property alteration, including temperature, pH, electricity, pressure, moisture, light, microwaves, laser heating, solvents, and solvent vapors, making them versatile for various applications. The Figure 2.2 below shows working of the SMPs and also difference in stimuli for SMAs and SMPs (Figure 2.3).

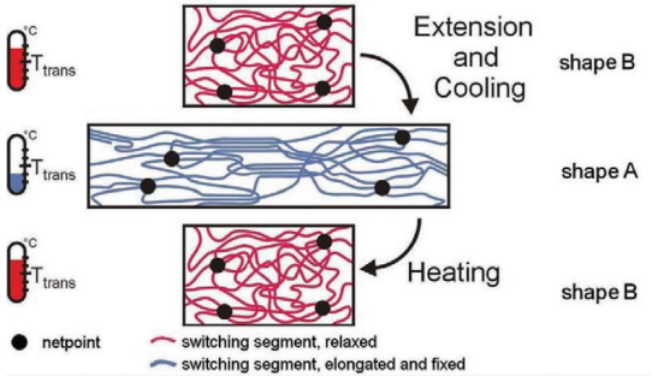

Figure 2.2: SMP phases [3].

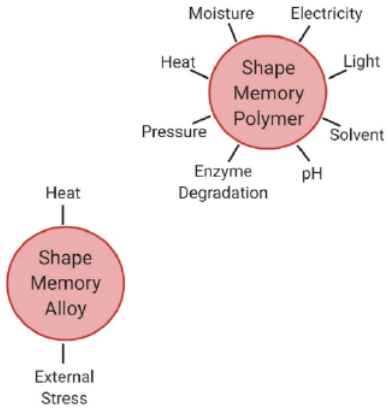

Figure 2.3: Different stimuli which SMA and SMP respond to [15].

2.1.3. Piezoelectric materials

Piezoelectric materials, another category of smart materials, derive their name from their ability to generate electricity in response to mechanical stress or pressure, as discovered by the Curie brothers [16]. Conversely, they can also deform under an applied electric field, exhibiting the inverse piezoelectric effect. These materials find widespread applications across industries, including automotive, energy harvesting, medical devices, and non-invasive imaging, owing to their unique properties. The image below provides a visual representation of the working principle:

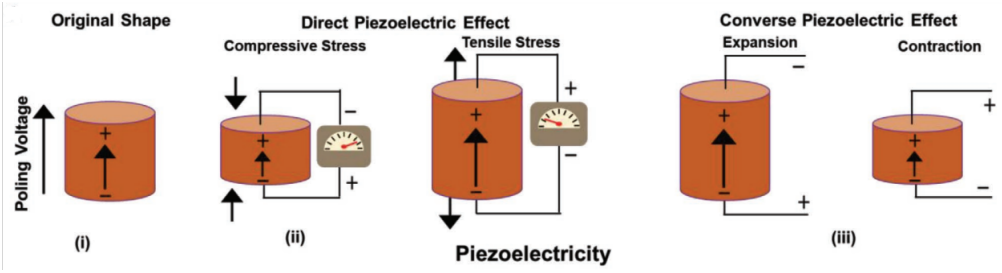

Figure 2.4: Piezoelectric material's working principle [17].

2.1.4. Electrical and magnetic based materials

Magnetostrictive materials, belonging to the realm of smart materials, undergo dimensional changes in response to a magnetic field, a phenomenon known as the magnetostrictive effect, first observed by James Joule in 1842 [3]. Terfenol-D and Galfenol are among the commonly used magnetostrictive materials, finding applications in ultrasound transducers, sensors, actuators, and industrial machinery [3].

Magnetorheological fluids, a specialized type of smart material, exhibit reversible changes in viscosity when subjected to a magnetic field, enabling applications in automotive shock absorbers, adaptive suspension systems, industrial machinery, and touch-sensitive devices [3].

Electrorheological fluids, akin to magnetorheological fluids, experience changes in viscosity under an electric field, offering solutions in adaptive suspension systems, robotic grippers, and industrial machinery [3].

These smart materials, with their diverse applications and inherent adaptive qualities, are increasingly utilized in the field of soft robotics, enabling the development of dynamic systems that mimic natural movements and adapt to their surroundings [1, 3].

These were a few classes of smart materials, but this report will focus on a special class of smart materials called as (smart)Hydrogels, which is discussed further in the next section.

2.2. Introduction to smart hydrogels

A hydrogel, a type of polymer network, exhibits the ability to alter its material properties through intermolecular interactions with water, which can result in swelling or shrinking. Notably, hydrogels demonstrate a higher mechanical compliance compared to biological tissue, alongside high permeability to various molecules and ionic conductivity, rendering them promising for diverse applications. Hydrogels can be classifed as follows:

2.2.1. Based on Source

Hydrogels can be categorized into two primary groups based on their source: natural and synthetic. Natural hydrogels are derived from biological origins, such as collagen, gelatin, and alginate, which are typically biocompatible and biodegradable, making them suitable for various biomedical applications [2, 6]. Synthetic hydrogels, on the other hand, are man-made polymers, such as polyvinyl alcohol (PVA), polyacrylamide (PAM), and polyethylene glycol (PEG) [2, 6]. These synthetic hydrogels offer greater control over their chemical composition and properties, allowing for customization to meet specific requirements in diverse industrial and medical applications [18].

2.2.2. According to Polymeric Composition

The method of preparation yields several significant classes of hydrogels:

- Homopolymeric hydrogels consist of a polymer network derived from a single type of monomer. These hydrogels may have a cross-linked skeletal structure based on the nature of the monomer and polymerization technique [19].
- Copolymeric hydrogels are composed of two or more different monomer species, with at least one hydrophilic component, arranged in various configurations along the polymer network chain [20].
- Multipolymer or Interpenetrating polymeric hydrogels (IPN) contain two independent cross-linked polymer components, either synthetic, natural, or both, forming a network. Semi-IPN hydrogels consist of one cross-linked polymer component and one non-cross-linked polymer component [21].

2.2.3. Based on Configuration

Hydrogels can be classified by their physical structure and chemical composition [22]:

- Amorphous (non-crystalline): These hydrogels lack a definite structure and are characterized by their disordered arrangement of polymer chains. This configuration often results in a higher degree of flexibility and an ability to absorb large quantities of water, thus making them suitable for applications where high absorbency and flexibility are required.
- Semicrystalline: Semicrystalline hydrogels possess both amorphous and crystalline regions within their structure. This blend provides a balance between flexibility and mechanical strength. The crystalline regions offer structural stability, and the amorphous areas maintain flexibility and water absorption. A combination like this is beneficial in applications where both mechanical integrity and absorbency are needed.
- Crystalline: Hydrogels with a crystalline configuration have highly ordered polymer chains. Their structure typically provides the hydrogel with enhanced mechanical strength and less flexibility compared to amorphous and semicrystalline hydrogels. Crystalline hydrogels are often used in applications where mechanical robustness is critical compared to absorbency.

2.2.4. Type of Cross-linking

Hydrogels fall into two categories based on the nature of cross-link junctions:

- Chemically cross-linked networks: These hydrogels feature permanent junctions formed through covalent bonds [5]. The chemical cross-linking provides stable and robust networks, which ensure that the hydrogel maintains its shape and strength even under stress or in varying environmental conditions. This type of cross-linking is typically achieved through polymerization techniques that introduce cross-linking agents, which result in a three-dimensional network that is less likely to

dissolve in water .

- Physically cross-linked networks: In contrast, physically cross-linked hydrogels possess transient junctions created by physical interactions such as ionic interactions, hydrogen bonding, or hydrophobic interactions [23]. These physical cross-links are reversible and can be broken and reformed under different conditions, allowing the hydrogel to respond dynamically to environmental changes. This type of hydrogel is often used in applications where reversible behavior is advantageous, such as in drug delivery systems or as actuators in soft robotics [24].

2.2.5. Physical Appearance

Hydrogels can be categorized based on their physical appearance, which is primarily determined by the polymerization technique employed during their synthesis. Depending on the method used, hydrogels can take up various forms such as matrices, films, or microspheres [22]. Matrices, the most common form, are continuous networks or blocks that are particularly useful in bulk applications like wound dressings, where their ability to retain moisture and conform to the shape of the wound is essential. Hydrogel films are thin layers designed for surface applications, such as coatings or membranes, and are often utilized in drug delivery systems and protective layers due to their controlled release capabilities. Additionally, hydrogels can be shaped into microspheres—tiny spherical particles that are especially advantageous in drug delivery [22]. These microspheres can be engineered to release therapeutic agents gradually over time, and their small size facilitates easy injection and distribution within the body. The physical appearance of a hydrogel plays a crucial role in determining its suitability and effectiveness across a variety of medical, pharmaceutical, and industrial applications.

2.2.6. According to Network Electrical Charge

Hydrogels can be classified into four groups based on the presence or absence of electrical charge on the crosslinked chains [22]:

- Nonionic (neutral): These hydrogels do not carry any net charge. They are neutral in nature, which often results in a stable and predictable swelling behavior, which make them suitable for various biomedical applications.
- Ionic (including anionic or cationic): Ionic hydrogels include both anionic (negatively charged) and cationic (positively charged) types. These hydrogels can interact with oppositely charged molecules or ions in their environment, which can lead to unique swelling behaviors and responsiveness to changes in pH or ionic strength. Such properties are often exploited in drug delivery systems where controlled release is essential.
- Amphoteric electrolyte (ampholytic): Amphoteric hydrogels contain both acidic and basic groups, allowing them to carry both positive and negative charges depending on the pH of their environment. This duality enables these hydrogels to exhibit complex responses to pH changes, making them useful in applications requiring dynamic adaptability.
- Zwitterionic (polybetaines): Zwitterionic hydrogels possess both anionic and cationic groups within each structural repeating unit. This unique configuration allows them to maintain a high degree of hydration and resist protein adsorption, which is particularly advantageous in developing biocompatible materials for medical applications.

2.2.7. Based of reaction to external stimuli

According to studies cited by [2–4], hydrogels can be further categorized into thermoresponsive, chemicalresponsive, electrical-responsive, magnetically-responsive, and photoresponsive types. These classifications form the foundation of the main hydrogel types that are being researched and applied. However, there is also room to consider additional categories involving less commonly applied stimuli-responsive materials such as dissolution, humidity, and redox states. This categorization extends beyond the application of hydrogels as actuators in soft grippers [11].

Among these categories, thermoresponsive hydrogels represent a significant classification. These hydrogels can adjust their volume in response to temperature changes. The phase transition behavior of thermoresponsive polymers, as discussed in [7, 25, 26], dictates the operational temperature range of these hydrogels. Two distinct types of thermoresponsive hydrogels exist: those exhibiting lower

critical solution temperature (LCST) and upper critical solution temperature (UCST). In the study of [2], the principle is illustrated, featuring poly(acrylic acid-co-acrylamide) hydrogel, a UCST hydrogel, and PNIPAM, an example of an LCST hydrogel. The former swells as temperature rises, absorbing water molecules, while the latter shrinks at higher temperatures and expands at lower temperatures, this can be seen in Figure 2.5. This dichotomy in behavior distinguishes the responses of hydrogels with LCST and UCST, delineating their unique properties and potential applications.

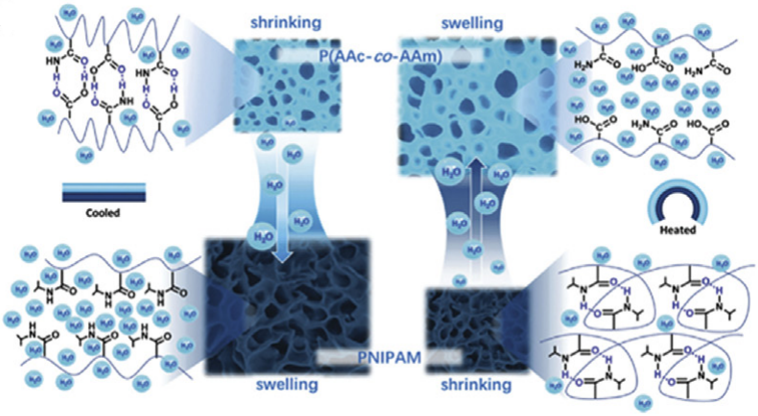

Figure 2.5: Schematic illustration showing the working principles of thermoresponsive hydrogels [2].

Electroresponsive hydrogels, categorized as Electroactive Polymers (EAPs), exhibit reversible mechanical deformation in response to electrical stimuli, as detailed in [3, 4]. In essence, these intelligent materials have the remarkable capability to convert electrical input into mechanical movement. Notably, EAPs offer several advantages, including high resistance to fracture, effective vibration damping, and the ability to withstand substantial deformation under high force conditions, as highlighted in [27].

Among the various types of EAPs discussed in the literature, dielectric elastomer actuators (DEAs) and ionic polymer-metal composites (IPMCs) stand out as two widely employed examples [4]. DEAs, characterized by two electrodes separated by a thin elastomer membrane, operate through electrostatic attraction when a high voltage is applied between the hydrogels. This results in compressive forces acting on the elastomer membrane, causing it to stretch, as illustrated in Figure 2.6 and Figure 2.7. Conversely, IPMCs employ a polymer membrane containing electrolytes instead of a thin elastomer membrane. Upon application of voltage, the electrolytes migrate towards the electrodes, inducing differential swelling and consequent bending, as depicted in Figure 2.6.

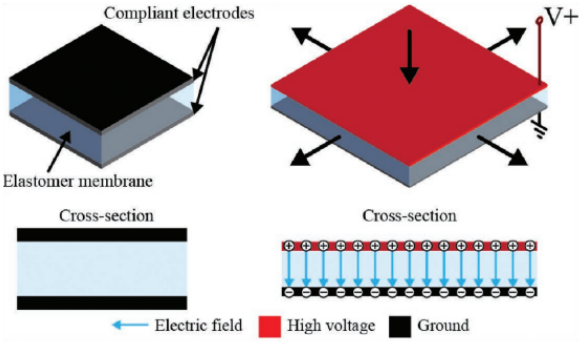

Figure 2.6: DEA [27].

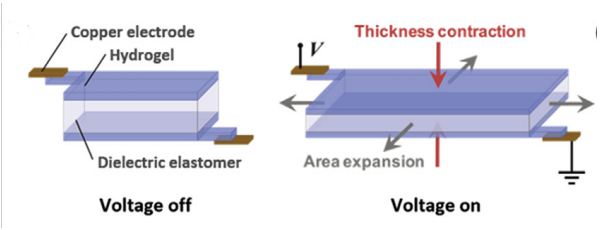

Figure 2.7: Hydrogel beased DEA [2].

While IPMCs are not inherently based on hydrogels, the underlying principle of electrically induced osmotic pressure can be adapted to hydrogels [2, 27]. This principle involves hydrogels with functional groups of specific charges and counter ions placed in an aqueous environment. Upon application of an electric field, mobile counter ions move towards the electrodes, creating a net charge [2]. Consequently, ions in the aqueous environment with similar charges as the functional groups are attracted to the electrodes, resulting in asymmetric swelling of the hydrogel, as demonstrated in Figure 2.9. This innovative mechanism underscores the potential of electroresponsive hydrogels in various applications requiring precise control and actuation, particularly in soft robotics and biomedical devices.

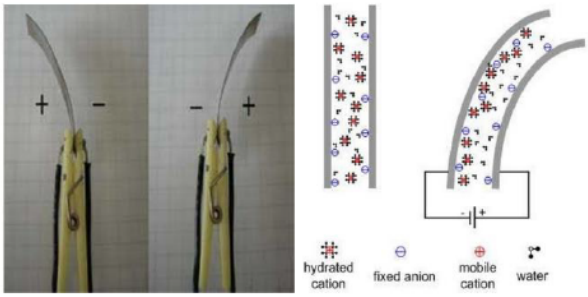

Figure 2.8: IPMC [27].

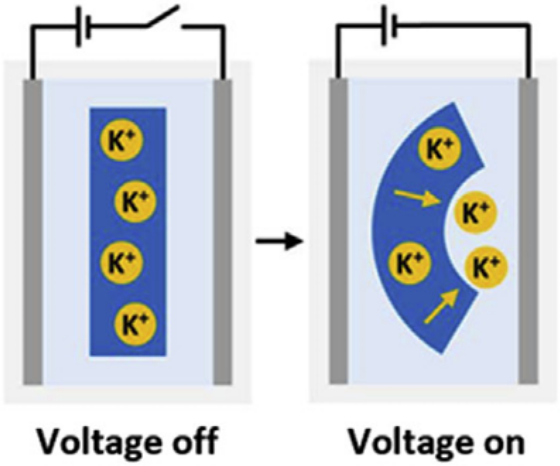

Figure 2.9: Hydrogel beased IPMC [2].

Magnetic-responsive hydrogels, a subset of hydrogels, are activated by exposure to a magnetic field. Incorporating magnetic particles into the hydrogel material is essential for its activation, typically achieved through the inclusion of paramagnetic or ferromagnetic additives, as described in [4]. These magnetic particles serve as mediators, transferring the magnetic force from an external magnetic field to the hydrogel structure, thereby inducing a change in its shape. This mechanism is visually depicted in Figure 2.10.

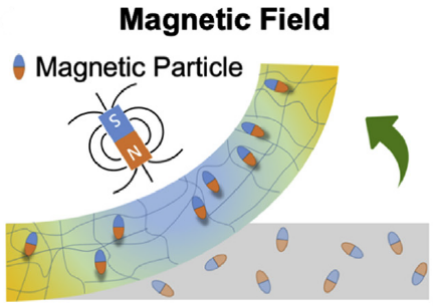

Figure 2.10: Schematic illustration showing the working principles of magnetoresponive hydrogels [4].

Expanding on magnetically responsive hydrogels, their unique ability to be controlled remotely through magnetic fields makes them promising candidates for various applications. In the field of soft robotics, for instance, these hydrogels could enable the development of robots capable of precise movements and shape changes without the need for direct physical contact or complex mechanisms. Additionally, in biomedicine, magnetically responsive hydrogels hold potential for targeted drug delivery systems or tissue engineering applications, where controlled manipulation at the micro or nano scale is desired. The versatility and controllability offered by magnetically responsive hydrogels open up exciting

avenues for innovation in both research and practical applications.

Chemically responsive hydrogels represent another category within the realm of hydrogels, offering distinct functionalities driven by environmental chemical cues that translate into mechanical responses, such as swelling or shrinking, as outlined in [2]. These hydrogels primarily comprise two main types: solvent-based and pH-based.

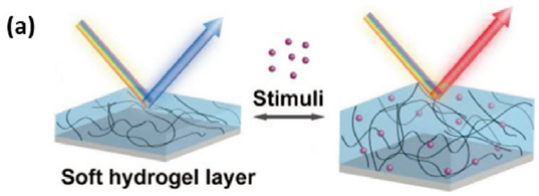

Figure 2.11: Schematic illustration showing the working principles of Chemically responsive hydrogels [2].

Solvent-responsive hydrogels undergo activation when there is a discrepancy in hydrophobicity between the solvent and the polymer network and this disparity prompts the hydrogel to either expand or contract [28]. The degree of volumetric change is directly influenced by the variance in hydrophobicity, with greater differences resulting in more pronounced swelling or shrinking. Notably, a universal trend is observed where hydrogels tend to shrink in organic solvents and swell in water, as depicted in Figure 2.11.

On the other hand, pH-responsive hydrogels exhibit responsiveness to fluctuations in pH levels. This behavior stems from alterations in the osmotic pressure within the hydrogel network during changes in pH, as elucidated in [4]. Typically composed of polyelectrolytes containing functional groups, these hydrogels form ionic barriers that selectively permit ions of opposite charges to be absorbed while preventing ions of similar charges. This selective ion localization induces changes in volume, leading to mechanical actuation of the hydrogel, as depicted in Figure 2.13.

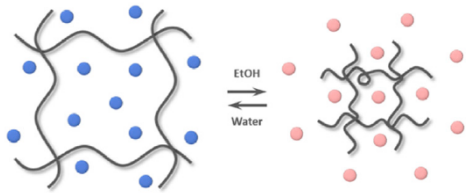

Figure 2.12: Schematic representation of solvent based hydrogels [2].

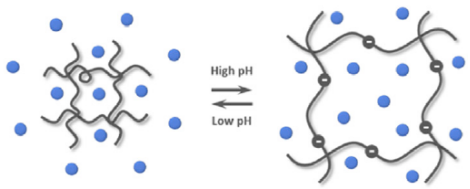

Figure 2.13: Ph responsive hydrogels [2].

Light irradiation serves as the triggering mechanism for photoresponsive hydrogels, prompting alterations in their volume or shape [2]. Within the domain of photoresponsive hydrogels, two primary categories are distinguished: reversible cross-linking reactions and photothermal excitation. These distinctions rely on the presence of photoactive moieties within the hydrogel, which is essential for both reversible cross-linking and photothermal excitation processes [29].

Reversible cross-linking entails mechanisms such as photoisomerization and photocleavage, facilitating dynamic changes in the hydrogel structure upon exposure to light. Conversely, photothermal excitation involves reversible dehydration-hydration processes, leveraging light-induced alterations in the hydrogel's hydration state for shape or volume modifications, as discussed in [4].

2.3. Hydrogel synthesis/preparation

2.3.1. Hydrogel synthesis

Hydrogels are polymer networks known for their hydrophilic characteristics, typically composed of hydrophilic monomers. However, hydrophobic monomers are sometimes incorporated to modify the hy-

drogel's properties for specific applications.

Hydrogels can be derived from synthetic or natural polymers [2]. Synthetic polymers, which are inherently hydrophobic and chemically robust compared to natural polymers, tend to degrade more slowly but provide greater mechanical strength [6]. This characteristic requires careful consideration during design. Similarly, natural polymers can be used in hydrogel production if they possess appropriate functional groups or have been modified with polymerizable groups [23].

In essence, a hydrogel is a hydrophilic polymer network cross-linked to form an elastic structure. Therefore, any method capable of creating a cross-linked polymer can be employed to produce hydrogels [22]. Copolymerization/cross-linking via free-radical polymerizations is a common technique, where hydrophilic monomers are reacted with multifunctional cross-linkers [22]. Additionally, water-soluble linear polymers, whether from natural or synthetic sources, are cross-linked through chemical reactions, ionizing radiation-induced free radicals, or physical interactions such as entanglements and electrostatic forces. A variety of polymerization techniques are employed to achieve the desired hydrogel properties.

Generally, the essential components of hydrogel preparation encompass monomers, initiators, and cross-linkers [5, 22]. To regulate polymerization heat and final hydrogel properties, diluents like water or other aqueous solutions are employed. Subsequently, the hydrogel mass undergoes washing to eliminate impurities stemming from the preparation process, such as unreacted monomers, initiators, cross-linkers, and undesired byproducts. This can be seen in Figure 2.14.

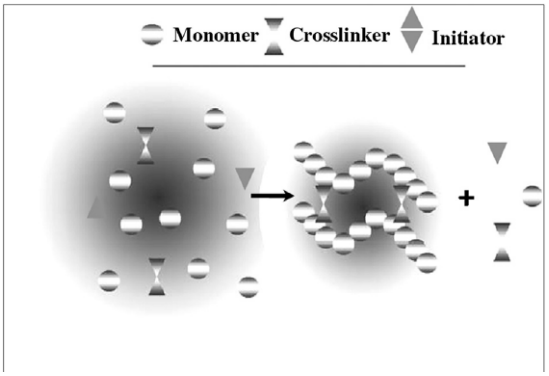

Figure 2.14: Schematic illustration of hydrogel synthesis using Monomer, crosslinker and initiators [5].

Bulk polymerization offers a straightforward approach for producing hydrogels, utilizing a variety of vinyl monomers [5]. These hydrogels can be crafted from one or more types of monomers, allowing for customization of physical properties tailored to specific applications. Typically, a small quantity of cross-linking agent is incorporated into the hydrogel formulation. Polymerization initiation usually occurs via radiation, ultraviolet light, or chemical catalysts, with the choice of initiator contingent upon the monomer types and solvents utilized [5].During bulk polymerization, only monomer and monomer-soluble initiators are involved, resulting in high polymerization rates and degrees. However, viscosity increases significantly with conversion, leading to heat generation during polymerization [5]. Controlling the reaction at low conversions mitigates these issues. Bulk polymerization yields a homogeneous hydrogel, initially producing a glassy, transparent polymer matrix that becomes soft and flexible upon immersion in water [5].

Solution polymerization/cross-linking involves mixing ionic or neutral monomers with multifunctional cross-linking agents, with polymerization initiated thermally via UV irradiation or redox initiator systems [5]. The presence of a solvent acts as a heat sink, distinguishing solution polymerization from bulk polymerization. The resulting hydrogels require washing with distilled water to remove impurities, with phase separation occurring if the water content exceeds equilibrium swelling levels. Solvents commonly used for solution polymerization include water, ethanol, water-ethanol mixtures, and benzyl alcohol. According to Javad Alaei et al. [30], hydrogel production in industrial settings involves solution, reversed suspension, and reversed emulsion polymerizations. Figure 2.15 illustrates a schematic diagram of a typical solution polymerization process. It outlines the key steps involved in hydrogel

manufacturing at semi-pilot and industrial scales.

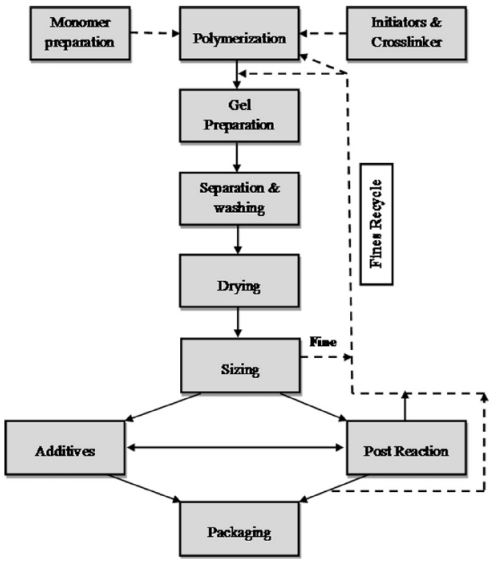

Figure 2.15: Schematic illustration of solution polymerization procedure [5, 30].

Suspension polymerization, or inverse-suspension polymerization, sometimes also called as Dispersion polymerization, presents notable advantages. It yields products in the form of powder or microspheres (beads), eliminating the need for grinding. This method adopts a water-in-oil (W/O) process instead of the more common oil-in-water (O/W) approach, hence termed inverse suspension [5]. Here, monomers and initiators are dispersed within the hydrocarbon phase as a homogeneous mixture. The size and shape of resin particles are primarily influenced by factors such as the viscosity of the monomer solution, agitation speed, rotor design, and dispersant type [31]. Detailed discussions on hetero-phase polymerizations have been previously documented [32, 33]. Given the thermodynamic instability of dispersion, continuous agitation and the addition of a low hydrophilic-lipophilic-balance (HLB) suspending agent are required. Recently, the inverse-suspension method has found widespread application in the production of polyacrylamide-based hydrogels due to its efficacy in removing and managing hazardous residual acrylamide monomers in the polymer [5]. Figure 2.16 illustrates a schematic diagram of the suspension polymerization process for hydrogel production. Critical parameters for preparing hydrogel beads via suspension polymerization largely remain undisclosed or proprietary in the literature.

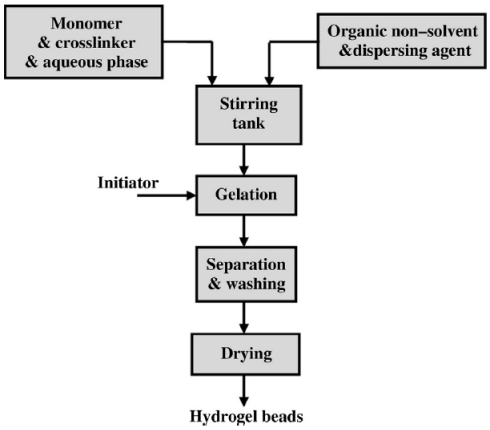

Figure 2.16: Schematic illustration of suspension polymerization procedure [5].

In general, hydrogels produced through bulk polymerization typically exhibit a weak structure. To enhance their mechanical properties, hydrogels can be surface-grafted onto a stronger support. This

technique involves initiating free radicals on the surface of a robust support material, followed by direct polymerization of monomers onto it, resulting in a chain of monomers covalently bonded to the support. Various polymeric supports have been employed in the synthesis of hydrogels using grafting techniques [5, 34, 35].

Utilizing ionizing high-energy radiation such as gamma rays [36] and electron beams, which serve as initiators for the creation of hydrogels from unsaturated compounds. Irradiating an aqueous polymer solution induces radical formation on the polymer chains [36]. Additionally, the radiolysis of water molecules generates hydroxyl radicals, which also interact with the polymer chains, resulting in the formation of macro-radicals. The recombination of these macro-radicals across different chains leads to the establishment of covalent bonds, ultimately forming a cross-linked structure. Polymers such as poly(vinyl alcohol), poly(ethylene glycol), and poly(acrylic acid) exemplify materials cross-linked through the radiation method [22]. The principal advantage of radiation initiation over chemical initiation lies in the production of relatively pure and initiator-free hydrogels. These were a few core methods for synthesis of hydrogels, but a vast majority of hydrogels are either physically cross-linked or chemically cross-linked, where different types of polymerizations are used to form those cross-links in the polymers (Figure 2.17). Pablo Sánchez-Cid et. al. [23] and Muhammad Faheem Akhtar et. al. [22] present a deeper look into the physical and chemical cross-linking processes and their following polymerization techniques.

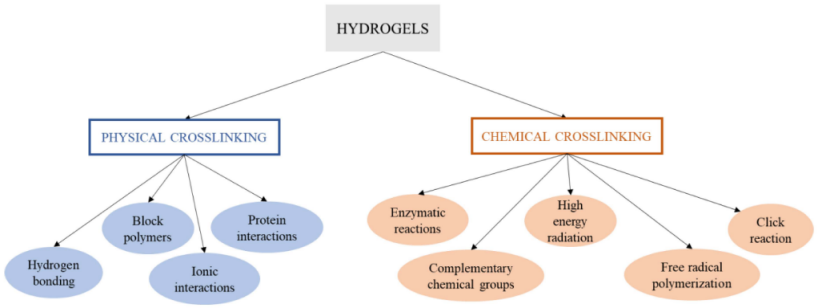

Figure 2.17: Schematic illustration of different Physical and chemically cross-linking methods for synthesis of hydrogels [23].

2.3.2. Testing of hydrogel

Due to their biodegradable, biocompatible, and non-toxic nature, hydrogels have garnered significant attention in pharmaceutical and biomedical engineering. Prior to their application, certain characteristics of hydrogels, such as swelling behavior, mechanical properties, and toxicity, must undergo thorough evaluation. Key qualities of hydrogels include:

Swelling and shrinking

Hydrogels are versatile materials that can expand in water, retaining a significant amount of water within their structure without breaking down. Their swelling behavior, a defining characteristic, is influenced by environmental factors such as ionic strength, pH, and temperature [37]. Comprising polymers cross-linked through various techniques, hydrogels are considered single molecules, making them highly responsive to slight changes in their surroundings [38, 39]. Several factors, including cross-linking ratio, ionic conditions, synthesis method, and polymer composition, affect the equilibrium and kinetics of swelling. The swelling ratio, which compares the weight of the swollen gel to its dry state, quantifies this behavior, with strongly cross-linked hydrogels exhibiting lower swelling ratios and vice versa [40].

The chemical structure, particularly the presence of hydrophilic and hydrophobic groups, significantly influences hydrogel swelling. Hydrogels rich in hydrophilic groups tend to swell more than those with hydrophobic groups. Additionally, temperature and pH play crucial roles in hydrogel expansion. pH-sensitive hydrogels, for example, expand due to the ionization of hydrophilic groups in response to pH changes [41]. Electrostatic repulsion within polymer chains contributes to the breakdown of secondary bonding, facilitating water diffusion into the hydrogel network. The process of hydrogel swelling involves water diffusion, unwinding of polymer chains, and development of the hydrogel network [42–44]. When hydrated, hydrogels are known to transition from a dry, smooth state to a rubbery, expanded state

known as swelling. The mechanism of water passage and exit from the hydrogel matrix is governed by diffusion processes [42–44]. Figure 2.18 illustrates the swelling and de-swelling of hydrogels.

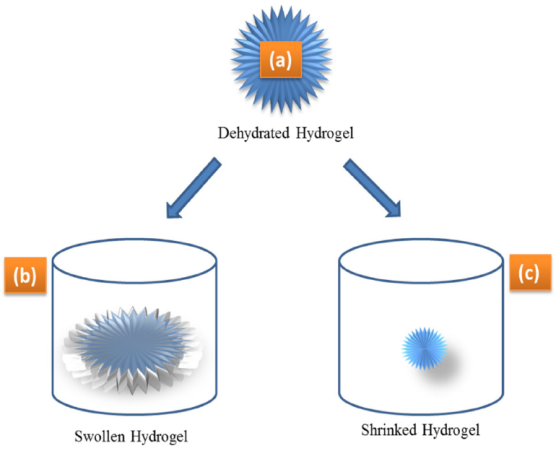

Figure 2.18: Schematic illustration of a) Dehydrated/Equilibrium state, b)Swollen hydrogel after being immersed in water, c) Shrunken hydrogel after being dehydrated by providing heat [45].

This phenomenon, hydrogel swelling, plays a crucial role in determining various parameters such as cross-linking density, mechanical properties, and degradation rate. Typically, the swelling behavior of hydrogels is assessed through straightforward methods like swelling ratio measurements, and weight loss calculations (or) shrinking ratio measurements.

Swelling ratio, an important parameter, is typically determined by immersing the hydrogel in distilled water for a standardized duration, filtering it through a 30-mesh filter, and then calculating the swelling percentage using the equation:

$$Swelling\% = \frac{(W_s - W_i)}{W_i} \times 100\% \tag{2.1}$$

Where, W_s and W_i are weight of the hydrogel after swelling and initial weight of the hydrogel. For the weightloss and shrinking ratio calculations, the hydrogel is left open to the air for standardised duration, during which the water content from the hydrogel is evapourated or leaves the polymer. This is called as a dehydrated hydrogel. This dehydration causes hydrogel sample to loose volume and mass. Dehydrated hydrogel's weight is measured and is noted as W_d, and weightloss and shrinking ratio are calculated through the use of following equations:

$$Weightloss\% = \frac{(W_d}{W_i} \times 100\% \tag{2.2}$$

$$Shrinking\% = \frac{(W_d - W_i)}{W_i} \times 100\% \tag{2.3}$$

Where W_d is the dehydrated hydrogel's weight and W_i is the initial weight of the hydrogel, measured before dehydration.

Mechanical properties

The fundamental mechanical testing methods and equipment utilized for assessing polymeric materials are similarly applied to characterize the mechanical properties of hydrogels [45]. Like many polymers, hydrogels display time-dependent mechanical behavior due to the inherent viscoelasticity of the polymer network, coupled with an additional time-dependent deformation mechanism caused by fluid flow. Consequently, time considerations play a significant role in planning and conducting mechanical experiments on hydrogels, which can be analyzed in either the time or frequency domain [45]. Hydrogels

require specific mechanical properties tailored to their intended applications, which can be evaluated through various testing techniques and among the most common testing techniques are tension, compression (both unconfined and confined), local indentation using a probe, and frequency-based tests such as shear rheometry or dynamic mechanical analysis [45, 46]. Also by adjusting the extent of cross-linking, one can achieve the desired mechanical properties of the hydrogel. Increasing the degree of cross-linking can produce a stronger hydrogel. However, as the degree of cross-linking rises, the percent elongation of the hydrogels decreases, leading to a more brittle structure. Thus, there exists an optimal degree of cross-linking to create a hydrogel that is moderately robust yet elastic [45, 47].

The elastic properties of hydrogels are achieved through the manipulation of parameters such as Young's modulus [48], tensile strength [49], failure strain [50], and compressive strength [51]. Elasticity refers to a material's ability to deform instantly under mechanical loading. Young's modulus, or tensile modulus, quantifies the resistance of an elastic material to stress and is defined as the ratio of tensile stress to strain, with tensile stress measured as force per unit area [48, 52]. Young's modulus can also assess the intrinsic elasticity of viscoelastic biomaterials [53]. Tensile strength indicates the stress at the breaking point during elongation of the hydrogel, while compressive strength denotes the ability to withstand loading-induced size reduction [54]. Stiffness describes the resistance to deformation under mechanical loading, often identified as the slope of the linear portion of the stress–strain curve for hydrogels [55]. It's important to distinguish strength from stiffness, as strength reflects a material's resistance to fracture or failure due to excessive deformation [56].

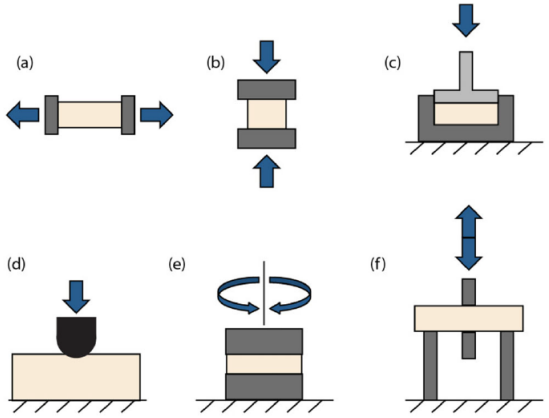

Figure 2.19: Schematic illustration of a) Tensile test, b) Unconfined compression test c) Confined compression test, d) Indentation test, e) Shear rheometry, f) dynamic mechanical analysis [46].

The Universal Test-frame is the primary tool utilized for mechanical characterization of materials, offering versatility across a broad spectrum of experimental tests. While most frames operate along a single axis (uniaxial), there has been a rise in the use of biaxial instruments in recent years [46]. The mechanisms for motion actuation vary, with common options including servohydraulic systems and electromechanical systems, while systems driven by speaker coils are less common. These systems can accommodate both tension and compression testing, with different hardware configurations for sample contact. Effective execution of tensile tests relies heavily on secure sample gripping, which can be challenging, especially for compliant and hydrated specimens like hydrogels. Strategies to address this challenge may involve the use of cardboard tabs, double-sided tape, or adhesive to enhance grip on the hydrogels [46]. For compressive testing, samples can be either unconfined, compressed between two non-porous platens, or confined within a container and compressed against a single porous platen. The latter method is particularly relevant for multiphase materials, as it allows for fluid motion out of the sample through the porous platen, a concept further explored in the section on 'Poroelasticity'. Universal Test-frames vary in size, ranging from large-scale machines used in civil engineering testing to small, modern machines optimized for soft biological materials or biomedical components, such as hydrogels. Typical load cells for such testing typically have a maximum load capacity of 5 or 10 N [46].

Another technique for assessing the mechanical properties of hydrogels is indentation testing Figure 2.19(d). In this method, a probe with a known geometry is used to indent the hydrogel at a specific point

to a predetermined depth, and then the force required to create the indentation is measured [46]. The data obtained from this test typically results in a force-displacement curve, which is commonly used to determine the elastic modulus of the material [57]. The popularity of the indentation method stems from its ability to evaluate mechanical strength at various points on a material, eliminating the need to prepare grips for hydrated materials as required in tensile and compression tests [58].

Rheology techniques offer valuable insights into the gelation and shear thinning behavior of hydrogels. In oscillatory rheometry, stress responses are measured when a hydrogel sample undergoes sinusoidal shear deformation at a specified frequency. This deformation is typically induced between two parallel plates, a cone and plate setup, or coaxial cylinders [59, 60]. The viscoelastic behavior at a given frequency is characterized by the storage modulus, $G_0(x)$, representing elasticity, and the loss modulus, $G_00(x)$, representing energy dissipation contributing to the stress response (G⁄), where $G(x) = G_0(x) + iG_00(x)$. If the hydrogel behaves as an ideal elastic solid, stress remains precisely in phase with the applied sinusoidal strain deformation, and the stress is directly proportional to the strain, defining the shear modulus. Conversely, if the hydrogel behaves as a purely viscous material, stress is proportional to the rate of strain deformation, defining viscosity [61].

Viscoelastic hydrogels exhibit both elastic and viscous characteristics during deformation. Similar to other polymers, hydrogels can transition between solid and liquid states depending on the time scale or frequency of mechanical loading. Initially, a polymer sample behaves as a solid and elastic material until exposed to stress for a specific duration or subjected to frequency-dependent loading. However, after prolonged stress exposure, a hydrogel may behave like a liquid or viscous material. While dynamic mechanical analysis primarily analyzes polymers in their solid state, rheology techniques are suitable for studying the viscoelastic properties of both solid and liquid states of hydrogels. Consequently, rheometers are instrumental in characterizing the gelation process [62]. Microrheology techniques have emerged to measure the viscoelastic behavior of hydrogels throughout their thickness. This method involves embedding micro-scale probe particles within the hydrogel and subjecting them to low-frequency stress or strain stimulation [63].

Up untill this section, basics and background of hydrogels, their preparation methods, and testing of their mechanical properties and behavior characterization have been covered. The next section explores PNIPAM Hydrogel, a thermoresponsive, biocompatible hydrogel. It is one of the most studied and applied thermoresponsive hydrogel, and this project's choice to manufacture and test it's characteristics and see how it can be applied in the field of soft robotics.

2.4. PNIPAM hydrogel

Currently, there's a wide spectrum of stimuli-responsive polymeric systems under development, capable of detecting external cues and executing intelligent functions [64]. These systems primarily encompass polymeric solids, gels, solutions, surfaces, and interfaces. Among these, polymeric hydrogels are particularly noteworthy, representing a category of biomimetic functional materials composed of crosslinked hydrophilic networks with a high water content [65]. Unlike conventional solids, polymeric hydrogels exhibit distinct mechanical properties and responses to external stimuli due to their composite nature of solid and liquid components. Notably, these hydrogels can undergo significant volume changes through water exudation or absorption, leading to alterations in properties like microstructure, permeability, and mechanical strength [66].

Stimuli-responsive polymer-based hydrogels, such as those utilizing thermo-responsive poly(N-isopropylacrylamide)(PNIPAM), pH-responsive poly(acrylic acid) (PAAc), and ion-responsive polyelectrolytes, constitute a significant category of advanced smart materials [64]. These hydrogels have found diverse applications in fields such as drug delivery, self-healing, shape memory, sensors, soft robotics, tissue engineering, artificial muscles, and more. Figure 2.20 below, gives the applications of PNIPAM hydrogels.

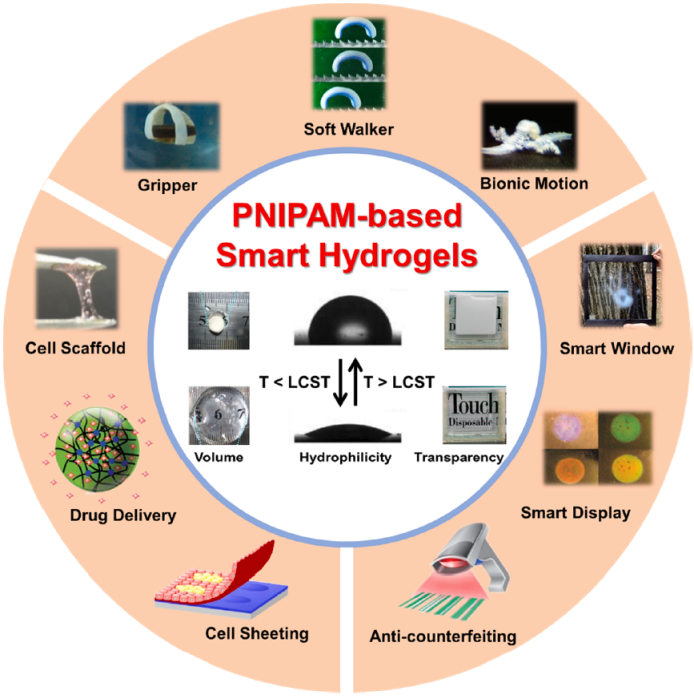

Figure 2.20: Application of PNIPAM hydrogels in different fields [66].

PNIPAM, a thermo-responsive polymer, gained prominence following Scarpa et al.'s 1967 report on its thermal phase transition behavior [67]. Since its synthesis in 1956, PNIPAM has become a major player in the realm of thermo-responsive polymer-based smart materials [68, 69]. The phase diagram of aqueous PNIPAM solutions was systematically investigated in 1968, a study that remains widely referenced [70]. In 1986, Pelton et al. pioneered the preparation of thermo-responsive microgels based on PNIPAM and with the evolution of biomedical applications. PNIPAM hydrogels have been harnessed for versatile purposes in selectively removing and delivering species, leveraging thermo-controlled dimensions to modulate substance movement in various mediums [71].

PNIPAM is characterized by its amide and isopropyl moieties, which exhibit a lower critical solution temperature (LCST, 32°C) in aqueous media. Smart hydrogels based on PNIPAM, synthesized by crosslinking PNIPAM or its derivatives, undergo a significant and reversible volume phase transition through swelling/shrinking near the LCST [72–74]. This process entails changes in several properties, including hydrophilicity [75], transparency [76, 77], and apparent electrostatic permittivity [78], alongside the size change during the volume phase transition. These captivating properties and functionalities of PNIPAM-based smart hydrogels have sparked considerable research interest. For instance, by co-polymerizing PNIPAM with more hydrophilic or hydrophobic monomers, both the volume phase transition temperature and the extent of swelling/shrinking can be readily controlled [79, 80]. It's noteworthy that the property alterations of these smart hydrogels can be induced through various means, including direct heating, indirect heating (such as via photothermal effects [81], Joule heating [82], and hysteresis effects [83]), photoionization [84], or photoisomerization [85], thereby enabling sensitivity to temperature, light, electrical fields, and magnetic fields. Crucially, the exceptional properties of PNIPAM-based smart hydrogels enable diverse smart functionalities, akin to those observed in cells and certain biological systems. For instance, the volume change capability allows these hydrogels to autonomously regulate or gate systems by modulating material transportation—such as blocking channels through swelling or opening them through shrinking [86]. This capability holds significant promise in fields like smart valves, water purification, drug delivery, and beyond.

PNIPAM hydrogel synthesis and mechanical properties

PNIPAM hydrogels synthesized via the free radical redox polymerization technique,
where N-isopropylacrylamide is the monomer, N,N-methylene-bis-acrylamide (MBA/BIS) is the crosslinker,

Ammoium persulfate/Sodium persulfate and Hydrogen peroxide/Tetramethylethylenediamine are used as the redox system initators (or Accelerators) [65, 66, 86]. In essence, as described in the hydrogel synthesis chapter, Monomer and crosslinker are first mixed, then initiators are added in one after another. Various factors come into play in determining their mechanical properties, such as the initial monomer concentration, crosslinker ratio, polymerization and measurement temperature, degree of swelling at the time of measurement, and the testing methodology employed [65]. Consequently, making precise comparisons of mechanical parameters proves challenging. Nonetheless, the Table 2.3 presents the diverse mechanical properties of PNIPAM hydrogels from various investigations.

Table 2.3: Mechanical properties of a native PNIPAM hydrogel [65].

Year	Monomer concentration (M)	Crosslinker Ratio	Measurement condition	Value (kPa)
1997	0.87	1.66e-02	At equilibrium, Tensile stress	9.8
1997	0.87	1.66e-02	At collapsed state, Tensile stress @ 65 degrees celsius	180
2002	0.71	1.18e-02	As prepared, Compressive stress, strain - 15%	6.12
2012	0.71	1.18e-02	At swollen state, Tensile stress , strain = 15%	5.63
2013	1.07	2.97e-02	At swollen state, Compressive stress using DMA, Strain = 10%	81
2013	0.21	1.20e-02	At swollen state, Compressive stress, strain = 15%	3.8
2013	0.21	1.20e-02	At swollen state, Temsile stress, strain = 15%	7.3
2013	1.0	1.00e-02	At swollen state, Scanning Force Mmicroscopy	6.6
2013	1.0	1.00e-02	At collapsed state, Scanning Force Microscopy, temp = 40 °C	13.9

In the Table 2.3, crosslinker ratio means moles of crosslinker/mol of monomers, temperature while measuring is the room temperature, stated otherwise. Lastly, DMA stands for Dynamic mechanical analysis.

The Young's modulus E_0 of PNIPAM hydrogel was initially reported in 1997 by Takigawa et al [87]. Their tensile test revealed a linear stress-strain curve for both swollen and collapsed gels, with E_0 approximately one hundred times higher in the collapsed state. The fracture strain was noted as 35% in the swollen state and 75% in the collapsed state. However, a later comprehensive study conducted by Puleo et al. [88] in 2013 revealed a non-linear stress-strain curve, leading them to propose the neo-Hookean model to explain it. Notably, they observed a fracture strain of 79% under compression compared to only 30% under tension, attributing the difference to variations in water behavior within the hydrogel matrix during the two types of tests. The Young's modulus calculated from rheological experiments using the complex modulus assumptions yielded a value of 1.2 kPa, significantly lower than those obtained from tensile tests, highlighting the significant impact of the measurement technique on the mechanical parameter's magnitude. Additionally, the polymerization temperature influences mechanical strength; lower temperatures result in slower kinetics and the formation of the material via fewer polymer chains of higher molecular weight, thus leading to increased strength. Across all studies listed in Table 2.3, polymerization generally occurred at room temperature (20–25°C), except for the study by Gundogan et al., who conducted the process at 5°C. Fei et al [89, 90]. reported unusually high compressive strength (81 kPa) in two studies, potentially attributed to their use of the highest concentration of crosslinker among all the studies.

The thermoresponsive deformations of PNIPAM hydrogels offer a mechanism for controlling their bending and unbending, enabling them to grasp objects and function as soft robots [65]. Unlike conventional rigid robots made of materials like metals and ceramics and actuated by electrical, hydraulic, or pneumatic mechanisms, soft robots have distinct advantages. They can operate easily in aqueous environments and emulate biological functions.

Poly(N-isopropylacrylamide) (PNIPAM) hydrogels possess unique properties that make them appealing for various applications. However, a key drawback is their inherent rigidity, which can limit their effectiveness in certain uses. To address this limitation, researchers have explored combining NiPAAm with other monomers to create Double-network and Interpenetrating network hydrogels, which offer enhanced flexibility and performance [65, 66].

Despite their promise, PNIPAM hydrogels face challenges, particularly in balancing flexibility with mechanical strength. The review concludes that while significant progress has been made in understanding and utilizing hydrogels in soft robotics, further research is needed to optimize these materials for large scale applications, ensuring they can meet the mechanical demands of various environments

while maintaining their unique responsive characteristics.

2.5. Conclusion

Chapter 2 provided a comprehensive review of smart materials with a focus on hydrogels and their applications in soft robotics. The chapter began by discussing the fundamental principles of smart materials and their ability to respond to external stimuli, making them ideal for innovative applications in fields like biomedical engineering and soft robotics. It then delved into the specifics of hydrogels, particularly thermoresponsive hydrogels like Poly(N-isopropylacrylamide) (PNIPAM), highlighting how their mechanical and responsive properties can be tailored through controlled synthesis processes.

The review also delves into the various classifications of hydrogels based on their source, polymeric composition, configuration, and response to external stimuli. It also explored various synthesis and characterization techniques, including indentation tests, rheometry, and swelling-deswelling tests, which are crucial for assessing the material's mechanical properties and thermoresponsive behavior.

In conclusion, Chapter 2 established the critical factors that influence hydrogel performance and laid the groundwork for the experimental work to follow. It underscored the potential of hydrogels in soft robotics and the need for ongoing research to optimize their properties for specific applications.

3

Methodology

3.1. Synthesis of hydrogels

This section details the methodology for synthesizing poly(N-isopropylacrylamide) (PNIPAM) hydrogels using free radical polymerization. We will discuss the role of different components involved and compare the use of hydrogen peroxide (H_2O_2) and N,N,N',N'-Tetramethylethylenediamine (TEMED) as reaction accelerators.

3.1.1. Free radical polymerization

Free radical polymerization is a widely used technique for polymer synthesis that involves three key steps: initiation, propagation, termination [5, 22]. The process begins when initiator molecules decompose to generate reactive free radicals. These free radicals then react with monomer molecules, such as N-isopropylacrylamide (NIPAM) in this study, forming new radicals that further react with additional monomers to extend the polymer chains. This chain reaction continues until the process is halted by either radical coupling or disproportionation [22]. In radical coupling, two free radicals combine, effectively neutralizing each other and stopping the polymerization. In disproportionation, a hydrogen atom is transferred from one radical to another, resulting in the formation of a stable molecule and an unsaturated molecule, thereby terminating the reaction. Throughout this process, crosslinkers introduce links between the polymer chains, creating a three-dimensional network that ultimately forms the hydrogel.

3.1.2. Monomers, Crosslinkers, Initiators, and Accelerators

- **Monomer:** N-isopropylacrylamide (NIPAM) is the fundamental monomer used in this hydrogel synthesis. The concentration of NIPAM plays a crucial role in determining the polymer chain density within the hydrogel network. This directly influences the hydrogel's mechanical properties, such as stiffness and swellability. For instance, higher concentrations of NIPAM result in a denser polymer network, which can lead to a positive impact on the stiffness and swelling ability.
- **Crosslinker:** Crosslinkers like N,N'-methylenebisacrylamide (BIS/MBA) or ethyleneglycol dimethacrylate (EGDMA) are used to link individual polymer chains, forming a three dimensional gel network. The amount of crosslinker added significantly affects the hydrogel's mechanical behavior. A higher crosslinker concentration generally leads to increased stiffness and reduced swelling capacity, as the dense network limits the polymer chains' ability to move and expand in the presence of water.
- **Initiator:** Initiators such as ammonium persulfate (APS) or potassium persulfate (KPS) are crucial for starting the polymerization reaction. These compounds decompose to produce free radicals, which initiate the polymerization by reacting with the monomers.
- **Accelerator:** Accelerators, such as TEMED (N,N,N',N'-Tetramethylethylenediamine) or hydrogen peroxide (H_2O_2), enhance the rate of free radical generation by the initiator, leading to faster polymerization.

The materials used for synthesis of poly(N-isopropylacrylamide) (PNIPAM) hydrogels are given in Table 3.1:

Table 3.1: Materials used for synthesis of PNIPAM hydrogel.

Type	Chemical
Monomer	N-isopropylacrylamide (NIPAM)
Cross-linker	N,N'-methylenebisacrylamide (BIS or MBA)
Initiator	Ammonium persulfate (APS)
Accelerator	N,N,N′,N′-Tetramethylethylenediamine (TEMED) & Hydrogen peroxide (H_2O_2)

3.1.3. Synthesis procedure

The synthesis of PNIPAM hydrogels follows a structured free radical polymerization process. The procedure begins by dissolving the N-isopropylacrylamide (NIPAM) monomer, crosslinker (such as N,N'-methylenebisacrylamide or BIS), and initiator (ammonium persulfate, APS) in deionized water. The concentrations of these components are crucial, as they directly influence the mechanical properties of the resulting hydrogel. To ensure homogeneity, the solution is stirred thoroughly. To eliminate oxygen, which can inhibit polymerization, the solution is often degassed by bubbling nitrogen gas through it. Following degassing, Accelerator (TEMED or H_2O_2) is added to the solution which helps in decomposition of the initiator into free radicals and facilitates gelation. The accelerator is added once the solution is transferred into the mold of choice. The polymerization can be further controlled, where cooling the solution will slowdown polymerization and heating the solution will hasten the polymerization. After gelation, the hydrogels are often purified through dialysis to remove any unreacted monomers or other impurities, ensuring the hydrogel meets the desired specifications.

The Figure 3.1 is a stepwise flowchart of the synthesis procedure.

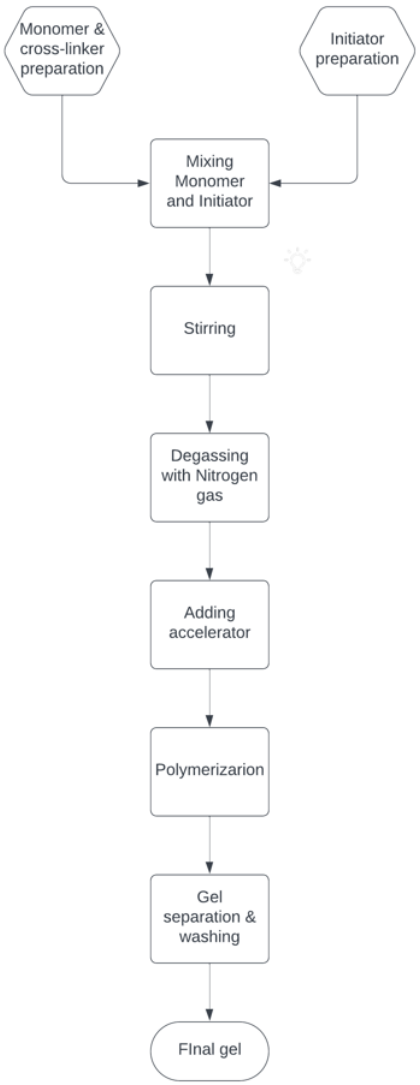

Figure 3.1: PNIPAM hydrogel preparation procedure.

However, achieving consistent and desired hydrogel properties can be challenging. Because synthesizing PNIPAM hydrogels can be like conducting a symphony. Just like a flawless performance requires all the instruments to play in harmony, several factors need to work together for successful gelation [5, 65, 86]. Here are some common reasons why some hydrogel formations might be out of tune:

- **The Wrong Chemistry:** Hydrogels are sensitive to the exact recipe. Double-check the ratios of NIPAM monomer, crosslinker, and initiator. Even minor deviations can disrupt the delicate balance needed for gelation.
- **Silent Conductors:** Crosslinking agents are crucial for forming the hydrogel network. Using the wrong type or an insufficient amount can lead to a weak or incomplete gel.
- **Varying tempo:** Temperature and pH can significantly impact gelation. Ensure the reaction conditions are within the optimal range for PNIPAM hydrogels (typically neutral pH and moderate temperature, around 60-70°C (If using H_2O_2)).
- **Unruly Audience:** Contaminants in the reagents or equipment can act like a disruptive audience, hindering the orderly assembly of the hydrogel network.
- **Rushing the Crescendo:** Gelation can take time. Ensure the reaction proceeds for a sufficient duration to allow for complete network formation.

- **Cacophony of Components:** Uneven mixing can lead to patchy gelation. Just like musicians need to rehearse together, thorough stirring and mixing of the components are essential.
- **Wrong Solvent, Wrong Song:** The choice of solvent can significantly affect gelation. Ensure to use a solvent compatible with your chosen hydrogel components.
- **Discordant Bubbles:** Air bubbles can act like discordant notes, disrupting the gelation process. Degassing the solution can help eliminate them.
- **Dehydrated Dancers:** Polymer chains need water to interact and form the gel network. Ensure the reaction mixture provides sufficient hydration.
- **Molecular Weight Matters:** The molecular weight of ther polymer can influence gel formation. Experiment with different molecular weight NIPAM to see if it affects the results.

3.1.4. TEMED vs. Hydrogen peroxide:

Following the exploration of the synthesis procedure and potential influencing factors, the selection of an appropriate accelerator emerges as a critical step in PNIPAM hydrogel synthesis. Both N,N,N',N'-Tetramethylethylenediamine (TEMED) and hydrogen peroxide (H_2O_2) act as accelerators in the free radical polymerization process for synthesizing PNIPAM hydrogels. However, they differ significantly in their influence on the reaction rate and the resulting hydrogel properties.

TEMED:

- **Mechanism:** TEMED acts as a strong nucleophile, readily donating electrons to the initiator (APS or KPS) molecules. This significantly accelerates the decomposition of the initiator, leading to a rapid generation of free radicals.
- **Impact on Reaction:** The rapid generation of free radicals translates to a faster polymerization process. This can be beneficial for situations where time is a constraint. However, the fast initiation can also lead to less control over the polymerization.
- **Resulting Hydrogel:** The faster reaction with TEMED might result in a broader distribution of polymer chain lengths within the hydrogel network. This can potentially affect the hydrogel's mechanical properties, such as stiffness and swelling behavior.

Hydrogen peroxide:

- **Mechanism:** H_2O_2 decomposes slowly at room temperature, generating free radicals at a more moderate rate compared to TEMED. This slower initiation allows for better control over the polymerization process.
- **Impact on Reaction:** The slower decomposition of H_2O_2 leads to a more gradual initiation of free radicals and a slower overall polymerization rate. While this might extend the reaction time, it also allows for better control over the polymer chain growth and distribution.
- **Resulting Hydrogel:** The more controlled polymerization with H_2O_2 can lead to a narrower distribution of polymer chain lengths within the hydrogel network. This can potentially result in hydrogels with more uniform properties and potentially improved mechanical characteristics.

The choice between TEMED and H_2O_2 depends on the type of application, specific needs and desired hydrogel properties:

- **For speed:** It is better to use TEMED if reaction time is a critical factor, even if it comes at the expense of some control over the polymer chain distribution.
- **For control:** It is better to use H_2O_2 if precise control over the polymerization process and a narrower chain length distribution are crucial for achieving the desired hydrogel properties.

In some cases, researchers might explore alternative accelerator systems or optimize the concentration of these accelerators to achieve a balance between reaction speed and control over the polymerization process.

3.2. Characterization of hydrogel

Following the successful synthesis of PNIPAM hydrogels, a crucial step lies in deciphering their physicochemical & mechanical properties thus unlocking their potential applications. This is achieved through meticulous characterization techniques that provide a comprehensive understanding of the hydrogel's behavior and performance. Here, we will delve into three prominent methods that offer valuable insights into the world of PNIPAM hydrogels:

3.2.1. Rheology: Delving into Viscoelasticity

Rheology remains a powerful technique that unveils the intricate interplay between flow and deformation behavior in materials subjected to applied stress or strain [91, 92]. It essentially quantifies how a material moves and reshapes itself when pressured or stretched. For PNIPAM hydrogels, rheology offers invaluable insights into their viscoelastic properties, a crucial aspect for many biomedical applications. Key rheological parameters include:

- Viscosity: This parameter reflects a material's resistance to flow. In the context of hydrogels, viscosity dictates their injectability or pumpability, a critical factor for drug delivery applications.
- Elasticity: This signifies a material's ability to store and recover energy upon deformation. For hydrogels designed to maintain their shape, a high degree of elasticity is essential.
- Storage Modulus (G'): This parameter serves as a quantitative measure of elasticity. A higher storage modulus indicates a stiffer and more solid-like hydrogel.
- Loss Modulus (G"): This parameter reflects the "fluidity" of the hydrogel. A higher loss modulus suggests a more fluid-like behavior with greater energy dissipation.

Rheometers are advanced instruments used to measure the rheological properties of materials like hydrogels. These instruments apply various deformation modes, such as oscillatory shear stress or strain, to assess the hydrogel's behavior across different frequencies or stress/strain levels. By analyzing the rheological data, one can gain deep insights into the gel's strength, network structure, and potential applications. For instance, a hydrogel with a high storage modulus and a low loss modulus is ideal for load-bearing applications, such as cartilage replacements [45, 86]. In contrast, a hydrogel with a lower storage modulus and higher loss modulus may be better suited for controlled drug release, where a more gradual release profile is desired.

Strain sweeps, which involve gradually increasing the applied strain, provide information about the hydrogel's rigidity or stiffness and help identify the Linear Viscoelastic Region (LVR) [91, 93, 94]. The LVR is the range in which the storage modulus (G') and loss modulus (G") remain independent of the applied strain. Beyond this threshold, the gel exhibits nonlinear behavior. Essentially, the LVR represents the linear portion of the G' and G" vs. strain curves. After conducting strain sweeps, a specific strain value from the LVR is selected for use in frequency sweeps. Frequency refers to the rate at which oscillatory stress or strain is applied, and during a frequency sweep, the gel is exposed to a range of frequencies to measure its response at each one.

The rheometeric tests, including strain sweeps and frequency sweeps, conducted in studies such as [91–96], have inspired the testing methods employed in this thesis.

3.2.2. Indentation Testing: Probing Mechanical Properties

While rheology provides a nuanced view of the hydrogel's response to various stimuli, indentation testing offers a more direct approach for assessing mechanical properties [93, 97]. Imagine gently pressing a fingertip into the hydrogel. Indentation testing replicates this concept using a specialized tip, typically a flat-ended cylinder or a sharp cone [98]. By measuring the force required to penetrate the hydrogel and the extent to which it recovers, valuable information can be gleaned about:

- Stiffness: Analogous to the slope of a hill, the steeper the force-displacement curve, the stiffer the hydrogel.
- Yield Strength: This parameter represents the maximum force the hydrogel can withstand before it starts to deform permanently.

- Elastic Recovery: This parameter quantifies how well the hydrogel ”recovers” its original shape after the pressure is released. A good recovery indicates a more elastic material.

Indentation testing is a relatively rapid and straightforward technique compared to rheology. However, it primarily focuses on the surface properties and might not capture the complex viscoelastic behavior deep within the hydrogel as effectively as rheometry. The indentation tests performed in these various studies such as [93, 97–102] have inspired the testing method employed in this thesis.

3.2.3. Swelling and Shrinking Ratio Measurements: A Simple Yet Powerful Technique

Moving beyond the realm of complex instrumentation, swelling and shrinking ratio measurements offer a simple yet powerful method for characterizing PNIPAM hydrogels [93, 94, 96]. This technique quantifies the hydrogel's ability to absorb water and change its weight and volume in response to environmental cues. This response is particularly interesting for PNIPAM hydrogels due to their thermoresponsive nature.

Here's how it works:

- The hydrogel is weighed in its Equilibrium state, i.e. the state it is in after synthesis and washing.
- The hydrogel is then immersed in a specific solvent or buffer solution at a controlled temperature, typically below the lower critical solution temperature (LCST) of PNIPAM (around 32°C). At this temperature, the hydrogel readily absorbs water and swells.
- Conversely, above the LCST (32°C) the hydrogel releases water and shrinks.
- The swelling percentage is calculated by the difference in swollen weight and equilibirum weight and that value divided by the swollen weight.
- The De-swelling ratio is calculated by dividing the difference between swollen weight and dried weight by the dried weight.

The experiment can be repeated at different temperatures to observe the hydrogel's response across a temperature range . PNIPAM hydrogels exhibit a significant decrease in weight and volume as the temperature rises above the LCST. This phenomenon is due to the collapse of the polymer chains within the hydrogel network as they become hydrophobic at higher temperatures [93, 98, 99]. Understanding the swelling and shrinking behavior of PNIPAM hydrogels is crucial for various applications. For example, hydrogels designed for controlled drug delivery can be tailored to release their payload (drug) at specific temperatures based on their swelling and deswelling behavior.

Beyond drug delivery, PNIPAM hydrogels with tailored swelling behavior can find applications in various fields. For example, they can be used as temperature-sensitive actuators for a soft robotic gripper, where the swelling or shrinking ability causes forces and those forces can be used for actuation of the soft robotic finger, or provide a stiffness enhancement layer based on their stiffness in the swollen or deswollen states. By understanding and optimizing the swelling and shrinking properties of PNIPAM hydrogels, researchers can unlock a vast array of possibilities for innovative materials with the potential to revolutionize numerous applications. As mentioned previously in the synthesis section, the amount of monomer and crosslinker added have an effect on the swelling ability of the hydrogels. Increasing monomer content should have a positive impact on the swelling ability as it increases the length and number of polymer chains resulting in more space for water to take up. Conversely for increasing amount of crosslinker, the number of crosslinks (bridges) built between the polymer chains increases, thus resulting in lesser space for water to enter the network [65, 101, 102].

3.3. Unlocking Diverse Shapes: A Method for Fabricating Shaped Hydrogels with Open Molds

Crafting hydrogels with specific shapes and sizes presents a unique challenge: achieving well-defined structures while minimizing the disruptive influence of dissolved oxygen, particularly when using open molds. This research tackles this very hurdle, proposing a method to achieve diverse hydrogel shapes and sizes while mitigating oxygen's negative effects.

3.3.1. The Oxygen Obstacle in Free Radical Polymerization

As established, PNIPAM hydrogel formation relies on free radical polymerization. Here's the catch: oxygen acts as a villain, snatching free radicals and prematurely halting the polymerization chain. This results in incompletely formed hydrogels with compromised mechanical properties.

3.3.2. The Open Mold Quandary

While closed molds offer the advantage of reduced oxygen exposure, they often become battlegrounds during demolding due to sticking of the gels. This research proposes a strategic maneuver: utilizing open molds made of silicone (For easy demolding) within a custom-built nitrogen enclosure. This approach aims to achieve shaped hydrogels while mitigating the negative impacts of oxygen and retaining the ease of demolding associated with open molds.

3.3.3. The Solution: Deoxygenation and Open Molds in a Nitrogen Sanctuary

This research employs a two-pronged strategy:

- **Stripping Away Oxygen:** Before transferring the PNIPAM solution to the open molds, it will undergo a deoxygenation process using nitrogen gas purging. This significantly reduces dissolved oxygen, paving the way for a more complete polymerization process.
- **Open Molds, Nitrogen Embrace:** The open silicone molds will be placed within a custom-built enclosure specifically purged with nitrogen gas. This controlled environment minimizes oxygen exposure throughout the polymerization process, mimicking the benefits of closed molds while allowing for the ease of demolding associated with open molds. The enclosure was constructed from polymethyl methacrylate (PMMA) plastic sheets for clear visibility.

3.3.4. The Method: A Step-by-Step Guide

- **Deoxygenating the Solution:** The PNIPAM solution will be prepared using standard synthesis procedure. Prior to transferring the solution to the molds, nitrogen gas purging will be employed to remove dissolved oxygen.
- **Polymerization under Nitrogen's Protection:** The open silicone molds will be placed inside the nitrogen enclosure. The deoxygenated solution will then be poured into the molds and the accelerator is added.
- **Curing in a Nitrogen Atmosphere:** After pouring, the enclosure will be filled with nitrogen gas to maintain a low-oxygen environment for the duration of the polymerization process. After a few hours, the cured/polymerized hydrogels can be carefully removed from the open molds due to the non-stick properties of the silicone.

3.3.5. The Beauty of This Approach

- **Preserves Open Mold Advantages:** This method allows for the continued use of open molds, simplifying the demolding process. Also helping in creating as many shapes and sizes as possible.
- **Curbing Oxygen's Influence:** The nitrogen enclosure significantly reduces oxygen exposure, comparable to using closed molds.
- **Adaptable to Diverse Molds:** This approach can be adapted to various open mold geometries, offering greater flexibility in shaping and sizing of the hydrogels.

This method presents a valuable approach for fabricating PNIPAM hydrogels with diverse shapes using open molds while minimizing the detrimental effects of oxygen on the polymerization process. It offers a well-balanced solution, combining ease of demolding with oxygen control, and thus expanding the possibilities for shaping hydrogels. Lastly, following the fabrication of shapes of hydrogels, swelling and de-swelling experiments will also be conducted to evaluate the change in their respective volumes.

3.3.6. Simulation analysis

In addition to the experimental procedures, simulations conducted by a previous researcher [11] were utilized to model the swelling behavior of thermoresponsive hydrogels, specifically PNIPAM (Poly(N-isopropylacrylamide)) hydrogels. These simulations aimed to predict the final dimensions of hydrogel

shapes after undergoing temperature-induced swelling and shrinking processes.

3.3.7. Simulation Procedure

The simulation of the swelling behavior of thermoresponsive hydrogels was conducted using the Finite Element Method (FEM) implemented through the ABAQUS software package. The procedure aimed to replicate the conditions under which the hydrogels were experimentally tested, focusing on their response to temperature changes.

Model Development

A three-dimensional geometric model of the hydrogel shapes (sqaure slabs, rectangular slabs, and circular disks) was created within the FEM software. To better capture the unique swelling behavior of PNIPAM hydrogels, a UHYPER (User-defined Hyperelastic) material model was implemented. This allowed for the incorporation of a more detailed free energy function that accounts for polymer network stretching and polymer-fluid mixing interactions [11].

The UHYPER model utilized in the simulations incorporated the Flory-Huggins interaction parameter (χ), which quantifies the interaction between the polymer and the solvent. The model was designed to be temperature-dependent, allowing it to accurately reflect the thermoresponsive nature of the hydrogels. By using UHYPER, the simulations could account for the complex material behavior more accurately than standard material models [11].

Meshing and Boundary Conditions

The hydrogel models were discretized using a three-dimensional mesh, with higher mesh density in areas of expected high deformation to ensure accurate results. Boundary conditions were applied to replicate the physical constraints, that the hydrogels would encounter during experiments. This included fixed constraints on specific faces to mimic attachment points and interfaces with other materials [11].

To simulate the swelling process, a temperature change was applied across the model, driving the hydrogel to swell or shrink depending on the thermal conditions. The swelling was modeled by adjusting the free energy function within the UHYPER model, which allowed the simulation to capture the hydrogel's response to temperature variations accurately [11].

Assumptions and Simplifications

Several assumptions were made to simplify the simulation process while ensuring its computational feasibility. The hydrogel was assumed to be in a homogeneous free-swelling state, with uniform swelling in all directions. A fixed swelling ratio was used to represent the equilibrium state, where the hydrogel swells uniformly without internal gradients.

Simulation Execution and Data Analysis

The simulation was executed under controlled temperature conditions, simulating the swelling and deswelling cycles the hydrogels underwent experimentally. Results such as the final dimensions were extracted and compared with experimental data. The use of the UHYPER material model provided a more detailed understanding of the material's behavior, though some discrepancies between the simulation and experimental results maybe observed.

3.4. Conclusion

Chapter 3 detailed the methodology and experimental procedures employed to synthesize and characterize PNIPAM hydrogels. The chapter covered the use of free radical polymerization to create PNIPAM hydrogels with varying monomer and crosslinker concentrations, aimed at exploring their effects on the mechanical and thermoresponsive properties of the material. The synthesis procedure was carefully designed with the aim to have control over the factors like stiffness, elasticity, and swelling capacity.

The chapter also outlined the characterization techniques, including rheometry, indentation tests, and swelling-deswelling experiments, which will be used to systematically evaluate the hydrogels' mechanical properties and swelling behavior. Additionally, simulations using Finite Element Method (FEM) were conducted to model the swelling behavior of the hydrogels, offering a computational perspective that might complement the experimental work.

Overall, Chapter 3 provides a comprehensive account of the methodologies used in this research, setting the stage for the subsequent analysis and discussion of results. The approaches described here were designed to ensure a thorough understanding of how synthesis parameters affect the behavior of PNIPAM hydrogels, with both experimental and simulation methods aiming to provide insights into their potential applications in soft robotics.

4

Design of Experiments

4.1. Materials and Equipment

N-isopropylacrylamide (NiPAAm), N,N′-Methylenebisacrylamide (MBA), ammonium persulfate (APS), N,N,N′,N′-tetramethylethylenediamine (TEMED), and Hydrogen peroxide (H_2O_2) were purchased from Sigma-Aldrich. the following equipment is used for both the synthesis of the hydrogels and also the characterisation/mechanical testing.

List of equipment:

- Zwick Z010 Universal testing machine.
- Zwick 500N load cell.
- TA Instruments Discovery HR-3 rheometer.
- Mettler toledo excellence XSR Analytical balance.
- IKA RET basic hotplate with magnetic stirrer.
- Elix essential 5 water purification system.
- Emag Emmi-60HC ultrasonic cleaning device.
- Prusa MK III 3d printer.
- Eco-flex 30 silicone.
- Nitrogen chamber.

4.2. Aim of the experiments

This study investigates the influence of the amount of monomer & crosslinker on the stiffness and swelling ability of poly(N-isopropylacrylamide) (PNIPAM) hydrogels. PNIPAM exhibits thermoresponsive behavior, meaning their physical properties change in response to temperature variations. This behavior is primarily due to the polymer's unique interaction with water molecules, which is influenced by temperature. The hypothesis is that the stiffness and swelling ability of the hydrogels are influenced by variations in the amount of monomer and crosslinker (also crosslinking density).

A wide range of monomer and crosslinker masses were used, shown in Table 4.1. This range is intended to showcase the mechanical properties and behavior of the gels at low, medium, and high monomer and crosslinker concentrations. The key factor in this investigation is the amount of crosslinker added to the solution, as it directly influences the crosslinking ratios and also the crosslinking density. Essentially, as the amount of crosslinker increases, the crosslinking density also increases. It is important to note that this study focuses solely on the conceptual understanding of how crosslinker concentration impacts crosslinking density, without performing any estimation or quantification of the crosslinking density.

Table 4.1: Masses of monomer and crosslinker investigated.

Monomer (g) (NiPaam)	0.2g	0.5g	1g	1.5g	2g
Crosslinker (g) (MBA)	0.01g	0.03g	0.05g	0.07g	0.09g

Monomer and crosslinker are not the only components used in the preparation of the hydrogels. The amounts of initiator (APS), accelerator (TEMED), and solvent (water) are also provided below. While the initiator and accelerator can influence the properties and behavior of the gel, this study primarily focuses on the effects of the monomer-to-crosslinker ratio/monomer and crosslinker concentrations. Therefore, the quantities of initiator and accelerator are kept to a minimum and remain consistent across all variations of the monomer and crosslinker concentrations. This is shown in Table 4.2.

Table 4.2: Amounts of initiator, accelerator and solvent used.

Initiator (APS) (g)	0.01g
Accelerator (TEMED)	2-3 drops/ (approximstely) 45 μl
Solvent (water) (ml)	20ml

Lastly, the Table 4.3 showcases the molar ratio of NiPaam to MBA, NiPaam wt% and wt% of MBA wrt NiPaam.

Table 4.3: Monomer and crosslinker concentrations used, with molar ratios, wt% of Nipaam and wt% of MBA wrt NiPAAm.

NiPAAm (g)	MBA (g)	Molar Ratio (NiPAAm/MBA)	wt% NiPAAm	wt% MBA wrt NiPAAm
0.2	0.01	27.18	0.99%	5.00%
0.2	0.03	9.06	0.99%	15.00%
0.2	0.05	5.45	0.98%	25.00%
0.2	0.07	3.89	0.98%	35.00%
0.2	0.09	3.02	0.98%	45.00%
0.5	0.01	67.98	2.43%	2.00%
0.5	0.03	22.66	2.43%	6.00%
0.5	0.05	13.64	2.43%	10.00%
0.5	0.07	9.73	2.42%	14.00%
0.5	0.09	7.57	2.42%	18.00%
1.0	0.01	135.97	4.75%	1.00%
1.0	0.03	45.32	4.74%	3.00%
1.0	0.05	27.28	4.73%	5.00%
1.0	0.07	19.47	4.73%	7.00%
1.0	0.09	15.14	4.72%	9.00%
1.5	0.01	203.95	6.96%	0.67%
1.5	0.03	67.97	6.95%	2.00%
1.5	0.05	40.92	6.94%	3.33%
1.5	0.07	29.21	6.93%	4.67%
1.5	0.09	22.71	6.93%	6.00%
2.0	0.01	271.94	9.07%	0.50%
2.0	0.03	90.63	9.06%	1.50%
2.0	0.05	54.55	9.05%	2.50%
2.0	0.07	38.93	9.04%	3.50%
2.0	0.09	30.27	9.03%	4.50%

The formulae used and one example calculation is described as:

$$\text{Molar Ratio (NIPAAm/MBA)} = \frac{\frac{\text{Mass of NIPAAm (g)}}{\text{Molar Mass of NIPAAm (g/mol)}}}{\frac{\text{Mass of MBA (g)}}{\text{Molar Mass of MBA (g/mol)}}} \tag{4.1}$$

$$\text{wt\% NIPAAm} = \left(\frac{\text{Mass of NIPAAm (g)}}{\text{Mass of NIPAAm (g)} + \text{Mass of MBA (g)}}\right) \times 100 \tag{4.2}$$

$$\text{wt\% MBA wrt NIPAAm} = \left(\frac{\text{Mass of MBA (g)}}{\text{Mass of NIPAAm (g)}}\right) \times 100 \tag{4.3}$$

Example Calculations: For 2g monomer and 0.05g crosslinker contents:

$$\text{Molar Ratio (NIPAAm/MBA)} = \frac{\frac{2.0\,\text{g}}{113.12\,\text{g/mol}}}{\frac{0.05\,\text{g}}{154.17\,\text{g/mol}}} = \frac{0.0177\,\text{mol}}{0.000324\,\text{mol}} = 54.59 \tag{4.4}$$

$$\text{wt\% NIPAAm} = \left(\frac{2.0\,\text{g}}{2.0\,\text{g} + 0.05\,\text{g}}\right) \times 100 = \left(\frac{2.0\,\text{g}}{2.05\,\text{g}}\right) \times 100 = 97.56\% \tag{4.5}$$

$$\text{wt\% MBA wrt NIPAAm} = \left(\frac{0.05\,\text{g}}{2.0\,\text{g}}\right) \times 100 = 2.5\% \tag{4.6}$$

4.3. Syntehsis experiments

With the aim of the study established, a full factorial Design of Experiments (DoE) was conducted to determine the influence of each individual parameter, specifically the monomer and crosslinker, on the properties of the hydrogels. The primary objective of this DoE was to comprehensively understand the behavior of the hydrogels and identify a formulations(s) (monomer and crosslinker concentrations) that achieves favorable stiffness and swelling ability.

To begin with, synthesis experiments were performed to compare the effects of using different accelerators, namely "H_2O_2" and "TEMED," on the hydrogel properties. These initial experiments were crucial for assessing the impact of each accelerator on the yield of the gels, specifically how gelation was influenced by each accelerator. Additionally, the opacity of the gels was investigated as a separate characteristic to determine any variations in transparency resulting from the change in amount of crosslinker in the solution. By examining these differences, the study aimed to refine the synthesis process and ensure the production of hydrogels with consistent and desirable characteristics. This comparative analysis provided valuable insights that informed the subsequent steps of the research and contributed to the overall goal of optimizing the hydrogel formulation.

Hydrogel Synthesis Procedure

1. Weigh Monomer (NiPaam), Crosslinker (MBA) & initiator (APS) and add them into 20ml solvent (DI water).
2. Magnetically Stir Solution for 30 minutes (see Figure 4.1(b)).
3. Immersion in ultrasound cleaner (5 minutes) (see Figure 4.1(a)).
4. Magnetically stir the solution for 10 minutes.
5. Degas the Solution with nitrogen gas for 15 minutes (see Figure 4.1(b)).
6. Add Accelerator TEMED (or) H_2O_2.
7. Polymerization.
8. Inspect Gel after 24 hours.

4.4. Indentation experiments

To evaluate the stiffness of the hydrogels, indentation tests were performed using a Zwick/Roell Z010 Universal Testing Machine. The Zwick Z010 is a versatile and highly precise testing machine designed for various mechanical tests, including tension, compression, bending, and indentation.

(a) Solution in the Ultrasound Cleaner.

(b) Magnetic Stirring and Degassing

Figure 4.1: Magnetic Stirring, Degassing and ultrasouns cleaner processes.

(a) Solvent with Chemicals

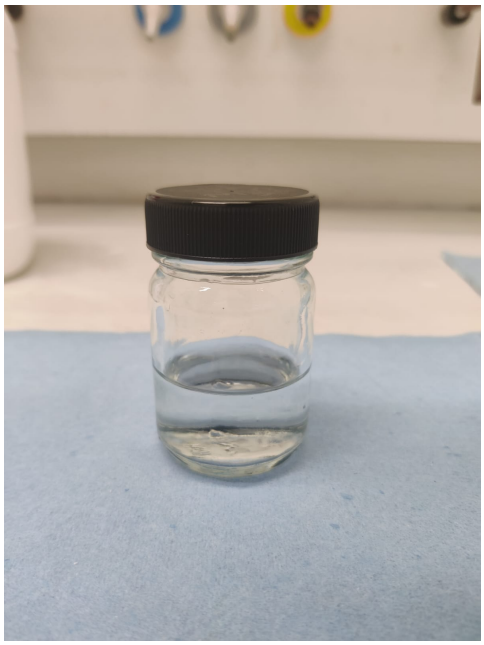

(b) Solution after Mixing

Figure 4.2: Comparison of Solvent with Chemicals and Solution after Mixing

Equipment Details

- **Model**: Zwick/Roell Z010
- **Type**: Universal Testing Machine
- **Capacity**: 10 kN

- **Control System**: TestControl III
- **Load Cell**: High-precision load cell with a capacity of 500N.
- **Crosshead Speed Range**: 0.0005 mm/min to 3000 mm/min
- **Software**: TestXpert III for data acquisition and analysis

Custom Indenter Details

- **Diameter**: 6 mm
- **Length**: 50 mm
- **Material**: Carbon Steel

Test Procedure

Preparation

- The hydrogel samples were prepared as per the synthesis procedure and allowed to polymerize for 24 hours.
- The sample is as shown in Figure 4.4.

Setup

- The Zwick Z010 machine was equipped with a custom indenter, which is 6 mm in diameter and 50 mm in length, made of carbon steel (Shown in Figure 4.3).
- The machine was calibrated to ensure accurate force and displacement measurements.

Test Execution

- Each hydrogel sample was placed on the testing platform.
- The indenter was aligned with the sample to ensure uniform indentation.
- The test was initiated, and the indenter was driven into the sample at a controlled speed of 0.5mm/sec.
- The indentation depths were 5mm and 10mm and corresponding force were recorded continuously throughout the test.
- One cycle of loading and unloading was done on the samples.
- Each sample of hydrogel was tested 3 times below LCST and 3 times above LCST.

Parameters Measured

- **Indentation Depth**: Indentation depth was set at 5mm and 10mm.
- **Force Applied**: The force exerted by the indenter on the sample.
- **Stiffness**: Calculated from the slope of the force-displacement loading curve (Untill the point of max depth).

Data Analysis

- The TestXpert III software was used to analyze the force-displacement data.
- The stiffness of each hydrogel sample was determined from the slope of the force-displacement loading curve (Untill the point of max depth).

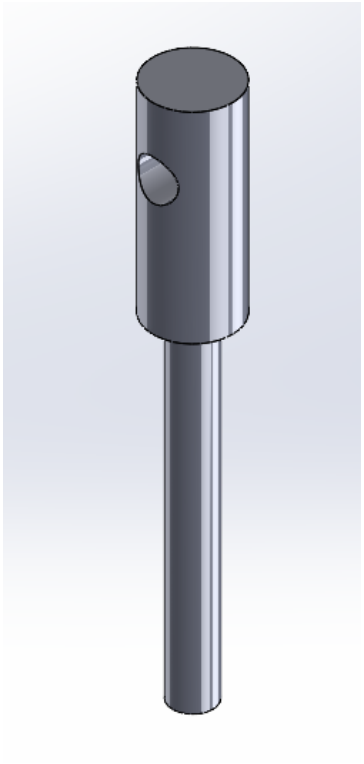

Figure 4.3: Indenter CAD Model.

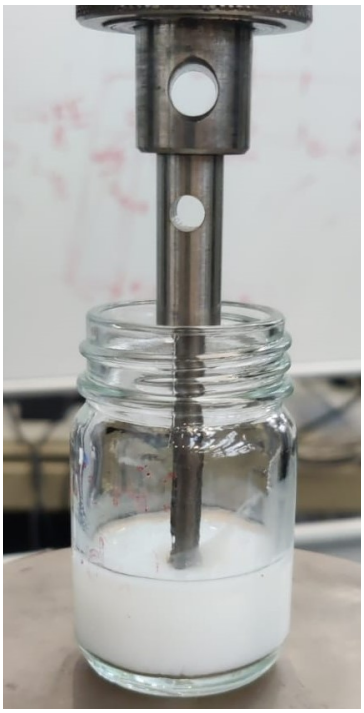

Figure 4.4: Indenter in use.

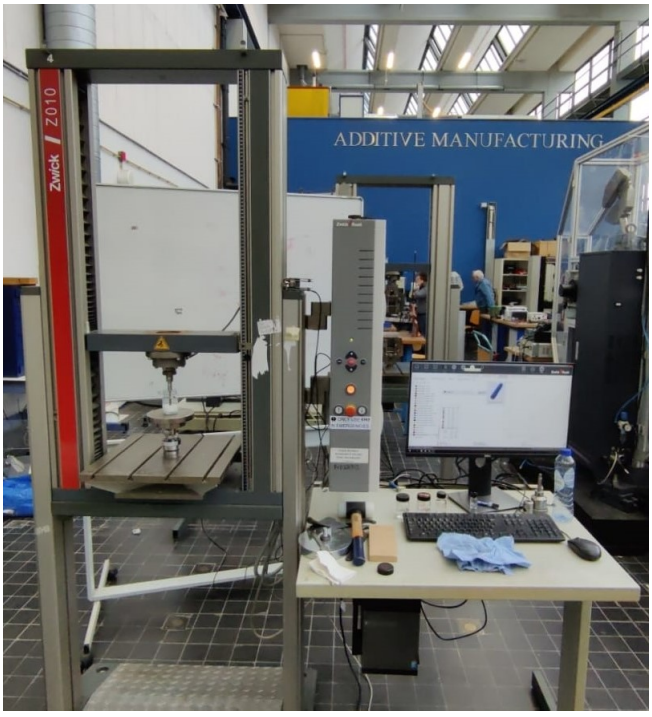

Figure 4.5: Indentation test setup.

4.5. Rheometer experiments

To evaluate the mechanical properties of the hydrogels, particularly their rigidity or stiffness, strain sweep tests were performed using a TA Instruments DHR-3 Rheometer. The DHR-3 is a highly ad-

vanced rheometer designed for precise measurement of rheological properties.

Equipment Details

- **Model**: TA Instruments Discovery HR-3
- **Type**: Rheometer
- **Measurement Range**: Broad torque range for high sensitivity
- **Control System**: Advanced Peltier temperature control system
- **Software**: TRIOS software for data acquisition and analysis

Test Procedure

Preparation

- The hydrogel samples were prepared according to the synthesis procedure and allowed to polymerize for 24 hours.
- Samples were cut into uniform 20mm discs with thickness of 2-2.5mm to ensure consistency during testing.
- After 24 hours, hydrogel samples were washed a couple of times by changing the water and let soak in water over night untill the time of experiments. These samples have been labeled as swollen samples.

Setup

- The Discovery DHR-3 rheometer was equipped with a sand galzed parallel plate geometry.
- The sample was placed between the parallel plates, ensuring uniform contact.
- The gap between the plates was adjusted to the required measurement gap.

Test Execution

- The test was initiated by applying an oscillatory strain to the hydrogel sample.
- The strain amplitude was gradually increased (strain sweep) from 0.001 to 10 (absolute strain) to cover a wide range of strains.
- The storage modulus (G') and loss modulus (G") were recorded as functions of strain.
- Measurements were taken below LCST (25°C) and above LCST (38°C).
- Solvent traps were used to minimize the evapouration of the solvent.

Parameters Measured

- **Storage Modulus (G')**: Represents the elastic or stored energy in the hydrogel, indicating its stiffness.
- **Loss Modulus (G")**: Represents the viscous or dissipated energy, indicating the hydrogel's viscous/flow behavior.
- **Complex Modulus (G*)**: Combined measure of both storage and loss moduli.

Data Analysis

- The TRIOS software was used to analyze the strain sweep data.
- The linear viscoelastic region (LVR) was identified from the storage modulus (G') vs. strain plot, where G' remains constant.
- The rigidity or stiffness of each hydrogel sample was assessed based on the mean value of G' (Mean of G' values over the strain range).

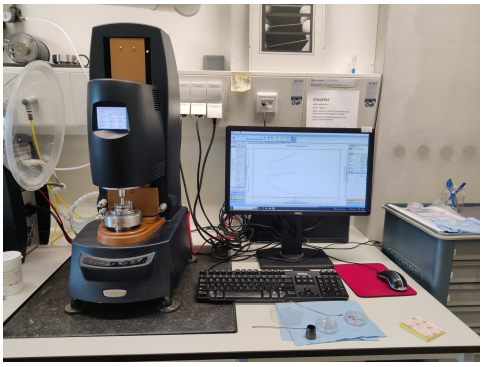

Figure 4.6: TA Discovery DHR-3 rheometer.

Figure 4.7: Rheometer setup with solvent trap.

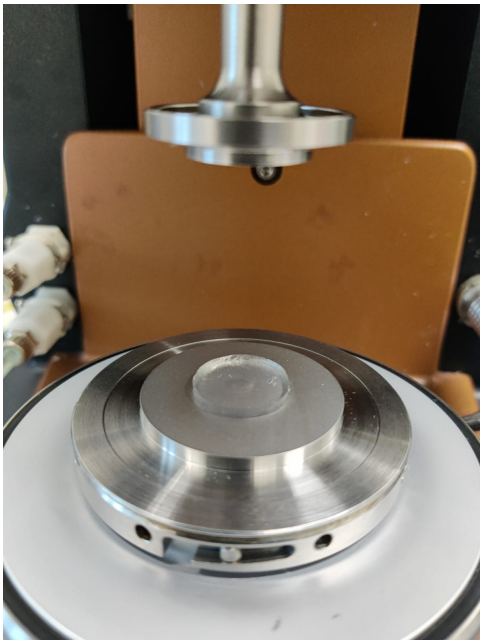

Figure 4.8: Hydrogel sample below LCST.

Figure 4.9: Hydrogel sample above LCST.

Figure 4.10: Below LCST loaded sample.

Figure 4.11: Above LCST loaded sample.

4.6. Swelling and De-swelling experiments

The swelling and deswelling experiments aim to evaluate the hydrogels' ability to absorb and release water at different monomer and crosslinker concentrations. This is crucial for understanding the hydrogel's behavior in different environmental conditions and its potential applications.

Equipment and Materials

- Prepared hydrogel samples.
- Distilled/Purified water.
- Analytical balance.
- Petri dishes/Sample bottles.
- Hot water (For De-swelling exeperiments).

Procedure

Swelling Experiment

1. **Preparation**:
    - The hydrogel samples were prepared according to the synthesis procedure and allowed to polymerize for 36 hours.
    - Samples were prepared of the same shape and size, but with different amounts of monomer and crosslinker.
2. **Initial Weighing**:
    - Weigh the hydrogel samples using an analytical balance and record their initial weights (W_0).
3. **Swelling**:
    - Place the hydrogel samples in sample boxes.
    - Add a sufficient amount of purified water (20°C) to fully immerse the samples.
    - Allow the samples to swell for periods of 24 hours and 48 hours.
4. **Final Weighing**:

- After the swelling period, gently remove the hydrogel samples from the water.
- Blot the surface with filter paper/parafilm to remove excess water.
- Weigh the swollen hydrogel samples and record their final weights (W_t).

5. **Calculation of Swelling Ratio**:
   - Calculate the swelling percentage (Q) using the formula:

$$Q = \frac{W_t - W_0}{W_0} \tag{4.7}$$

   Where W_t is the weight of the swollen hydrogel and W_0 is the initial weight.

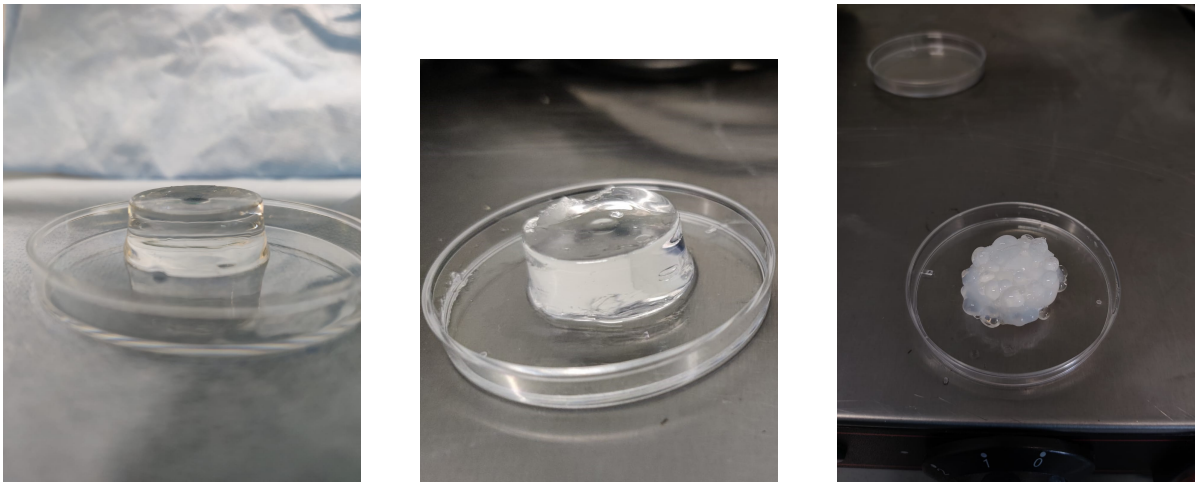

(a) Sample before Swelling. **(b)** Swollen sample **(c)** De-swollen Sample

Figure 4.12: Comparison of Hydrogel Samples Before Swelling, After swelling, and After De-swelling

Deswelling Experiment

1. **Initial Swollen State**:
   - Use the swollen hydrogel samples from the swelling experiment.
   - Record their weights if not already done after the swelling period.
2. **Deswelling**:
   - For deswelling, place the swollen samples in a water which is at a temperature above the lower critical solution temperature (LCST) (32°C) of the hydrogel.
   - 60°C water in this research (hot tap water used).
3. **Intermittent Weighing**:
   - Weigh the hydrogel samples at regular intervals (e.g., every 10 minutes) to monitor the deswelling process (optional).
   - Maximum deswelling time is set at 30 minutes.
   - Record the weights of the deswollen hydrogel samples (W_d).
4. **Final Weighing**:
   - Continue the deswelling process until the samples reach a constant weight (Incase of intermittent weighing).
   - Record the final weights (W_f).
5. **Calculation of Deswelling Ratio**:

- Calculate the deswelling percentage (D) using the formula:

$$D = \frac{W_t - W_f}{W_t} \tag{4.8}$$

- Where W_t is the initial swollen weight and W_f is the final weight after deswelling.

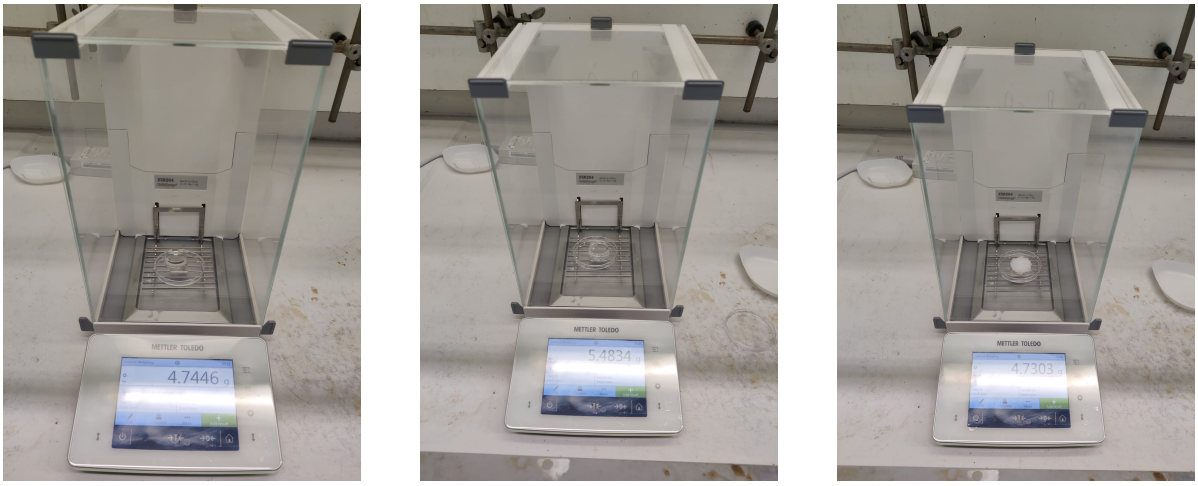

(a) Weight of sample before swelling (4.7446g).

(b) Weight of sample after swelling (5.4834g).

(c) Weight of sample after shrinking (4.7303g).

Figure 4.13: Comparison of Hydrogel Sample Weights: Equilibrium, swollen and shrunken states.

Extreme Swelling & De-swelling experiment

The extreme swelling and deswelling experiment aims to evaluate the ability of dried hydrogel samples to reabsorb water and return to their hydrated state. This test is crucial for understanding the hydrogel's long-term stability and reusability, while also showcasing swelling in an extreme case. This experiment was done with two varying amounts of crosslinker namely 0.03g and 0.05g, while the amount of monomer was 2g for both the samples.

Equipment and Materials

- Dried hydrogel samples.
- Distilled/Purified water.
- Analytical balance.
- 120ml sample bottles.

Procedure

Drying of Hydrogel Samples

1. Prepare hydrogel samples according to the synthesis procedure and allow them to polymerize for 24 hours.
2. Place the hydrogel samples in an open-air environment or in a vaccum oven to dry out the hydrogel samples.
3. The current samples were dried in open air for 4 weeks.

Initial Weighing

1. Weigh the dried hydrogel samples using an analytical balance and record their initial dry weights (W_d).

Water Uptake/rehydration

1. Place the dried hydrogel samples in the 120ml sample bottles.

2. Add a sufficient amount of distilled water (temp below LCST) to fully immerse the samples.
3. Allow the samples to rehydrate for 24 hours at room temperature.

Intermittent Weighing (Optional)

1. For more detailed data, weigh the hydrogel samples at regular intervals (e.g., every hour) to monitor the water uptake process.
2. Gently blot the surface of the hydrogel with filter paper/para film before weighing to remove excess water.

Final Weighing

1. After the 24-hour rehydration period, gently remove the hydrogel samples from the water.
2. Blot the surface with filter paper/para film to remove excess water.
3. Weigh the rehydrated hydrogel samples and record their final weights (W_r).

Calculation of Water Uptake Ratio

1. Calculate the swelling percentage (U) using the formula:

$$U = \frac{W_r - W_d}{W_d} \tag{4.9}$$

2. Where W_r is the weight of the rehydrated hydrogel and W_d is the initial dry weight.

4.7. Shapes of Hydrogels

This section details the steps for fabricating PNIPAM hydrogels with various shapes and sizes using open molds and a nitrogen enclosure.

4.7.1. Materials

- PLA filament for 3D printing
- Ecoflex 30 silicone
- PNIPAM precursors (NiPaam, MBA, APS & TEMED)
- Solvent (water)
- Nitrogen gas
- Standard lab equipment (magnetic stirrer)
- Custom nitrogen enclosure (refer to Figure 4.15 for pictures)

4.7.2. Procedure

Mold Preparation

1. Design and 3D print Polylactic acid plastic (PLA) molds for desired shapes and sizes.
2. Cast Ecoflex 30 molds using the PLA molds and later demold from PLA.

PNIPAM Solution

1. Prepare the PNIPAM solution according to your chosen protocol (Free radical polymerization in this research).
2. Purge the solution with nitrogen gas for a designated time (For 15-20 minutes) to remove any dissolved oxygen.

Hydrogel Formation

1. Assemble the nitrogen enclosure and ensure a nitrogen gas supply.
2. Place the open Ecoflex 30 molds inside the enclosure.
3. Carefully transfer the deoxygenated PNIPAM solution into the molds.
4. Initiate polymerization by adding the accelerator.
5. Keep the nitrogen gas flow till the polymerization is complete (4-6 hours minimum)

Demolding and Analysis

1. After the polymerization time is complete, remove the enclosure and stop the flow of nitrogen gas.
2. Gently demold the hydrogels from the Ecoflex 30 molds.
3. Analyze the fabricated hydrogels using visual inspection to assess shape, uniformity, and air bubbles.
4. Measure the dimensions of the hydrogels to perform further swelling and de-swelling experiments.
5. Measure the dimensions of the hydrogels post swelling and desweling, and compare with the simulation results, as mentioned in section 3.3.6.

The following figures are of the 3d printed molds and silicone molds cured from the 3d printed molds.

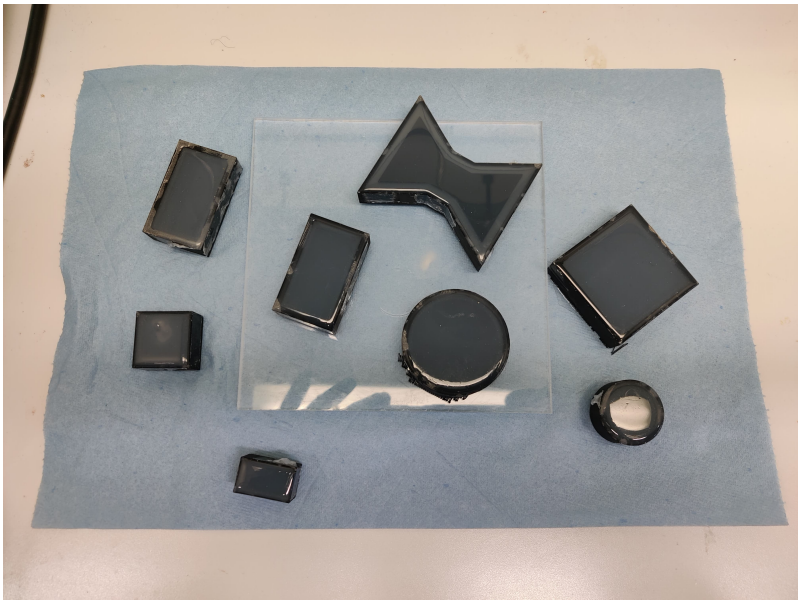

(a) Cured silicone samples

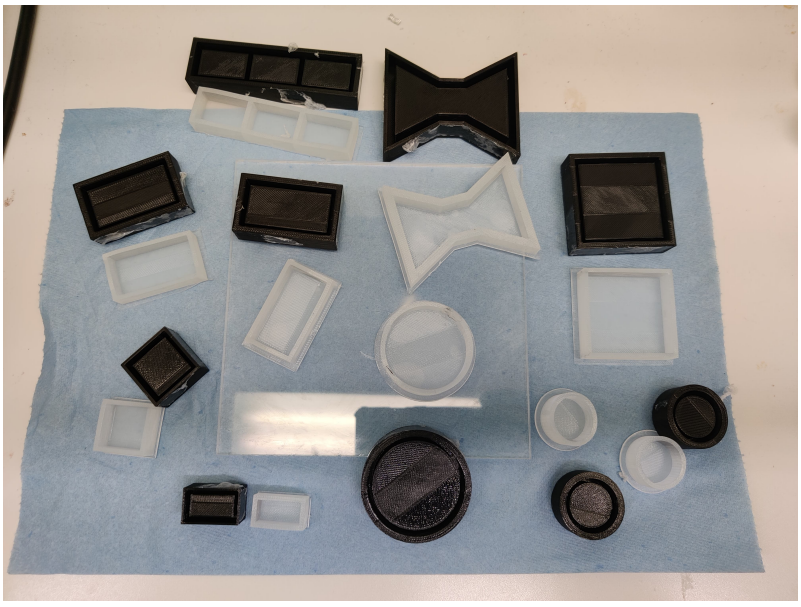

(b) Demolded silicone samples

Figure 4.14: Images of cured and demolded silicone samples.

The following figures are of the Nitrogen enclosures used to minimize the exposure to oxygen:

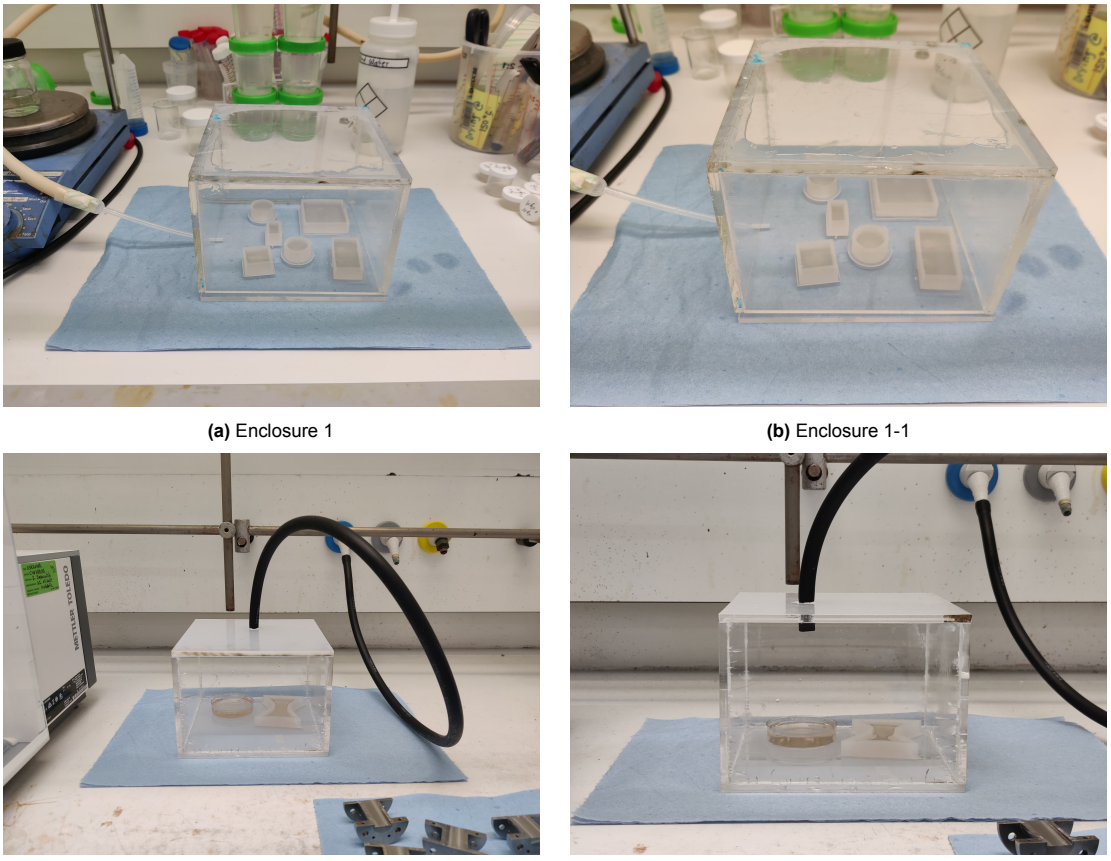

(a) Enclosure 1

(b) Enclosure 1-1

(c) Enclosure 2

(d) Enclosure 2-1

Figure 4.15: Images of enclosures built.

4.8. Conclusion

Chapter 4 provided a detailed overview of the design and execution of experiments aimed at understanding the synthesis and characterization of PNIPAM hydrogels. The chapter began by outlining the materials and equipment used, ensuring that all procedures were conducted under controlled conditions to maintain the integrity of the experimental results. The primary focus was on understanding how different concentrations of monomers and crosslinkers impact the mechanical properties and thermoresponsive behavior of the hydrogels.

The chapter also described the various experiments conducted, including synthesis experiments to produce hydrogels with varying properties, indentation tests to measure stiffness and elasticity, rheometer tests to evaluate viscoelasticity and also stiffness, and swelling-deswelling experiments to assess the hydrogels' responsiveness to temperature changes. Each of these experiments was meticulously planned to isolate and study specific aspects of the hydrogels' performance, providing a comprehensive dataset that would later be analyzed in subsequent chapters.

In conclusion, Chapter 4 successfully established the experimental framework necessary for a thorough investigation of PNIPAM hydrogels. The methodologies employed were designed to generate reliable and repeatable results, forming a solid foundation for the analysis and discussion of these materials' potential applications in soft robotics and other fields. The experiments outlined in this chapter are crucial for understanding how to optimize hydrogel synthesis to meet specific performance criteria.

5

Results and Discussion

5.1. Synthesis experiments

To systematically investigate the effects of monomer and crosslinker concentrations on the gelation process and properties of hydrogels, a full factorial design was employed. The design included five different monomer concentrations (0.2g, 0.5g, 1g, 1.5g, 2g) and five different crosslinker concentrations (0.01g, 0.03g, 0.05g, 0.07g, 0.09g), resulting in a total of 25 unique combinations. For each combination, the initiator (APS) mass was kept constant at 0.01g, and two different accelerators, TEMED and hydrogen peroxide, were tested to evaluate their effects on the gelation process.

All of the samples were prepared by dissolving the mentioned amounts of monomner (NiPaam), Corsslinker (MBA) and initiator (APS) in 20ml solvent (water). The samples were magnetically stirred for 15 minutes, then immersed in the ultrasound cleaner for 5 minutes to ensure breakdown of all the solid particles, then magnetically stirred for 15 minutes again. This procedure was done to make sure the solution looks completely clear indicating dissolution of the solid chemicals (see Figure 4.2). Next, the solution was seperated into two 10ml tubes, and individually degassed for 15 minutes to ensure removal of dissolved oxygen. Lastly accelerators (30% H_2O_2 and TEMED) (2-3 drops) were added into the corresponding tubes and left aside for 24 hours to ensure complete polymerisation.

The following table summarizes the full factorial design used for the synthesis experiments: (Refer Table 5.1)

Comparison of Accelerators

5.1.1. Hydrogen Peroxide

Hydrogen peroxide as an accelerator did not yield satisfactory gelation at room temperature. It was observed that:

- **No Gels**: Gelation did not occur even after 72 hours. The solution stayed the same.
- **Gelation Requirement**: The solution required heating to initiate polymerization.
- **Effect of Heating**: Heating the solution yielded gels with holes in them, they were brittle to touch and would break due to their own weight.
- **Monomer Concentrations**: At lower monomer concentrations (0.2g, 0.5g, 1g), the gelation was poor, forming only a few lumps of gel in the tubes.

Given these outcomes, hydrogen peroxide was deemed unsuitable for this experiment due to its inconsistent results and the necessity for heat, which negatively impacted the gelation quality.

5.1.2. TEMED

TEMED, on the other hand, produced gels almost instantly at room temperature. Key observations include:

- **0.2g Monomer**: Remained liquid and did not form a solid gel, although polymerization occurred, as evidenced by a white, viscous liquid at higher crosslinker concentrations (refer appendix B).
- **0.5g Monomer**: Formed a gel, but it was more viscous than solid.
- **1g Monomer**: Successfully yielded a solid gel.
- **1.5g Monomer**: Successfully yielded a solid gel.
- **2g Monomer**: Successfully yielded a solid gel.

Based on these observations, TEMED was selected as the superior accelerator for the synthesis of hydrogels due to its ability to produce reproducible gels rapidly at room temperature. The photos of the gels prepared can be found in the appendix B. A few of the gels could not be photographed, either due to the gel being checked for how it feels physically, or some of them were discarded by the time photographs were taken.

5.1.3. Impact of Crosslinker Concentration on Gel Opacity

An additional observation was the change in the opacity of the gels as the crosslinker concentration increased:

- **Low Crosslinker Concentrations (0.01g, 0.03g)**: The gels remained transparent, suggesting a homogenous network without significant aggregation of polymer chains. At these concentrations, the polymer chains were sufficiently spaced to avoid aggregation.
- **Moderate Crosslinker Concentration (0.05g)**: The gels became slightly turbid or hazy, indicating the onset of aggregation of polymer chains. This suggests that increasing the crosslinker concentration begins to promote aggregation of polymer chains.
- **Higher Crosslinker Concentration (0.07g)**: The gels became off-white, suggesting increased aggregation. This more pronounced aggregation is likely due to the higher density or quantity of crosslinker, which may have caused substantial polymer chain aggregation.
- **Highest Crosslinker Concentration (0.09g)**: The gels turned pearl white, indicating substantial aggregation, which led to brittleness. At this concentration, the network became so dense that large aggregated regions formed, likely disrupting the gel's homogeneity

This change in opacity with increasing crosslinker concentration highlights its impact on the microstructure of the gels, where higher concentrations promote aggregation due to the formation of a tighter and denser network.

Table 5.1: Full Factorial Design for Synthesis Experiments

Monomer Mass (g)	Crosslinker Mass (g)	Initiator Mass (g)	Accelerator	Solvent (ml)
0.2	0.01	0.01	TEMED	10
0.2	0.01	0.01	Hydrogen Peroxide	10
0.2	0.03	0.01	TEMED	10
0.2	0.03	0.01	Hydrogen Peroxide	10
0.2	0.05	0.01	TEMED	10
0.2	0.05	0.01	Hydrogen Peroxide	10
0.2	0.07	0.01	TEMED	10
0.2	0.07	0.01	Hydrogen Peroxide	10
0.2	0.09	0.01	TEMED	10
0.2	0.09	0.01	Hydrogen Peroxide	10
0.5	0.01	0.01	TEMED	10
0.5	0.01	0.01	Hydrogen Peroxide	10
0.5	0.03	0.01	TEMED	10
0.5	0.03	0.01	Hydrogen Peroxide	10
0.5	0.05	0.01	TEMED	10
0.5	0.05	0.01	Hydrogen Peroxide	10
0.5	0.07	0.01	TEMED	10
0.5	0.07	0.01	Hydrogen Peroxide	10
0.5	0.09	0.01	TEMED	10
0.5	0.09	0.01	Hydrogen Peroxide	10
1.0	0.01	0.01	TEMED	10
1.0	0.01	0.01	Hydrogen Peroxide	10
1.0	0.03	0.01	TEMED	10
1.0	0.03	0.01	Hydrogen Peroxide	10
1.0	0.05	0.01	TEMED	10
1.0	0.05	0.01	Hydrogen Peroxide	10
1.0	0.07	0.01	TEMED	10
1.0	0.07	0.01	Hydrogen Peroxide	10
1.0	0.09	0.01	TEMED	10
1.0	0.09	0.01	Hydrogen Peroxide	10
1.5	0.01	0.01	TEMED	10
1.5	0.01	0.01	Hydrogen Peroxide	10
1.5	0.03	0.01	TEMED	10
1.5	0.03	0.01	Hydrogen Peroxide	10
1.5	0.05	0.01	TEMED	10
1.5	0.05	0.01	Hydrogen Peroxide	10
1.5	0.07	0.01	TEMED	10
1.5	0.07	0.01	Hydrogen Peroxide	10
1.5	0.09	0.01	TEMED	10
1.5	0.09	0.01	Hydrogen Peroxide	10
2.0	0.01	0.01	TEMED	10
2.0	0.01	0.01	Hydrogen Peroxide	10
2.0	0.03	0.01	TEMED	10
2.0	0.03	0.01	Hydrogen Peroxide	10
2.0	0.05	0.01	TEMED	10
2.0	0.05	0.01	Hydrogen Peroxide	10
2.0	0.07	0.01	TEMED	10
2.0	0.07	0.01	Hydrogen Peroxide	10
2.0	0.09	0.01	TEMED	10
2.0	0.09	0.01	Hydrogen Peroxide	10

The synthesis experiments revealed that TEMED is the optimal accelerator for hydrogel formation at room temperature, providing consistent gelation across different monomer and crosslinker concentra-

tions. In contrast, hydrogen peroxide proved unsuitable due to its inconsistent results and the necessity for heat, which negatively impacted gel quality. The experiments also highlighted the significant impact of crosslinker concentration on the opacity of the gels, where higher crosslinker concentrations led to more pronounced aggregation of polymer chains and the gel started to turn white. This finding emphasizes the importance of selecting appropriate accelerator and crosslinker concentrations to achieve the desired hydrogel properties. The photos of the gels can be found in the appendix B.

5.2. Indentation experiments

5.2.1. Selection tests

Indentation test is a straightforward method of testing hydrogel's stiffness. First, two sets of tests were done to investigate the dependence of stiffness on the amount of monomer and crosslinker. The indentation depth was set as 5mm and Indentation speed of 0.5mm/sec.

For the monomer variation test (see Figure 5.1), the amount of crosslinker (MBA) was set as 0.01g:

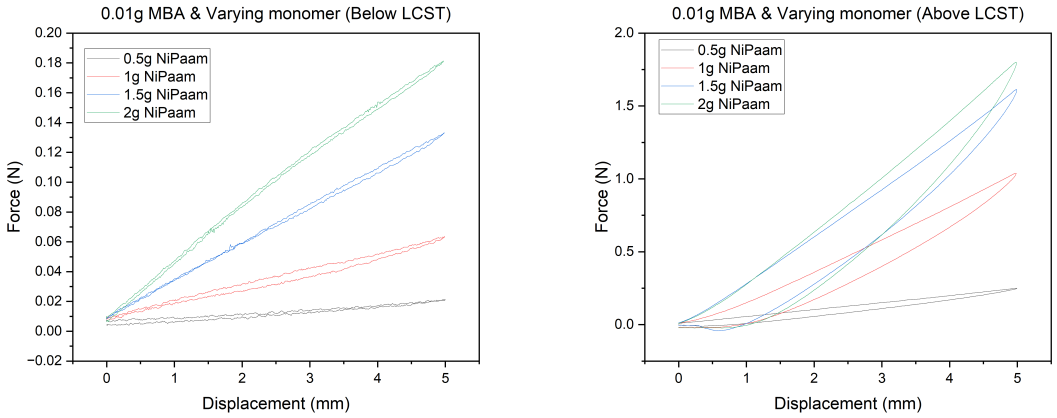

(a) 0.01g MBA & Varying monomer (Below LCST)

(b) 0.01g MBA & Varying monomer (Above LCST)

Figure 5.1: Force vs. Displacement graphs for different monomer concentrations at 0.01g MBA crosslinker concentration

The calcualted stiffness values are shown in Table 5.2:

Table 5.2: Stiffness values in N/m for varying monomer concentrations below and above LCST.

Monomer Concentration (g)	Stiffness Below LCST (N/m)	Stiffness Above LCST (N/m)
0.5g	3.51	52.07
1g	11.17	212.51
1.5g	25.08	331.78
2g	35.16	365.96

And now for the varying crosslinker test (see Figure 5.2), the amount of monomer mass was set as 1.5g as constant:

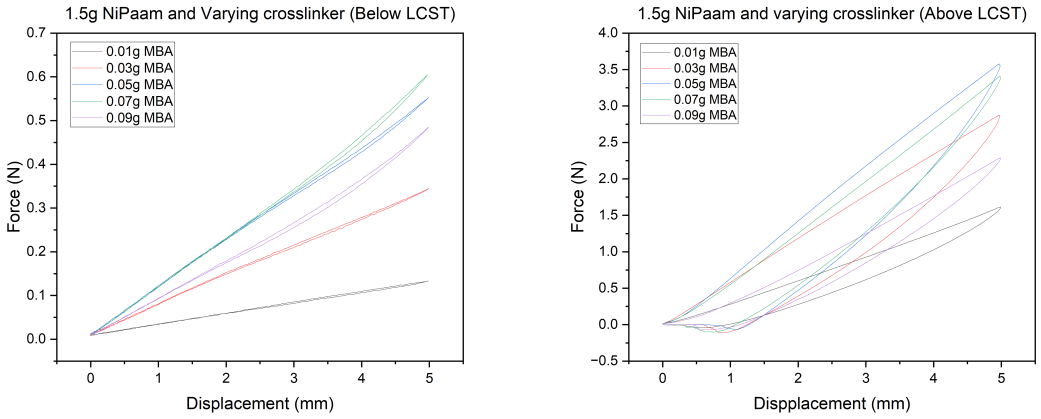

(a) 1.5g NiPaam & varying crosslinker (Below LCST)

(b) 1.5g NiPaam & varying crosslinker (Above LCST)

Figure 5.2: Force vs. Displacement graphs for different crosslinker concentrations at 1.5g NiPaam

Table 5.3 showcases the values of stiffness calculated for the varying crosslinker test:

Table 5.3: Stiffness values in N/m for varying crosslinker concentrations below and above LCST.

Crosslinker Concentration (g)	Stiffness Below LCST (N/m)	Stiffness Above LCST (N/m)
0.01g	25.142	324.195
0.03g	66.226	584.064
0.05g	106.468	742.977
0.07g	116.834	698.515
0.09g	92.059	475.627

The following observations were made from Figure 5.2 and Table 5.3:

- Stiffness has a positive effect with both increasing monomer and increasing crosslinker concentrations.
- 0.5g monomer mass yields a gel which is more viscous than solid, hence the least stiff gel within the monomer concentrations.
- 0.01g crosslinker concentration yields a solid gel, but is the least stiff gel within the crosslinker concentrations.
- Stiffness increases as the crosslinker concentration increases, but stiffness reduces at the higher concentrations (0.07g and 0.09g), this is likely due to the possibility that above 0.05g of crosslinker, excessive crosslinking takes place. Excessive crosslinking further leads to high aggreagtion of polymer chains..
- Following the reduction in stiffness, 0.09g is not going to be used for further testing.

Based on these observations, 0.5g monomer mass, 0.01g and 0.09g crosslinker masses are eliminated from further testing. Due to time constrains and also taking into account the amount of chemicals available, the following table of monomer, crosslinker values are tested for 10mm indentation depth. Where failure of the gels are expected, and a full factorial DoE was performed for the dependent variable stiffness.

Table 5.4: Final list of monomer and crosslinker for further testing

Monomer mass	1g		2g
Crosslinker mass	0.03g	0.05g	0.07g

All of the further testing is limited to this final list of monomer and crosslinker masses shown in Table 5.4.

5.2.2. Final indentation tests

The final indentation tests were performed with a depth of 10mm, to check if any of the hydrogels would fail or break. The following are the results:

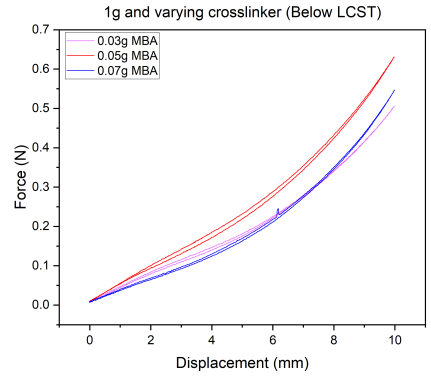

(a) 1g NiPaam & Varying crosslinker (Below LCST)

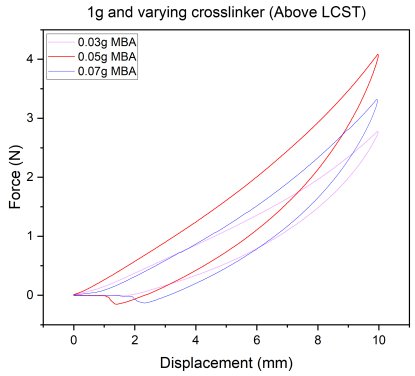

(b) 1g NiPaam & Varying crosslinker (Above LCST)

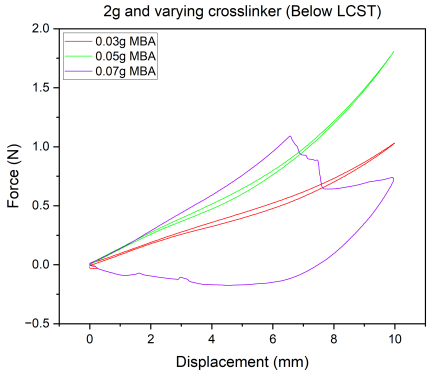

(c) 2g NiPaam & Varying crosslinker (Below LCST)

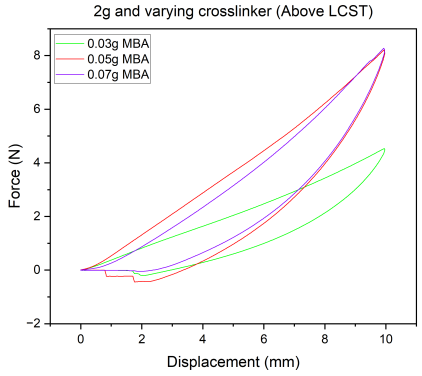

(d) 2g NiPaam & Varying crosslinker (Above LCST)

Figure 5.3: Force vs Displacement for 1g and 2g NiPaam with varying crosslinker amounts at different conditions.

From the Figure 5.3 stiffness values were caculated as the slope of the loading curve alone, and until the maximum point loading point (10mm). The calculated stiffness values are shown below in the Table 5.5 & Table 5.6.

Table 5.5: Stiffness of 1g monomer and varying crosslinker mass

Monomer (g)	Crosslinker(g)	Stiffness (N/m) (Below LCST)	Stiffness (N/m)(Above LCST)
1g	0.03g	46	271
1g	0.05g	58	399
1g	0.07g	50	336

Table 5.6: Stiffness of 2g monomer and varying crosslinker mass

Monomer (g)	Crosslinker(g)	Stiffness (N/m) (Below LCST)	Stiffness (N/m)(Above LCST)
2g	0.03g	96	444
2g	0.05g	167	825
2g	0.07g	77	855

The force-displacement graphs above in Figure 5.3(a) showcase that below LCST stiffness increases as the amount of corsslinker increases. 0.03g exhibits the lowest stiffness, while 0.07g exhibits mediocre stiffness and 0.05g showing the highest stiffness. The same trend remains even above LCST Figure 5.3(b) where 0.05g exhibits the highest stiffness. Things get interesting with the 2g monomer samples, where from the Figure 5.3(c) it can be seen that the stiffness trend remains the same, with 0.05g showcasing the highest stiffness, but the sample with 0.07g fails around 6mm depth. It can also be seen that the 2g monomer samples are more stiffer compared to that of 1g samples Figure 5.3(a,c). The highest force for 1g samples can be seen around 0.6N, and the highest force for 2g samples is close to 2N. This is due to the face that as the amount of monomer increases in the initial solution, the number of polymer chains formed also increases, and those chains are most likely of bigger length, thus resulting in a denser gel network.

The next notable observation from Figure 5.3(c) is that the gel with 2g monomer and 0.07g crosslinker fails around a 6mm indentation depth. This likely occurs because the higher crosslinker concentration leads to an increased crosslinking density, resulting in a more denser gel network. This restricts the movement of polymer chains, ultimately causing the gel to become brittle.

In the Figure 5.3(b,d) which are the force-displacement curves for gels tested above LCST. The gels show almost 4 times increase in stiffness compared to their respective below LCST states, showcasing the thermoresponsive effect of the PNIPAM hydrogels where they shrink and stiffen up above LCST. This can also be seen from the tables of calculated stiffnes values Table 5.5 and Table 5.6.

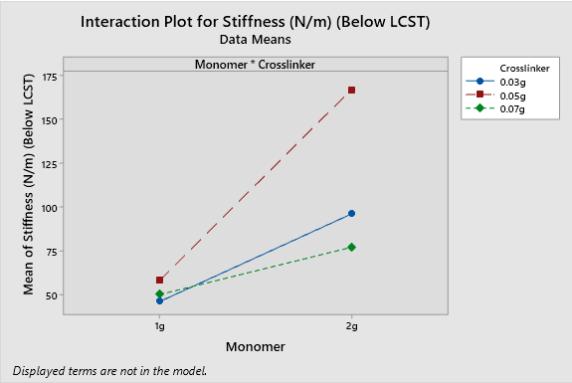

(a) Interaction Plot for Stiffness (N/m) (Below LCST)

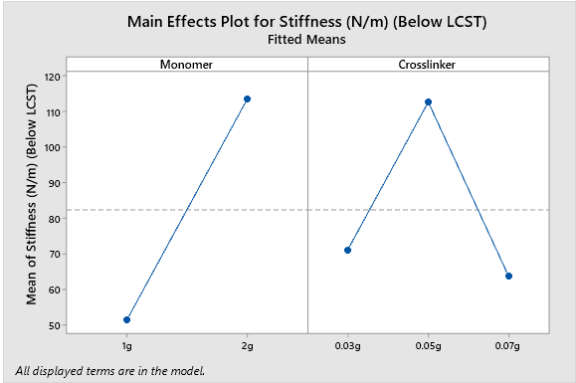

(b) Main Effects Plot for Stiffness (N/m) (Below LCST)

Figure 5.4: Comparison of Stiffness (N/m) Below LCST

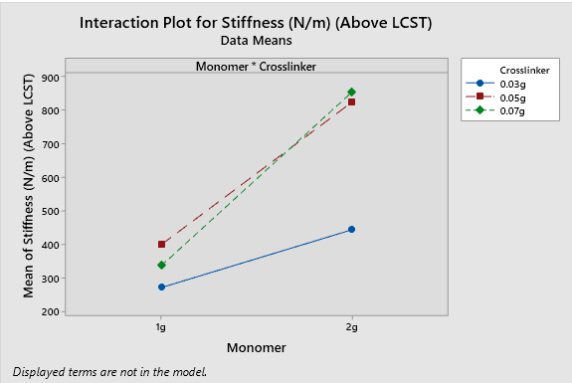

(a) Interaction Plot for Stiffness (N/m) (Above LCST)

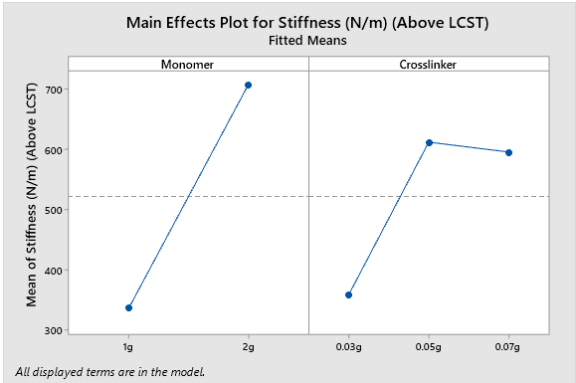

(b) Main Effects Plot for Stiffness (N/m) (Above LCST)

Figure 5.5: Comparison of Stiffness (N/m) Above LCST

The Figure 5.4 and Figure 5.5 illustrate how increasing crosslinker concentration leads to an increase in stiffness, while excessive crosslinking resulting in brittleness. Specifically, the sample with 2g monomer

and 0.03g crosslinker exhibits moderate stiffness, the sample with 2g monomer and 0.05g crosslinker shows the highest stiffness, and the sample with 2g monomer and 0.07g crosslinker shows the least stiffness, indicating the effects of excessive crosslinking. Interestingly, above the LCST, the trend is different, with the results showing 2g monomer and 0.03g crosslinker < 2g monomer and 0.05g crosslinker < 2g monomer and 0.07g crosslinker. This suggests that even though the gel with the 2g monomer and 0.07g crosslinker formulation fails below the LCST due to aggregation (see Figure 5.3(c)), it still functions effectively above the LCST.

Beyond the stiffness values calculated above, Young's modulus values have also been calculated. To calcualte Youngs's modulus, the force-displacement data was converted to stress-strain data using the following information:

1. Indenter dia (D): 6mm.
2. Original sample height (h): 30mm.
3. Force (F): 0.15N (one value from 1g and 0.03g F-D curve)
4. Displacement (d): 1.5mm (corresponding displacement value of the mentioned force)
5. Stress was calculated using: $\sigma = \frac{F}{A} = 5.3kPa$
6. Strain was calcualted using: $\epsilon = \frac{d}{h} = 0.05$
7. Stress-strain values were plotted and a linear regression was performed on the Linear part of the loading curve for the values of Young's modulus.

The tables below showcase the calcualted Young's modulus values. (Table 5.7 & Table 5.8):

Table 5.7: Young's modulus of 1g monomer and varying crosslinker samples.

Monomer (g)	Crosslinker(g)	Young's modulus (kPa) (Below LCST)	Young's modulus (kPa) (Above LCST)
1g	0.03g	53.96	438.91
1g	0.05g	93.53	633.31
1g	0.07g	110.01	551.84

Table 5.8: Young's modulus of 2g monomer and varying crosslinker samples.

Monomer (g)	Crosslinker(g)	Young's modulus (kPa) (Below LCST)	Young's modulus (kPa) (Above LCST)
2g	0.03g	66.92	522.24
2g	0.05g	112.23	692.15
2g	0.07g	138.14	605.38

From the Table 5.7 and Table 5.8, a consistent trend is observed, where increasing the crosslinker concentration has a positive impact on the mechanical properties, specifically on the stiffness of the gels. Additionally, increasing the monomer concentration also leads to a similar positive effect, enhancing the overall strength and resilience of the gel network. These trends align with findings in various studies, such as those by Sasson et al. (2012) [97], Kim et al. (2022) [98], Puleo et al. (2013) [99], Esteki et al. (2020) [100], Ahearne et al. (2008) [101], and Czerner et al. (2015) [102]. These studies consistently demonstrate that both increased crosslinker and monomer concentrations can enhance the mechanical integrity of hydrogels, resulting in improved stiffness and structural stability. This further corroborates the observations made in the present study, emphasizing the critical role of these parameters in tailoring the properties of hydrogels for specific applications.

In conclusion, The indentation experiments provided insights into the stiffness of hydrogels under varying monomer and crosslinker concentrations. It was observed that stiffness increases with higher monomer and crosslinker concentrations, indicating a denser and more crosslinked polymer network. However, at the highest crosslinker concentration, the stiffness reduced likely due to the increased aggregation of polymer chains. These findings suggest that while increasing crosslinker content generally enhances stiffness, and excessive crosslinking can lead to aggregation, reducing the material's overall mechanical integrity.

5.3. Rheometer experiments

Strain sweeps were performed on the gels to assess their response to varying levels of strain. The strain range, as previously mentioned, was set from 0.001 to 10 (absolute strain). The Figure 5.6 illustrates the variation of G' (storage modulus) and G" (loss modulus) with respect to strain. The gels were tested in three different states: equilibrium state, swollen state, and above LCST. These tests were conducted to evaluate the differences in stiffness and rigidity, which were determined by calculating the mean of the G' (storage modulus) curve.

The samples are designated as H_M1_C003, H_M1_C005, H_M1_C007, H_M2_C003, H_M2_C005, and H_M2_C007, corresponding to the formulations of hydrogel with 1g monomer with 0.03g crosslinker, hydrogel with 1g monomer with 0.05g crosslinker, and continuing in this pattern up to hydrogel with 2g monomer with 0.07g crosslinker. Each of these formulations was analyzed to understand how changes in monomer and crosslinker concentrations affect the mechanical properties of the gels under different strain conditions. For better understanding, refer Table 5.9.

Table 5.9: Sample names and their respective monomer and crosslinker concentrations.

Sample name	Monomer and crosslinker content
H_M1_C003	Hydrogel with 1g monomer & 0.03g crosslinker
H_M1_C005	Hydrogel with 1g monomer & 0.05g crosslinker
H_M1_C007	Hydrogel with 1g monomer & 0.07g crosslinker
H_M2_C003	Hydrogel with 2g monomer & 0.03g crosslinker
H_M2_C005	Hydrogel with 2g monomer & 0.05g crosslinker
H_M2_C007	Hydrogel with 2g monomer & 0.07g crosslinker

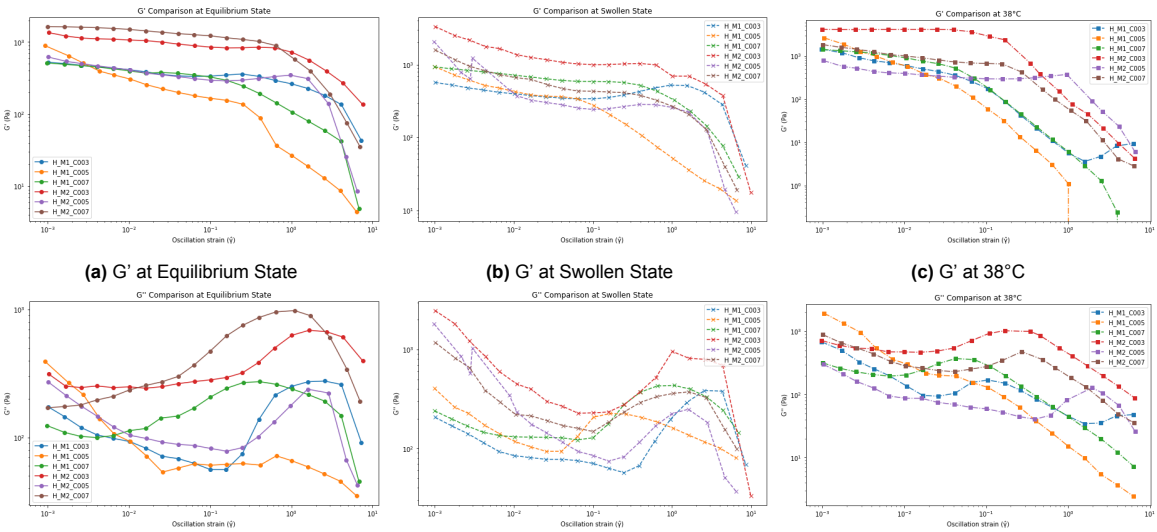

(a) G' at Equilibrium State **(b)** G' at Swollen State **(c)** G' at 38°C

(d) G" at Equilibrium State **(e)** G" at Swollen State **(f)** G" at 38°C

Figure 5.6: Comparison of G' and G" across different states and temperatures for all samples.

The Figure 5.6(a, b, c), showcases the G' vs strain is shown for the samples in different states, while Figure 5.6(d, e, f) represents G" vs strain for all the samples. The common trends observed indicate that hydrogels with a 2g monomer content are stiffer, exhibiting higher G' values, compared to those with a 1g monomer content. Similarly, the 2g monomer samples demonstrated higher energy dissipation, reflected in higher G" values, compared to the 1g monomer samples. Below given Table 5.10 contains the mean G' and G" values calculated throughout the strain region, and bar graphs (see Figure 5.7) gives a visualization.

Table 5.10: Magnitude values of G' and G" for all samples and states.

Sample	G' Equilibrium (Pa)	G' Swollen (Pa)	G' 38°C (Pa)	G" Equilibrium (Pa)	G" Swollen (Pa)	G" 38°C (Pa)
H_M1_C003	336.68	401.02	375.67	135.43	140.84	167.12
H_M1_C005	229.85	305.41	457.28	101.71	169.16	330.30
H_M1_C007	284.95	545.64	483.89	165.98	222.99	178.88
H_M2_C003	853.47	1232.62	2355.10	368.20	676.40	552.35
H_M2_C005	334.12	432.21	326.16	130.94	332.45	96.28
H_M2_C007	1072.37	529.19	670.04	452.60	339.52	317.44

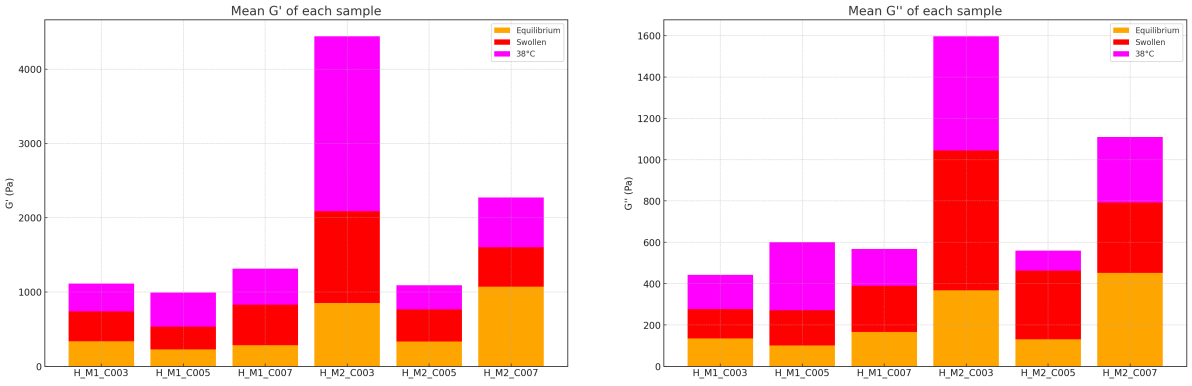

(a) Mean G' of each sample

(b) Mean G" of each sample

Figure 5.7: Comparison of Mean G' and G" magnitudes for each sample across different states.

Analysis of the results

Equilibrium State

In the equilibrium state (Figure 5.6(a) & Figure 5.7(a)), the hydrogels demonstrate varying degrees of stiffness, as indicated by their G' values. The H_M2_C007 hydrogel, which has a higher monomer content, exhibits the highest stiffness (1072.37 Pa), followed by the H_M2_C003 hydrogel, which also has a higher monomer content but less crosslinker compared to H_M2_C007. This suggests that higher monomer concentrations contribute to a more rigid network structure by increasing the number of polymer chains available for entanglement and crosslinking. This also showcases the effect of crosslinker concentration on the stiffness, but quite the opposite of what was seen in the indentation test.

The lower G' values observed for the H_M1_C005 and H_M1_C003 hydrogels, which have lower monomer content, indicate a less densely crosslinked network, resulting in reduced stiffness. The concentration of the crosslinker also plays a significant role. Although the H_M1_C005 and H_M1_C003 hydrogels have similar monomer content, the H_M1_C007 hydrogel has a higher crosslinker concentration, leading to a stiffer network despite having the same amount of monomer as the H_M1_C003 and H_M1_C005 hydrogel. This underscores the importance of both monomer and crosslinker concentrations in determining stiffness: sufficient monomer is necessary to create a dense network, and adequate crosslinkers are required to tie these polymer chains together, preventing them from slipping past each other under stress.

The G" values in the equilibrium state (Figure 5.6(d) & Figure 5.7(b)) highlight the viscous nature of the hydrogels. The H_M2_C007 hydrogel shows the highest G" (452.60 Pa), indicating higher energy dissipation likely due to internal friction within its more dense network structure. The H_M2_C003 hydrogel also exhibits significant energy dissipation (368.20 Pa), reflecting its robust network with a good balance of crosslinking and monomer content.

Strain softening was observed across all samples, where G' decreases with increasing strain, indicating that the gels become softer at higher strains. Additionally, the gels in the equilibrium state often failed (broke) or slipped out from between the plates at higher strains (at or above 1), likely due to exceeding the physical limits of the network structure (see Figure 5.8).

Swollen State

When swollen (Figure 5.6(b) & Figure 5.7(a)), the hydrogels absorb water, which influences their mechanical properties. The H_M2_C003 hydrogel maintains the highest G' (1232.62 Pa), indicating its ability to retain stiffness even in a swollen state. This suggests that a higher initial stiffness, due to higher monomer content, can lead to better performance after swelling. The observed changes in G' for all samples in the swollen state compared to equilibrium state, could be attributed to the balance between network expansion due to water uptake and the inherent stiffness provided by the polymer structure.

The G" values in the swollen state (Figure 5.6(e) & Figure 5.7(b)) indicate increased energy dissipation compared to the equilibrium state. The H_M2_C003 hydrogel again shows the highest G" (676.40 Pa), suggesting that this hydrogel dissipates more energy when deformed. This is followed by the H_M2_C007 hydrogel, which has a G" value of 339.52 Pa. These results imply that even as the gels swell and absorb water, their ability to dissipate energy remains significant, particularly in samples with higher monomer content.

Similar to the equilibrium state, strain softening was observed, with G' decreasing as strain increased. Gels in the swollen state also experienced failure and slippage at higher strains due to the added flexibility from the absorbed water, making them more prone to these issues (see Figure 5.8).

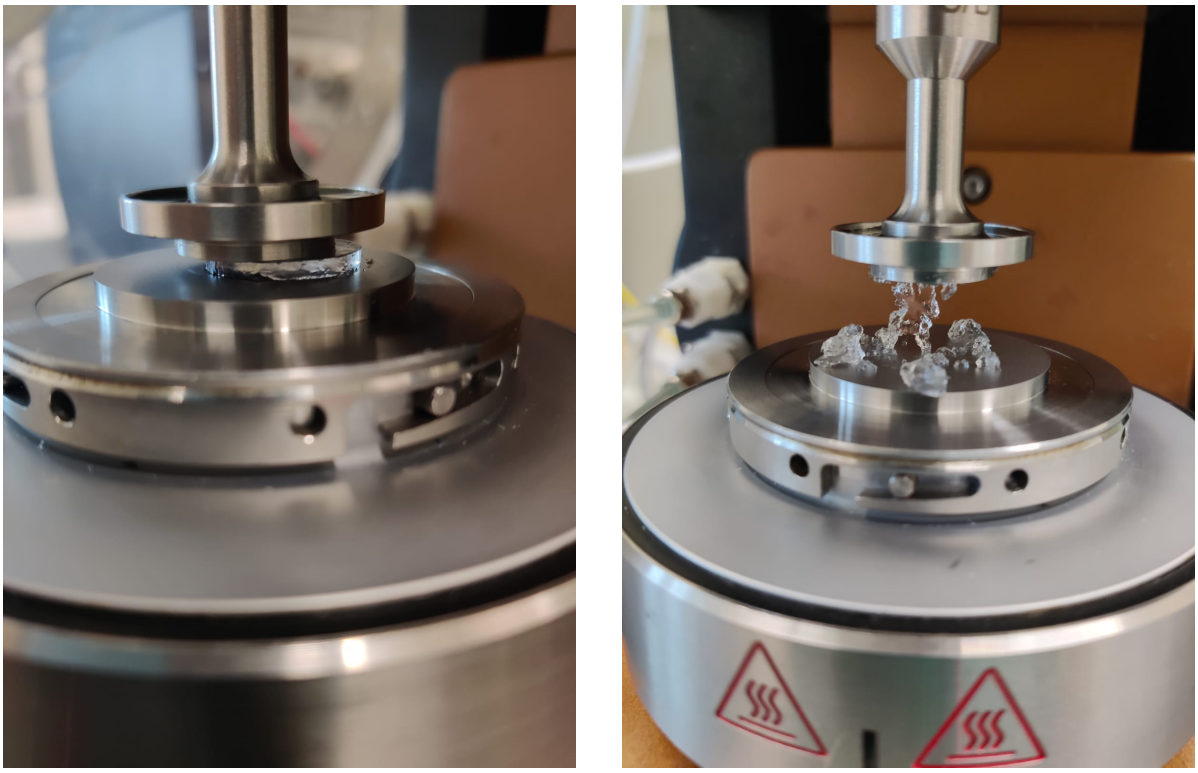

(a) Hydrogel slipping at higher strains.

(b) Hydrogel failure at high strains.

Figure 5.8: Hydrogels slipping or failing at higher strains.

At 38°C (Above LCST)

At 38°C (Figure 5.6(c) & Figure 5.7(a)), the hydrogels are above their LCST, leading to phase change and changes in mechanical properties. The H_M2_C003 hydrogel exhibits the highest G' (2355.10 Pa), indicating that it retains significant stiffness at elevated temperatures. This could be due to a combination of factors: the higher initial stiffness from the higher monomer content and a more thermally stable network structure. The H_M2_C007 hydrogel also shows substantial stiffness (670.04 Pa), but less than the H_M2_C003 hydrogel, possibly because it has a higher crosslinker concentration which might be more susceptible to thermal effects compared to the H_M2_C003 hydrogel's network.

The G" values at 38°C (Figure 5.6(f) & Figure 5.7(b)) reflect the complex behavior of the hydrogels under thermal conditions. The H_M2_C003 hydrogel shows the highest G" (552.35 Pa), indicating substantial energy dissipation due to phase change. The H_M1_C005 hydrogel also shows significant energy dissipation (330.30 Pa), reflecting its less stable network structure at elevated temperatures.

It is important to note that the steep drop in G' observed at 38°C for some samples may be partly due to experimental artifacts. As the hydrogels shrink and release water at this elevated temperature, slippage can occur between the top plate of the rheometer and the gel surface. This slippage could lead to an artificial increase in the measured loss modulus (G") and a corresponding decrease in the measured storage modulus (G').

Additionally, the Strain sweep graphs with G' and G" vs strain for each sample individually be found in appendix A.

In conclusion, Rheometer experiments showed that hydrogels exhibit varying stiffness and energy dissipation characteristics depending on their state (equilibrium, swollen, or above LCST). The results indicated that hydrogels with higher monomer content generally retained better stiffness across different states. In case of increasing crosslinker content, the effect of stiffness was quite the opposite (0.03g showcasing higher stiffness) compared to what was observed in indentation experiments. This is due to the fact that making 2-2.5mm gels was challenging, as incomplete polymerization would occur quite frequently. This effect is also likely due to the difference in testing principles and setups. The experiments also revealed the thermoresponsive behavior of PNIPAM hydrogels, where the stiffness significantly increased above the LCST. However, strain softening was observed consistently across all samples, highlighting that the gel's mechanical limits.

5.4. Swelling & De-swelling experiments

Swelling and deswelling experiments were conducted to examine how varying amounts of monomer and crosslinker influence the hydrogel's ability to absorb and release water.

Swelling experiments

The hydrogels were made following the list of final variatons as mentioned in the Table 5.4. All the hydrogels are of the same shape and size, and have been made in the same mold (Figure 5.10). Following are the results.

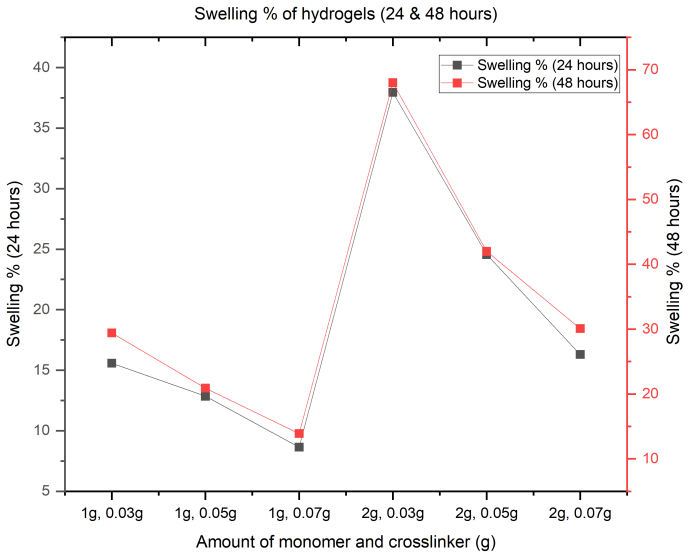

Figure 5.9: Swelling percentages of hydrogels at 24 and 48 hours.

Table 5.11: Swelling % of hydrogels at 24 and 48 hours.

Monomer & crosslinker mass	Weight before swelling (g)	Weight after swelling (24 hours)	Weight after swelling (48 hours)	Swelling % (24 hours)	Swelling % (48 hours)
1g & 0.03g	4.744g	5.483g	6.140g	15.6%	29.4%
1g & 0.05g	4.706g	5.311g	5.690g	12.9%	20.9%
1g & 0.07g	4.451g	4.836g	5.070g	8.7%	13.9%
2g & 0.03g	4.759g	6.565g	7.995g	38%	68%
2g & 0.05g	4.654g	5.797g	6.608g	24.6%	42%
2g & 0.07g	4.539g	5.279g	5.905g	16.3%	30.1%

Figure 5.9 and Table 5.11 offer valuable insights into the swelling behavior of PNIPAM hydrogels below their LCST (32°C). As expected, the data confirms that these hydrogels readily absorb water and swell in this temperature range.

The impact of both monomer and crosslinker content on swelling capacity becomes evident:

Monomer Content: A positive influence is observed (refer to Figure 5.9). As the amount of monomer increases, the number and length of polymer chains within the gel network also grow. This translates to the creation of more available space within the network for water molecules to occupy. Consequently, hydrogels with higher monomer content exhibit a greater swelling ability.

Crosslinker Content: This factor plays an opposing role (refer to Figure 5.9). Crosslinkers act as molecular bridges, tightly connecting individual polymer chains within the network. By adjusting the crosslinker concentration, one essentially controls the network's density and tightness. As the amount of crosslinker increases, the polymer chains become more tightly linked, resulting in a denser network with smaller spaces between the chains. This restricted space hinders the network's ability to expand and absorb water. Therefore, a higher crosslinker concentration in the synthesis solution leads to a decrease in the hydrogel's swelling ability.

Table 5.11 shows the weights of hydrogels before and after swelling. It can be observed that the weight of the hydrogels increases at both 24 and 48 hours, indicating water absorption. However, even at 48 hours, the hydrogel did not reach equilibrium with the water. The weight at 72 hours was not recorded, as the research focused on the 24-hour and 48-hour time points.

Similar trends are highlighted in studies such as [95, 96, 101, 102], which demonstrate how monomer and crosslinker concentrations influence the swelling ability of hydrogels. These studies primarily show that as crosslinker concentrations increase, the gel network becomes denser (with a tighter mesh), resulting in reduced water uptake. The swelling ability in those studies, was also assessed at different temperatures, both below and above the LCST. However, the temperature of the water was 20°C for this thesis.

In essence, the interplay between monomer and crosslinker content plays a crucial role in tailoring the swelling properties of PNIPAM hydrogels for specific applications. By carefully manipulating these factors, anyone can create hydrogels with desired water absorption and desorption characteristics.

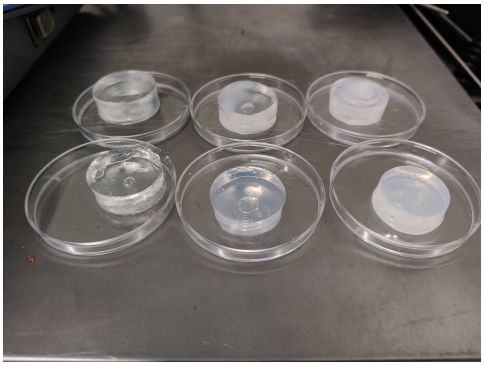

Figure 5.10: Swollen Samples of hydrogels

De-swelling experiments

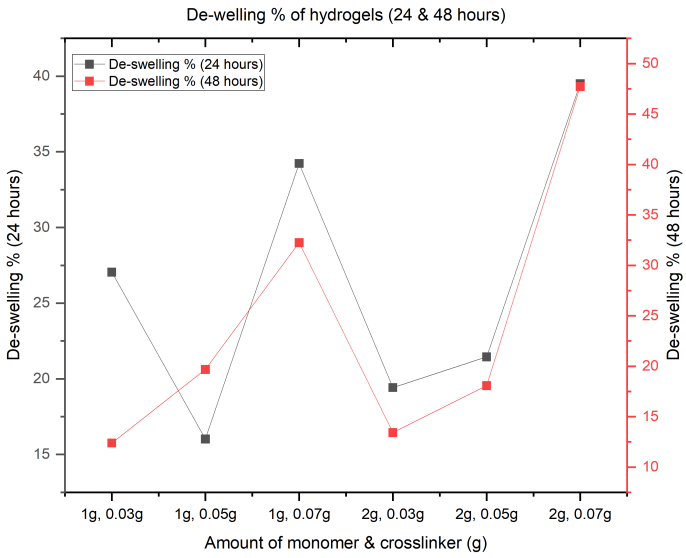

Figure 5.11: De-swelling percentages of hydrogels at 24 and 48 hours.

Table 5.12: De-swelling % of hydrogels at 24 and 48 hours.

Monomer & crosslinker mass	Weight before swelling (g)	Weight after swelling (24 hours)	Weight after swelling (48 hours)	De-swollen weight (24 hours)	De-swollen weight (48 hours)	De-swelling % (24 hours)	De-swelling % (48 hours)
1g & 0.03g	4.744g	5.483g	6.140g	3.999g	5.379g	27.1%	12.4%
1g & 0.05g	4.706g	5.311g	5.690g	4.459g	4.570g	16.0%	19.7%
1g & 0.07g	4.451g	4.836g	5.070g	3.180g	3.436g	34.2%	32.2%
2g & 0.03g	4.759g	6.565g	7.995g	5.290g	6.924g	19.4%	13.4%
2g & 0.05g	4.654g	5.797g	6.608g	4.554g	5.413g	21.4%	18.1%
2g & 0.07g	4.539g	5.279g	5.905g	3.194g	3.088g	39.5%	47.7%

Figure 5.11 and Table 5.12 reveal that deswelling in PNIPAM hydrogels is more nuanced than just network density. While a looser mesh (lower crosslinking) might seem to promote deswelling, the data shows an upward trend with increasing crosslinker content. This phenomenon can be explained by two key factors. First, denser networks formed by higher crosslinking likely exhibit stronger hydrophobic interactions. These interactions become more pronounced in response to deswelling stimuli, such

as heat, causing the hydrogels to expel a greater proportion of their trapped water compared to less dense networks. Second, denser networks hold less water overall due to their limited space (lower swelling), the stronger hydrophobic interactions still effectively drive out a significant portion of this water. Additionally, the extended heat exposure time likely plays a role, providing sufficient time for hydrogels with higher crosslinker content to expel a larger fraction of their water content.

Table 5.12 showcases the reduction in weight recorded after 30 minutes. It is observed that at higher crosslinker concentraion the weight reduces more compared to the lower crosslinker concentrations. As mentioned earlier, it is likely because the gel network representing a tight mesh does not take in much water, but will still push out the amount of water present in the gel matrix.

Deswelling behavior appears to be a complex interplay between the network structure, the response to external stimuli, and the deswelling kinetics. Further investigation is needed to fully understand the influence of factors like monomer and crosslinker content and their combined effects on deswelling behavior in PNIPAM hydrogels.

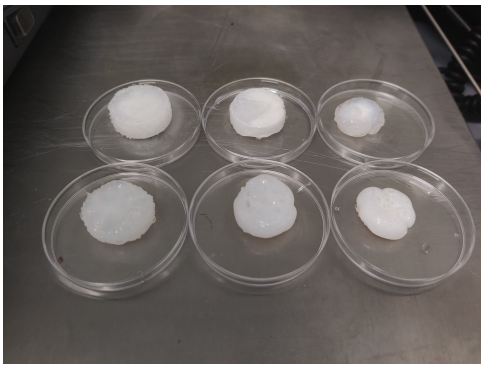

Figure 5.12: De-swollen samples of hydrogels.

In conclusion, swelling and deswelling experiments demonstrated the influence of monomer and crosslinker content on the hydrogels' ability to absorb and release water. Higher monomer content resulted in greater swelling capacity due to the increased availability of space within the polymer network for water molecules. Conversely, higher crosslinker content, while reducing overall swelling, enhanced the deswelling response by promoting stronger internal forces within the hydrogel network. These findings underline the delicate balance between monomer and crosslinker concentrations in optimizing hydrogel performance for specific applications.

Extreme Swelling & De-swelling experiment

Extreme Swelling & De-swelling experiments were done, mainly to check if a dried hydrogel can be revived. This experiment gives an idea of re-usability of the hydrogels. The results are shown in Figure 5.13.

(a) Dried Hydrogel Samples

(b) Dried Samples in Water (Top View)

(c) Dried Samples in Water (Side View)

Figure 5.13: Comparison of Dried Hydrogel Samples and their Rehydration Process

This experiment was performed only once, on two samples of different monomer-crosslinker recipes, namely 2g monomer and 0.03g & 0.05g Crosslinker. The bigger hydrogel in the Figure 5.13(a) was of 0.03g crosslinker and smaller one was of 0.05g crosslinker.

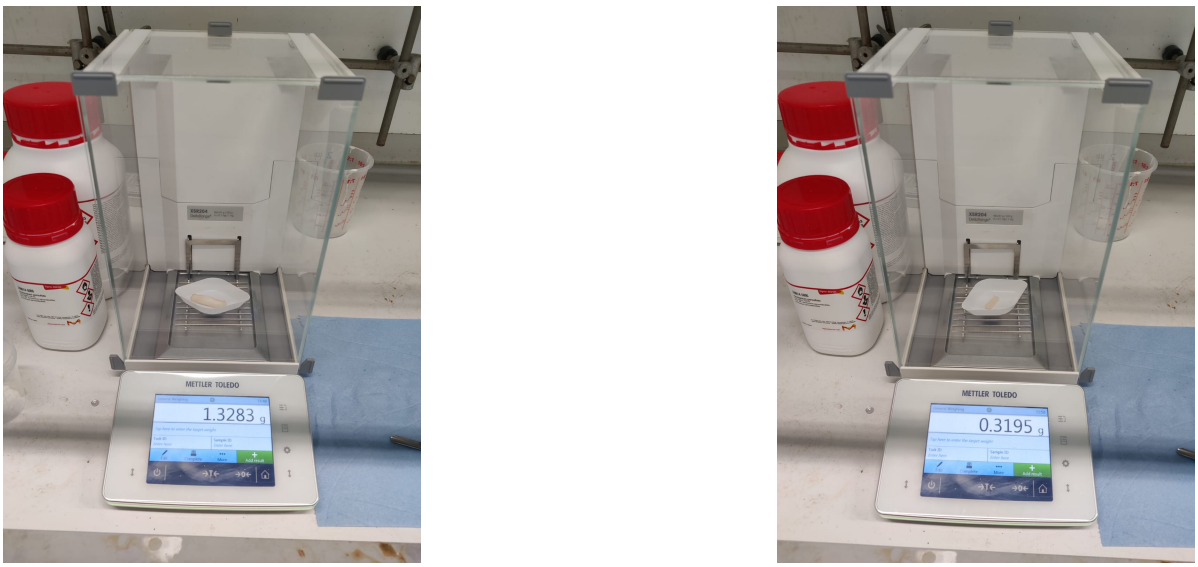

(a) Weight of big Hydrogel Sample (dried)

(b) Weight of Small Hydrogel Sample (dried)

Figure 5.14: Weight of the dried samples

Figure 5.14 shows that, the bigger hydrogel weighs 1.32g and the smaller one weighs 0.31g. These two samples were immersed in water and left for 24 hours, and then weighed again.

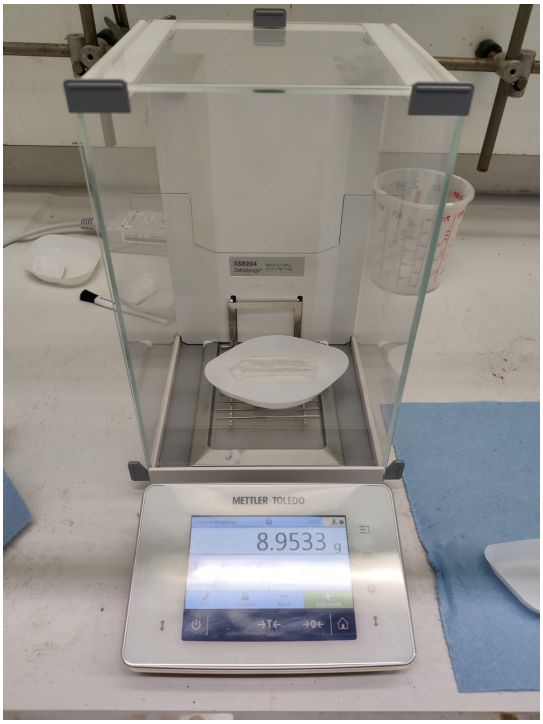

(a) Weight of Big Hydrogel Sample after Rehydration

(b) Big Hydrogel Sample after Rehydration

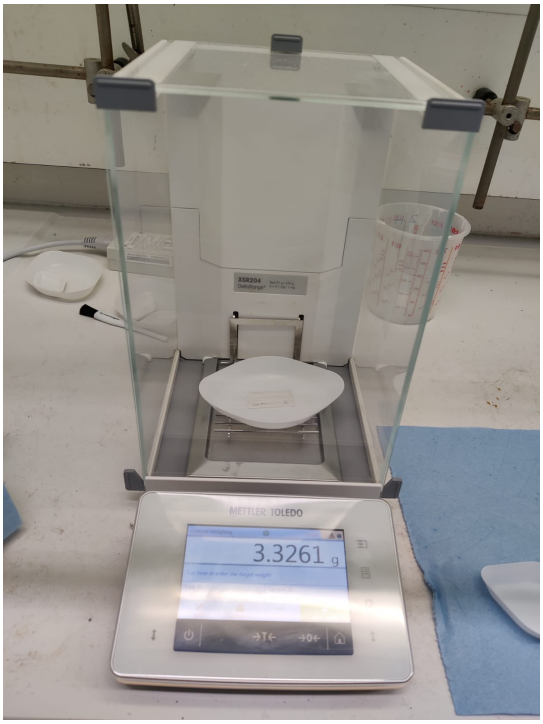

(c) Weight of Small Hydrogel Sample after Rehydration

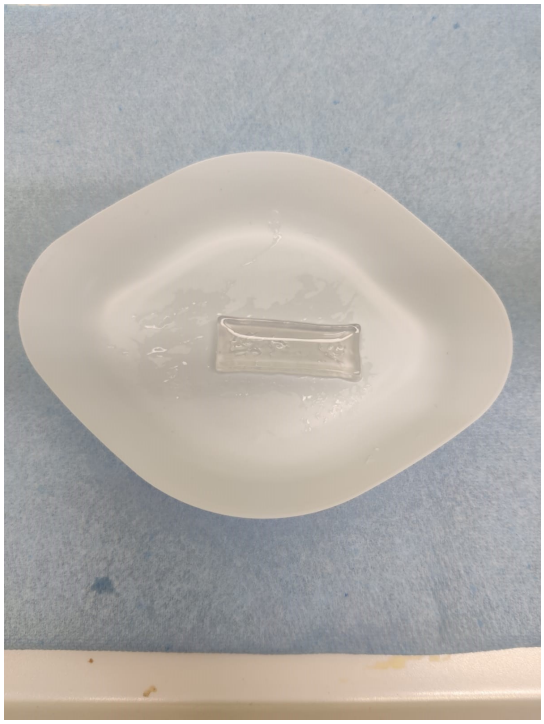

(d) Small Hydrogel Sample after Rehydration

Figure 5.15: Comparison of big and small hydrogel samples and their weights before and after rehydration.

Table 5.13: Swelling ratios of the samples.

Sample	Dry Weight (g)	Rehydrated Weight (g)	Water Uptake Ratio (U)	Water Uptake Ratio (%)
Sample 1 (0.03g crosslinker)	1.383	8.9533	5.474	547.4%
Sample 2 (0.05g crosslinker)	0.3195	3.3261	9.410	941.0%

From the Figure 5.15 and Table 5.13, It is clear that the hydrogels were able to absorb water and swell up again, essentially coming back to life, even after being dried for 4 weeks in open air. This experiment demonstrates the potential for hydrogels to be reused in applications where this is required. While the current time frame involved 4 weeks of drying, longer drying durations could be explored. Additionally, if time is a constraint, the hydrogel samples could be dried more quickly in a vacuum oven. This flexibility suggests that hydrogels could be effectively regenerated and reused, depending on the specific needs of the application.

5.5. Shapes of hydrogels

This experiment showcases a method to overcome the issue of dissolved oxygen which interfers with the polymerization and gelation of the hydrogels. Three shapes namely square slab, rectangular slab & circlular disks" were used and of two different sizes each. Poly (methyl methacrylate) (PMMA) plastic sheets were used to build the enclosure, super glue was used to glue them together and lastly silicone (Ecoflex-30) was applied on the edges to make it air and water tight. Two methods of filling the enclosure with nitrogen gas was used as shown the Figure 4.15. The Table 5.14 shows the different shapes and sizes made, including one special shape (Photos can be found in the appendix C).

Table 5.14: Shapes and sizes of hydrogels

Shapes	Length (mm)	Width (mm)	Diameter (mm)	Thickness (mm)
Sqaure slab	20	20	-	10
Square slab	40	40	-	10
Rectangular slab	20	10	-	10
Rectangular slab	40	20	-	10
Circular disk	-	-	20	10

(a) Shrunken 40mm rectangular slab length.

(b) Shrunken 40mm rectangular slab width.

(c) Shrunken 40mm rectangular slab thickness.

(d) Swollen 40mm rectangular slab length.

(e) Swollen 40mm rectangular slab width.

(f) Swollen 40mm rectangular slab thickness.

Figure 5.16: Comparison of Shrunken and Swollen Samples

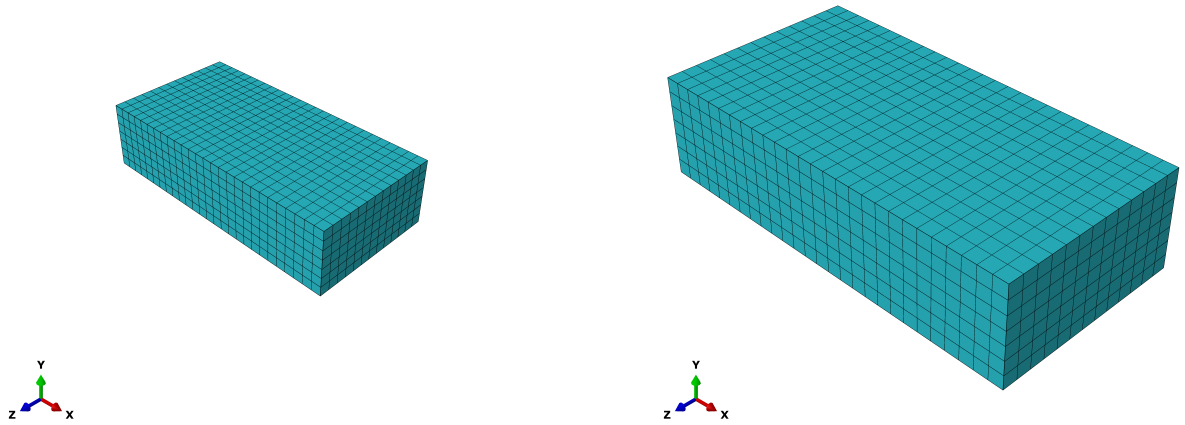

(a) Shrunken state of the 40x20 rectangular slab hydrogel.

(b) Swollen state of the 40x20 rectangular slab hydrogel.

Figure 5.17: Comparison of shrunken and swollen states in simulations

The Figure 5.16 showcase the rectangular slab of hydrogel at shrunken and swollen states made experimentally/physically, and the Figure 5.17 shows the shrunken and swollen states of the rectangular slab in simulations. The rest of the photos can be found in the appendix C. The findings from this experiment are as follows:

1. Too much nitrogen gas: The hydrogels became dry and lost some volume because the constant flow of nitrogen gas. Nitrogen gas not only minimized exposure to oxygen, but also removed moisture from the enclosures. Since the hydrogels are composed of approximately 85% water, they lost water content and began to dry up as a result.
2. Time for nitrogen gas was reduced from 24 hours to first 4 hours, and then to 1 hour. The time for degassing the solution with nitrogen gas was increased to 30 minutes. This proved to be a better solution.
3. The gels have a hint of copper color, and this is likely due to the fact that the solutions prepared were a couple of weeks old. But this did not affect the gelation. Nitrogen gas removing moisture might also have caused this.
4. The thickness after gelation was 8mm for all the models except 20mm dia circular disk. This reduction in thickness is likely due to the exposure to the nitrogen gas while polymerization, which removes moisture from the enclosures and from the gels as well.

Table 5.15: Dimensions of hydrogels at shrunken state and swollen state.

Shrunken dimensions				
Shape	Shrunken length(mm)	Shrunken width (mm)	Shrunken diameter (mm)	Shrunken thickness (mm)
Cube	18.32	18.34		6.79
Cube	39.99	39.99		7.15
Cuboid	18.34	7.65		6.52
Cuboid	40.26	18		6.42
Circular plate			18.19	9.47
Swollen dimensions				
Shape	Final length(mm)	Final width (mm)	Final diameter (mm)	Final thickness (mm)
Cube	22.13	22.13		9.34
Cube	46.69	46.69		10.02
Cuboid	21.7	9.51		10.3
Cuboid	43.04	21.42		9.33
Cylinder			22.47	12.08

Table 5.16: Dimensions of hydrogels in swollen state from simulations.

Swollen dimensions (Simulations)				
Shape	Final length(mm)	Final width (mm)	Final diameter (mm)	Final thickness (mm)
Cube	23.93	23.93		9.51
Cube	52.1	52.1		10.02
Cuboid	23.93	9.14		10.7
Cuboid	52.2	23.49		9.01
Cylinder			23.74	12.3

Hydrogels of various shapes were immersed in deionized water at 20°C for 24 hours (for swelling) and the hydrogels were dried in a vaccum oven for 4 hours (for deswelling). As indicated in Tables 5.15, the hydrogels exhibited significant swelling and de-swelling below and above their (LCST) (32°C). Table 5.16 shows the dimensions of the swollen hydrogels in the simulations. From these two tables it can be seen that there is a discrepancy between the simulation dimensions and the experimental dimensions. The dimensions, specifically length, width and diameter are not close to each other in comparison, while thickness values show very less deviation.

5.5.1. Discrepancies Between Simulation and Experimental Results

The comparison between the simulation and experimental results reveals some discrepancies, which can be attributed to several factors related to the assumptions made during the simulations and the inherent variability of the experimental setup:

1. **Assumptions of Homogeneous Swelling:** The simulations assumed a homogeneous free-swelling state for the hydrogel, leading to uniform swelling behavior in all directions. In reality, the swelling of hydrogels in experiments may not be perfectly uniform due to factors like local variations in material composition, solvent absorption, or environmental conditions. These inhomogeneities could have caused the experimental results to deviate from the idealized simulation predictions.
2. **Fixed Swelling Ratio:** The simulations employed a fixed swelling ratio, corresponding to a specific equilibrium state. This fixed ratio does not account for potential variations in swelling that may occur in experiments due to fluctuations in environmental conditions, such as changes in temperature, humidity, or solvent concentration. These real-world variations can lead to differences in the final dimensions of the hydrogel shapes compared to the simulation results.
3. **Simplified Material Behavior:** The Neo-Hookean model used in the simulations provides a simplified representation of the hydrogel's elastic properties and gel network. However, hydrogels exhibit complex, non-linear behaviors that include viscoelasticity and time-dependent deformation, which are not fully captured by this model. The gel network also might have been quite inhomogenous and as a result, the simulations may not accurately reflect the material's response under experimental conditions, leading to discrepancies.
4. **Constant Temperature Assumptions:** In the simulations, temperature conditions were assumed to be constant and uniform across the entire hydrogel. In contrast, during the experimental process, there might be temperature gradients or fluctuations that affect the swelling behavior of the hydrogel differently in various regions, leading to non-uniform swelling and resulting in discrepancies between the simulated and observed results.
5. **Experimental Variability's:** In addition to the assumptions made in the simulations, variations in the experimental setup, such as minor inconsistencies in the mold design, fabrication process, or measurement techniques, could also contribute to the differences observed between the experimental and simulation results.

The study of hydrogel shapes has demonstrated the intricate behavior of these materials under varying conditions. The experimental results highlighted that while the hydrogels generally exhibited significant swelling, the degree of swelling varied across different shapes and sizes, indicating a complex relationship between the shape and swelling behavior. The comparison between experimental results and simulation predictions revealed discrepancies, likely due to the assumptions and simplifications made

in the simulations. Factors such as homogeneous swelling, fixed swelling ratios, simplified material behavior, and constant temperature conditions in the simulations did not fully capture the nuances of the experimental setup, leading to differences in observed and predicted dimensions. Additionally, experimental variabilities, such as mold imperfections and measurement inconsistencies, further contributed to the discrepancies. Despite these differences, the research underscores the potential for using simulations as a predictive tool, while also emphasizing the need for careful consideration of real-world factors that influence hydrogel behavior.

5.6. Potential application

Given that this research makes a humble contribution to the extensive fields of smart hydrogels and soft robotics, a potential application is suggested. Through the experience of synthesizing the gels and testing their behavior and mechanical properties, one can use the gels either for actuation purposes or for stiffness enhancement purpose for a soft gripper. This research covers how the amount of monomer and crosslinker added to the initial solution can affect the swelling ability and stiffness of the hydrogels. From the results of this research it is observed that an optimal balance between swelling and stiffness can be achieved, or a gel can just have good swelling ability or a it can only have high stiffness. Based on this, the potential application can be a soft gripper which uses the hydrogels for either actuation or to add sufficient stiffness such that it can grab an object. The concept can be seen below Figure 5.18:

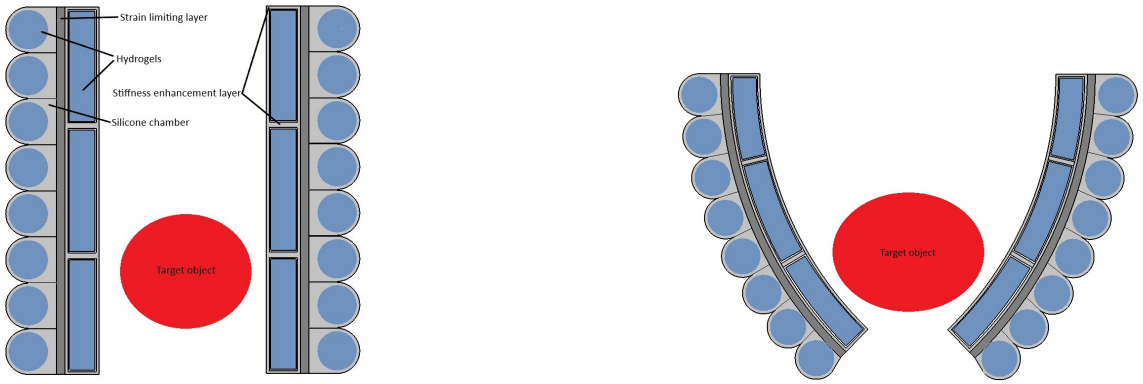

(a) Straight Configuration **(b)** Bent Configuration

Figure 5.18: Comparison of Hydrogel Gripper Configurations

If hydrogels are being used for actuation purposes, such as bending, it is advantageous to first completely dry the hydrogel. This process causes extreme shrinking, making it feel rigid, like plastic. The dried hydrogel can then be placed inside a silicone chamber with dimensions smaller than the hydrogel's original size. By introducing a few milliliters of water into the chamber via a syringe, the dry hydrogel will absorb the water and expand back to its original shape. Depending on the amount of water added, it may even swell beyond its original size over a few days. This increase in size generates sufficient force to bend the entire finger. The ability of a dry hydrogel to swell back to its original shape was demonstrated in the section 4.6. If hydrogels are used as a stiffness enhancement layer, they can provide significant support in increasing the block force—the force exerted by the gripper when fully actuated. During the indentation test (Figure 5.3(c) & Figure 5.3(d)), the hydrogel demonstrated a force of 8N for a displacement of 10mm when tested above LCST, in contrast to a maximum force of 1.8N below the LCST. These results indicate that hydrogels can substantially enhance the block force of a soft robotic gripper, particularly under elevated temperature conditions, thereby improving its overall gripping strength.

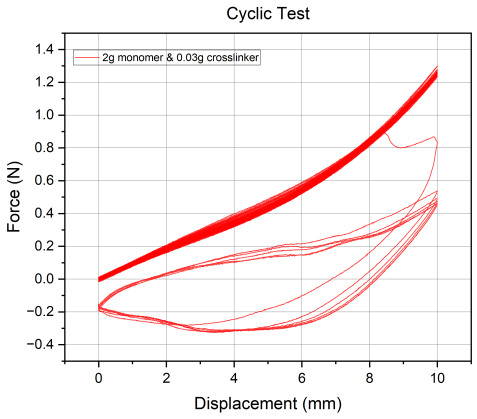

(a) Fatigue test below LCST.

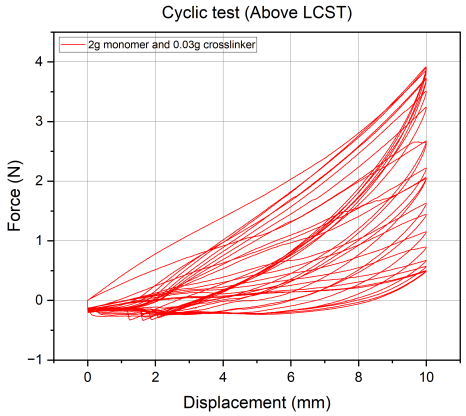

(b) Fatigue test above LCST.

Figure 5.19: Fatigue tests performed on hydrogel below and above LCST.

Figures 5.19(a,b) display the fatigue tests (via indentation) conducted on a hydrogel. When tested below the LCST (see Figure 5.19(a)), the hydrogel exhibited a consistent stress response up until the 45th cycle, where failure occurred. This indicates the durability of the hydrogel when it is below its LCST. In contrast, when tested above the LCST (see Figure 5.19(b)), the stress response gradually decreased after a few cycles, attributed to the hydrogel cooling down and transitioning back to its below LCST state. However, if the elevated temperature conditions are maintained, the stress response remains quite robust.

Lastly, one of the hydrogel shapes produced was a bowtie shape, as shown in Figure 5.20.

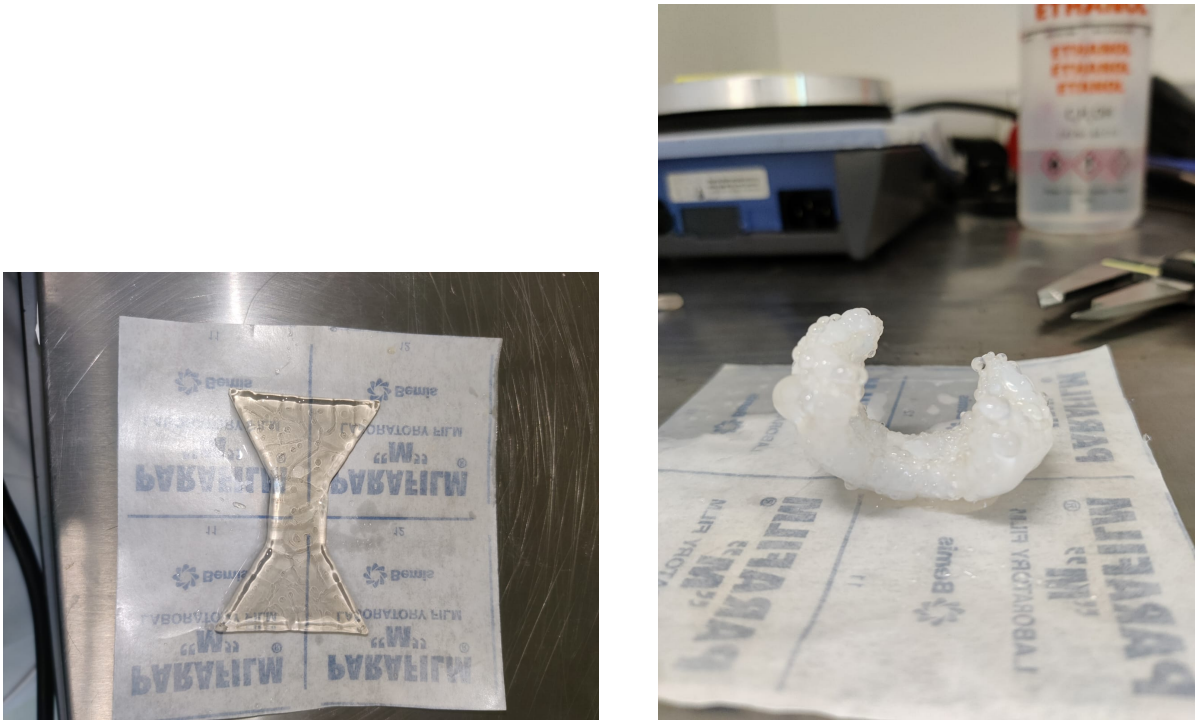

(a) Bow tie shaped hydrogel below LCST. **(b)** Bowtie shaped hydrogel after shrinking for 30 minutes.

Figure 5.20: Bowtie shaped hydrogel before and after shrinking.

This shape exhibited deformation during the shrinking process (see Figure 5.20(b)), likely due to an uneven distribution of the gel matrix caused by its geometry. This suggests that deformable shapes of hydrogels can be created, which, when used in a stiffness enhancement layer, can further contribute to the deformation of the soft gripper while also increasing its stiffness.

This chapter highlights the potential of PNIPAM hydrogels in soft robotics, particularly for enhancing stiffness and actuation. The material's responsiveness to temperature changes and its ability to increase block force above LCST make it a strong candidate for adaptable robotic systems. Fatigue tests also showcased the hydrogel's durability. Overall, these findings support the use of hydrogels in soft robotics, where their unique properties can enhance performance and functionality.

5.7. Conclusion

Chapter 5 presents a comprehensive analysis of the experimental results obtained from various tests conducted on PNIPAM hydrogels. The synthesis experiments successfully demonstrated the impact of varying monomer and crosslinker concentrations on the gelation process and final properties of the hydrogels. Through factorial design experiments, it was evident that the concentrations of monomer and crosslinker play a significant role in determining the mechanical properties and thermoresponsive behavior of the hydrogels.

In the indentation experiments, a clear relationship was established between the stiffness of the hydrogels and the concentration of monomer and crosslinker used. The results revealed that both higher monomer and crosslinker concentrations generally lead to increased stiffness, although excessive crosslinking can cause aggregation, which might negatively affect the material's mechanical properties. This finding was further supported by Young's modulus values calculated from force-displacement data, providing a quantitative measure of the mechanical strength of the hydrogels.

Rheological tests further explored the viscoelastic properties of the hydrogels under different strain conditions, examining the storage modulus (G') and loss modulus (G'') across various states of swelling. These experiments underscored the complex interplay between the hydrogel's internal network structure and its mechanical response to external stimuli, particularly temperature.

Swelling and de-swelling experiments provided insights into the hydrogel's capacity to absorb and release water, highlighting the effects of monomer and crosslinker content on this behavior. The findings indicated that while higher monomer content increases swelling capacity, higher crosslinker content decreased the swelling capacity of the gels. These observations are critical for tailoring hydrogels for specific applications where controlled swelling and deswelling are required.

Simulations using Finite Element Method (FEM) were also conducted to model the swelling behavior of the PNIPAM hydrogels. These simulations provided a computational perspective that complemented the experimental findings, offering predictions on how the hydrogels would respond to temperature-induced swelling and shrinking. The simulations highlighted some discrepancies when compared to experimental results, particularly in accurately predicting the material's behavior under operational conditions. However, they also provided valuable insights that can guide further refinement of the hydrogel models for more precise predictions.

Furthermore, the chapter explored potential applications of PNIPAM hydrogels, particularly in the field of soft robotics. A notable application highlighted is the use of these hydrogels in the development of a soft gripper. The thermoresponsive properties of PNIPAM hydrogels enable the gripper to adjust its stiffness and grip strength in response to temperature changes, making it suitable for handling delicate and irregularly shaped objects. This potential application not only showcases the adaptability and functionality of PNIPAM hydrogels but also underscores their relevance in advancing soft robotics technology.

Overall, Chapter 5 successfully demonstrates the intricate relationship between synthesis parameters and the resulting mechanical and responsive properties of PNIPAM hydrogels. The experiments, along with the simulation data, provide a solid foundation for understanding how to optimize these materials for practical applications, particularly in fields like soft robotics where both mechanical robustness and environmental responsiveness are essential. The potential applications discussed further illustrate the versatility of PNIPAM hydrogels and their promising role in future technological developments.

6

Conclusion & Future recommendations

6.1. Conclusion

This research focused on the synthesis, characterization of Poly(N-isopropylacrylamide) (PNIPAM) hydrogels, with an emphasis on their potential use in soft robotics. The study aimed to understand how various synthesis parameters, particularly the concentrations of monomer and crosslinker, affect the mechanical properties and behavior of these hydrogels. The primary objectives were to develop a reliable method for synthesizing PNIPAM hydrogels, characterize their thermoresponsive behavior, and assess their suitability for applications requiring controlled actuation and enhanced stiffness. The study was driven by the main research question: ”How can PNIPAM hydrogels be synthesized and characterized to optimze their mechanical properties and behavior for use in soft robotics?”

Subresearch Questions and Their Answers

The research was structured around several subresearch questions, which have been addressed in the respective chapters:

1. **How can PNIPAM hydrogels be synthesized effectively?**
This question was addressed in Chapters 2 & 3, where the synthesis process of PNIPAM hydrogels was detailed, including the materials, equipment, and specific steps involved.

2. **What are the factors that affect hydrogel synthesis and its final properties?**
Chapter 3 explored the factors influencing hydrogel’s gelation and final properties. Particularly the monomer and crosslinker concentrations. The study found that varying these concentrations significantly impacts the stiffness, swelling behavior, and overall mechanical properties of the hydrogels.

3. **What are the methods to characterize a hydrogel’s behavior?**
In Chapters 3 & 4, various experimental techniques were utilized to characterize the hydrogels, including rheometer tests, swelling and deswelling experiments. These methods provided insights into the thermal responsive behaviour of the hydrogels, where the hydrogels absorbed or released water based on the temperature variation. The effect of temperature on the mechanical properties was also seen through the experiments conducted.

4. **What are the methods to characterize hydrogel’s mechanical properties?**
In chapter 3 the experimental techniques that can be used to characterize the stiffness of the hydrogels were explained. Following that in the chapter 4 the mechanical properties of the hydrogels, ”stiffness” was characterized using rheometer and indentation experiments. These tests were essential in understanding how the hydrogels respond to stress/strain and temperature changes.

5. **How can hydrogels be fabricated in different shapes and sizes to be effectively used in soft robotics?**

Chapter 3 also addressed the feasibility of creating specific hydrogel shapes. The experimental results demonstrated the successful fabrication of hydrogels in various geometries, although some discrepancies were noted between the simulation and experimental outcomes (swelling wrt volume) likely due to the assumptions made in the simulations or measurement inconsistencies. Lastly the section 5.6 describes the potential application of PNIPAM hydrogels in a soft robotics gripper.

Main Research Question Answered

By systematically addressing these subresearch questions, the main research question has been answered. The synthesis of PNIPAM hydrogels has been successfully achieved, and their behavior and mechanical properties have been thoroughly characterized. The study provides a comprehensive understanding of how varying monomer and crosslinker concentrations affect the performance of these hydrogels, contributing valuable knowledge to the field of smart hydrogels and soft robotics.

Final Remarks

The findings of this research emphasize the importance of precise control over synthesis parameters to tailor PNIPAM hydrogels for specific applications. While simulations offered valuable predictions, the experimental results revealed the complexity of hydrogel behavior in real-world conditions, suggesting areas for improvement in modeling techniques.

This study focused on the synthesis, characterization, and application of PNIPAM hydrogels, with an emphasis on their potential use in soft robotics. The research demonstrated that adjusting monomer and crosslinker concentrations can finely tune the mechanical properties of these hydrogels, such as stiffness and swelling ability. The study also successfully fabricated hydrogels in various geometries, which is critical for practical applications in soft robotics.

Furthermore, the experimental results confirmed the thermoresponsive nature of PNIPAM hydrogels, showcasing their ability to undergo reversible volume changes in response to temperature variations—an essential feature for applications in soft robotics requiring controlled actuation and flexibility.

Lastly, the experimental results provided valuable insights into the behavior and mechanical properties of hydrogels, leading to the identification of potential applications in soft robotics. Hydrogels were shown to be useful either for actuation or as a stiffness enhancement layer. The creation of deformable hydrogel shapes, exemplified by the bowtie shape, further highlighted the versatility of these materials and their possible uses in advanced soft robotic systems.

6.2. Future recommendations

Building on the findings of this study, several avenues for future research have been identified. Firstly, further experimentation with varying concentrations of initiators and accelerators could yield deeper insights into the optimal synthesis conditions for PNIPAM hydrogels, potentially enhancing their mechanical properties and responsiveness. Additionally, exploring the combination of PNIPAM hydrogels with other smart materials could open new possibilities for creating multi-functional systems in soft robotics.

Another promising area for future research is predicting (simulating) the behavior of hydrogels under different monomer and crosslinker concentrations or varying crosslinking densities, and then comparing these predictions with the experimental behavior of gels. This would help assess the accuracy of simulations and identify ways to improve the models used, ultimately enabling the design of hydrogels with tailored mechanical and responsive properties for specific applications.

Furthermore, conducting frequency sweeps using a rheometer would provide valuable insights into the gel's recovery behavior, helping to understand its performance under repeated actuation cycles with varying environmental conditions. Such a study could offer essential data to improve the reliability of hydrogels and expand their applications in industrial and biomedical fields. Additionally, determining a method to perform tensile and compressive tests on the hydrogels would be highly beneficial. When combined with the indentation and rheometer experiments, these tests would provide a comprehensive understanding of the hydrogel's mechanical properties.

Finally, further exploration into creating and testing deformable shapes of hydrogels could open up new avenues in soft robotics, providing customized solutions for unique challenges in actuation and stiffness enhancement.

In conclusion, this research has laid a solid foundation for the development of PNIPAM hydrogels with tailored properties for use in soft robotics and other advanced technologies. The insights gained from this study will guide future efforts to refine these materials, ensuring their effective applications in the extensive field of soft robotics.

References

1. El-Atab, N. *et al.* Soft Actuators for Soft Robotic Applications: A Review. *Advanced Intelligent Systems* **2.** ISSN: 2640-4567 (10 Oct. 2020).
2. Lee, Y., Song, W. J. & Sun, J. Y. *Hydrogel soft robotics* Dec. 2020.
3. Shintake, J., Cacucciolo, V., Floreano, D. & Shea, H. *Soft Robotic Grippers* July 2018.
4. Ding, M. *et al. Multifunctional soft machines based on stimuli-responsive hydrogels: from free-standing hydrogels to smart integrated systems* Dec. 2020.
5. Ahmed, E. M. *Hydrogel: Preparation, characterization, and applications: A review* 2015.
6. Hydrogels review 2015.
7. Hydrogels review 2015.
8. Jani, J. M., Leary, M., Subic, A. & Gibson, M. A. *A review of shape memory alloy research, applications and opportunities* Apr. 2014.
9. Bahl, S., Nagar, H., Singh, I. & Sehgal, S. *Smart materials types, properties and applications: A review* in. **28** (Elsevier Ltd, 2020), 1302–1306.
10. N, G. & M, F. Smart Materials and Structures: State of the Art and Applications. *Nano Research & Applications* **04** (02 2018).
11. Jovanova, J. & Chen, Q. *Graduation project Modelling a novel design of soft grippers actuated by smart hydrogel* 2023.
12. Ölander, A. An electrochemical investigation of solid cadmium-gold alloys. *Journal of the American Chemical Society* **54,** 3819–3833 (1932).
13. Kauffman, G. B. *The Story of Nitinol: The Serendipitous Discovery of the Memory Metal and Its Applications*
14. Buehler, W. J., Gilfrich, J. V. & Wiley, R. C. Effect of Low□Temperature Phase Changes on the Mechanical Properties of Alloys near Composition TiNi. *Journal of Applied Physics* **34,** 1475–1477. ISSN: 0021-8979. eprint: `https://pubs.aip.org/aip/jap/article-pdf/34/5/1475/18328767/1475\_1\_online.pdf`. `https://doi.org/10.1063/1.1729603` (May 1963).
15. Holman, H., Kavarana, M. N. & Rajab, T. K. Smart materials in cardiovascular implants: Shape memory alloys and shape memory polymers. *Artificial organs* **45,** 454–463 (2021).
16. Sekhar, M. C. *et al. A Review on Piezoelectric Materials and Their Applications* Feb. 2023.
17. Karan, S. K. *et al. Recent Advances in Self-Powered Tribo-/Piezoelectric Energy Harvesters: All-In-One Package for Future Smart Technologies* Nov. 2020.
18. Zhao, W., Jin, X., Cong, Y., Liu, Y. & Fu, J. Degradable natural polymer hydrogels for articular cartilage tissue engineering. *Journal of Chemical Technology Biotechnology* **88,** 327–339 (2013).
19. Iizawa, T. *et al.* Synthesis of porous poly (N-isopropylacrylamide) gel beads by sedimentation polymerization and their morphology. *Journal of applied polymer science* **104,** 842–850 (2007).
20. Yang, L., Chu, J. S. & Fix, J. A. Colon-specific drug delivery: new approaches and in vitro/in vivo evaluation. *International journal of pharmaceutics* **235,** 1–15 (2002).
21. Maolin, Z., Jun, L., Min, Y. & Hongfei, H. The swelling behavior of radiation prepared semi-interpenetrating polymer networks composed of polyNIPAAm and hydrophilic polymers. *Radiation Physics and Chemistry* **58,** 397–400 (2000).
22. Akhtar, M. F., Hanif, M. & Ranjha, N. M. *Methods of synthesis of hydrogels … A review* Sept. 2016.

23. Jiménez-Rosado, P. ; & Romero, M. ; Citation: Sánchez-Cid. *Polymers* **2022,** 3023. https://doi.org/10.3390/polym (2022).
24. Hacker, M. C., Krieghoff, J. & Mikos, A. G. in *Principles of regenerative medicine* 559–590 (Elsevier, 2019).
25. Shi, Q. *et al. Bioactuators based on stimulus-responsive hydrogels and their emerging biomedical applications* Dec. 2019.
26. Bashir, S. *et al. Fundamental concepts of hydrogels: Synthesis, properties, and their applications* Nov. 2020.
27. Castiblanco, P. A., Ramirez, J. L. & Rubiano, A. Smart materials and their application in robotic hand systems: A state of the art. *Indonesian Journal of Science and Technology* **6,** 401–426. ISSN: 25278045 (2 2021).
28. Palleau, E., Morales, D., Dickey, M. D. & Velev, O. D. Reversible patterning and actuation of hydrogels by electrically assisted ionoprinting. *Nature Communications* **4.** ISSN: 20411723 (2013).
29. Li, L., Scheiger, J. M. & Levkin, P. A. Design and Applications of Photoresponsive Hydrogels. *Advanced Materials* **31.** ISSN: 15214095 (26 June 2019).
30. Alaei, J., Boroojerdi, S. H. & Rabiei, Z. Application of hydrogels in drying operation. *Petroleum & Coal* **47,** 32–37 (2005).
31. Ogata, T., Nagayoshi, K., Nagasako, T., Kurihara, S. & Nonaka, T. Synthesis of hydrogel beads having phosphinic acid groups and its adsorption ability for lanthanide ions. *Reactive and Functional Polymers* **66,** 625–633. ISSN: 13815148 (6 June 2006).
32. Hunkeler, D. Synthesis and characterization of high molecular weight water-soluble polymers. *Polymer international* **27,** 23–33 (1992).
33. Watanabe, N., Hosoya, Y., Tamura, A. & Kosuge, H. Characteristics of water-absorbent polymer emulsions. *Polymer international* **30,** 525–531 (1993).
34. Talaat, H. *et al.* Development of a multi-component fertilizing hydrogel with relevant techno-economic indicators. *Am-Euras J Agric Environ Sci* **3,** 764–70 (2008).
35. Qunyi, T. & Ganwei, Z. Rapid synthesis of a superabsorbent from a saponified starch and acrylonitrile/AMPS graft copolymers. *Carbohydrate Polymers* **62,** 74–79. ISSN: 01448617 (1 Oct. 2005).
36. Karadağ, E., Saraydın, D. & Güven, O. Radiation induced superabsorbent hydrogels. Acrylamide/itaconic acid copolymers. *Macromolecular Materials and Engineering* **286,** 34–42 (2001).
37. Boral, S., Gupta, A. N. & Bohidar, H. B. Swelling and de-swelling kinetics of gelatin hydrogels in ethanol-water marginal solvent. *International Journal of Biological Macromolecules* **39,** 240–249. ISSN: 01418130 (4-5 Nov. 2006).
38. Kim, S. Y., Shin, H. S., Lee, Y. M. & Jeong, C. N. Properties of electroresponsive poly (vinyl alcohol)/poly (acrylic acid) IPN hydrogels under an electric stimulus. *Journal of applied polymer science* **73,** 1675–1683 (1999).
39. Shih, H. & Lin, C. C. Cross-linking and degradation of step-growth hydrogels formed by thiol-ene photoclick chemistry. *Biomacromolecules* **13,** 2003–2012. ISSN: 15257797 (7 July 2012).
40. Qu, X., Wirsén, A. & Albertsson, A.-C. Structural change and swelling mechanism of pH-sensitive hydrogels based on chitosan and D, L-lactic acid. *Journal of applied polymer science* **74,** 3186–3192 (1999).
41. Zhang, R., Tang, M., Bowyer, A., Eisenthal, R. & Hubble, J. A novel pH- and ionic-strength-sensitive carboxy methyl dextran hydrogel. *Biomaterials* **26,** 4677–4683. ISSN: 01429612 (22 Aug. 2005).
42. Kline, S. *KINETICS OF DRUG RELEASE FROM HYDROGEL MATRICES* Ping I. Lee* 1985.
43. Dolbow, J., Fried, E. & Ji, H. Chemically induced swelling of hydrogels. *Journal of the Mechanics and Physics of Solids* **52,** 51–84. ISSN: 00225096 (1 Jan. 2004).

44. Ehrenhofer, A., Binder, S., Gerlach, G. & Wallmersperger, T. Multisensitive Swelling of Hydrogels for Sensor and Actuator Design. *Advanced Engineering Materials* **22.** ISSN: 15272648 (7 July 2020).
45. Ahmad, Z. *et al. Versatility of Hydrogels: From Synthetic Strategies, Classification, and Properties to Biomedical Applications* Mar. 2022.
46. Oyen, M. L. *Mechanical characterisation of hydrogel materials* 2014.
47. Li, X. *et al.* Hybrid dual crosslinked polyacrylic acid hydrogels with ultrahigh mechanical strength, toughness and self-healing properties via soaking salt solution. *Polymer* **121,** 55–63. ISSN: 00323861 (July 2017).
48. McKee, C. T., Last, J. A., Russell, P. & Murphy, C. J. Indentation versus tensile measurements of young's modulus for soft biological tissues. *Tissue Engineering - Part B: Reviews* **17,** 155–164. ISSN: 19373368 (3 June 2011).
49. Drury, J. L., Dennis, R. G. & Mooney, D. J. The tensile properties of alginate hydrogels. *Biomaterials* **25,** 3187–3199. ISSN: 01429612 (16 2004).
50. Virk, A. S., Hall, W. & Summerscales, J. Failure strain as the key design criterion for fracture of natural fibre composites. *Composites Science and Technology* **70,** 995–999. ISSN: 02663538 (6 June 2010).
51. Urayama, K., Taoka, Y., Nakamura, K. & Takigawa, T. Markedly compressible behaviors of gellan hydrogels in a constrained geometry at ultraslow strain rates. *Polymer* **49,** 3295–3300. ISSN: 00323861 (15 July 2008).
52. Roylance, D. Introduction to elasticity. *Cambridge, MA* **2139,** 7 (2000).
53. McKee, J. R. *et al.* Thermoresponsive nanocellulose hydrogels with tunable mechanical properties. *ACS Macro Letters* **3,** 266–270. ISSN: 21611653 (3 Mar. 2014).
54. Hadryś, D., Węgrzyn, T., Piwnik, J., Wszołek, L. & Węgrzyn, D. Compressive strength of steel frames after welding with micro-jet cooling. *Archives of Metallurgy and Materials* **61,** 123–126. ISSN: 17333490 (1 2016).
55. Pal, S. *et al. Chronic inflammation and cancer: potential chemoprevention through nuclear factor kappa B and p53 mutual antagonism* 2014. http://www.journal-inflammation.com/content/11/1/23.
56. Vedadghavami, A. *et al. Manufacturing of hydrogel biomaterials with controlled mechanical properties for tissue engineering applications* Oct. 2017.
57. Whitehead, A. J. & Page, T. F. *Nanoindentation studies of thin film coated systems* 1992.
58. Ahearne, M., Yang, Y. & Liu, K.-K. *Mechanical Characterisation of Hydrogels for Tissue Engineering Applications Hydrogels for Tissue Engineering* 2008.
59. Weitz, D., Wyss, H. & Larsen, R. Oscillatory rheology: Measuring the viscoelastic behaviour of soft materials. *GIT laboratory journal Europe* **11,** 68–70 (2007).
60. Zuidema, J. M., Rivet, C. J., Gilbert, R. J. & Morrison, F. A. A protocol for rheological characterization of hydrogels for tissue engineering strategies. *Journal of Biomedical Materials Research - Part B Applied Biomaterials* **102,** 1063–1073. ISSN: 15524981 (5 2014).
61. Grattoni, C. A., Al-Sharji, H. H., Yang, C., Muggeridge, A. H. & Zimmerman, R. W. Rheology and permeability of crosslinked polyacrylamide gel. *Journal of Colloid and Interface Science* **240,** 601–607. ISSN: 00219797 (2 Aug. 2001).
62. Ravanagh, G. M. & Ross-Murphy, S. B. *RHEOLOGICAL CHARACTERISATION OF POLYMER GELS* 1998.
63. Kloxin, A. M., Kloxin, C. J., Bowman, C. N. & Anseth, K. S. Mechanical properties of cellularly responsive hydrogels and their experimental determination. *Advanced Materials* **22,** 3484–3494. ISSN: 09359648 (31 Aug. 2010).
64. Neumann, M. *et al. Stimuli-Responsive Hydrogels: The Dynamic Smart Biomaterials of Tomorrow* Nov. 2023.

65. Haq, M. A., Su, Y. & Wang, D. *Mechanical properties of PNIPAM based hydrogels: A review* Jan. 2017.
66. Tang, L. *et al. Poly(N-isopropylacrylamide)-based smart hydrogels: Design, properties and applications* Jan. 2021.
67. Scarpa, J. S., Mueller, D. D. & Klotz, I. M. Slow hydrogen-deuterium exchange in a non-. alpha.-helical polyamide. *Journal of the American Chemical Society* **89,** 6024–6030 (1967).
68. Din, M. I. *et al.* Recent progress of poly (N-isopropylacrylamide) hybrid hydrogels: synthesis, fundamentals and applications–review. *Soft Materials* **16,** 228–247 (2018).
69. Nagase, K., Yamato, M., Kanazawa, H. & Okano, T. Poly (N-isopropylacrylamide)-based thermoresponsive surfaces provide new types of biomedical applications. *Biomaterials* **153,** 27–48 (2018).
70. Heskins, M. & Guillet, J. E. Solution properties of poly (N-isopropylacrylamide). *Journal of Macromolecular Science—Chemistry* **2,** 1441–1455 (1968).
71. Pelton, R. & Chibante, P. Preparation of aqueous latices with N-isopropylacrylamide. *Colloids and surfaces* **20,** 247–256 (1986).
72. Xia, L.-W. *et al.* Nano-structured smart hydrogels with rapid response and high elasticity. *Nature communications* **4,** 2226 (2013).
73. Erol, O., Pantula, A., Liu, W. & Gracias, D. H. Transformer hydrogels: A review. *Advanced Materials Technologies* **4,** 1900043 (2019).
74. Hirokawa, Y. & Tanaka, T. Volume phase transition in a nonionic gel. *The Journal of chemical physics* **81,** 6379–6380 (1984).
75. Sun, T., Song, W. & Jiang, L. Control over the responsive wettability of poly (N-isopropylacrylamide) film in a large extent by introducing an irresponsive molecule. *Chemical communications,* 1723–1725 (2005).
76. Wang, X. & Wu, C. Light-scattering study of coil-to-globule transition of a poly (N-isopropylacrylamide) chain in deuterated water. *Macromolecules* **32,** 4299–4301 (1999).
77. Wang, M. *et al.* Binary solvent colloids of thermosensitive poly (N-isopropylacrylamide) microgel for smart windows. *Industrial & Engineering Chemistry Research* **53,** 18462–18472 (2014).
78. Füllbrandt, M. *et al.* Dynamics of linear poly (N-isopropylacrylamide) in water around the phase transition investigated by dielectric relaxation spectroscopy. *The Journal of Physical Chemistry B* **118,** 3750–3759 (2014).
79. Keerl, M. & Richtering, W. Synergistic depression of volume phase transition temperature in copolymer microgels. *Colloid and Polymer Science* **285,** 471–474 (2007).
80. Gao, G. *et al.* Snap-buckling motivated controllable jumping of thermo-responsive hydrogel bilayers. *ACS applied materials & interfaces* **10,** 41724–41731 (2018).
81. Zhao, Y. *et al.* Soft phototactic swimmer based on self-sustained hydrogel oscillator. *Science robotics* **4,** eaax7112 (2019).
82. Yu, C. *et al.* Electronically programmable, reversible shape change in two-and three-dimensional hydrogel structures. *Adv. Mater* **25,** 1541–1546 (2013).
83. Ghosh, S. & Cai, T. Controlled actuation of alternating magnetic field-sensitive tunable hydrogels. *Journal of Physics D: Applied Physics* **43,** 415504 (2010).
84. Mamada, A., Tanaka, T., Kungwatchakun, D. & Irie, M. Photoinduced phase transition of gels. *Macromolecules* **23,** 1517–1519 (1990).
85. Satoh, T., Sumaru, K., Takagi, T. & Kanamori, T. Fast-reversible light-driven hydrogels consisting of spirobenzopyran-functionalized poly (N-isopropylacrylamide). *Soft Matter* **7,** 8030–8034 (2011).
86. Ansari, M. J. *et al. Poly(N-isopropylacrylamide)-Based Hydrogels for Biomedical Applications: A Review of the State-of-the-Art* July 2022.

87. Takigawa, T., Yamawaki, T., Takahashi, K. & Masuda, T. Change in Young's modulus of poly (N-isopropylacrylamide) gels by volume phase transition. *Polymer Gels and Networks* **5,** 585–589 (1998).

88. Puleo, G. *et al.* Mechanical and rheological behavior of pNIPAAM crosslinked macrohydrogel. *Reactive and Functional Polymers* **73,** 1306–1318 (2013).

89. Fei, R., George, J. T., Park, J. & Grunlan, M. A. Thermoresponsive nanocomposite double network hydrogels. *Soft Matter* **8,** 481–487 (2012).

90. Fei, R., George, J. T., Park, J., Means, A. K. & Grunlan, M. A. Ultra-strong thermoresponsive double network hydrogels. *Soft Matter* **9,** 2912–2919 (2013).

91. Stojkov, G., Niyazov, Z., Picchioni, F. & Bose, R. K. *Relationship between structure and rheology of hydrogels for various applications* Dec. 2021.

92. Choi, J. H. *et al.* Development of a Temperature-Responsive Hydrogel Incorporating PVA into NIPAAm for Controllable Drug Release in Skin Regeneration. *ACS Omega* **8,** 44076–44085. ISSN: 24701343 (46 Nov. 2023).

93. Visentin, F., Babu, S. P. M., Meder, F. & Mazzolai, B. Selective Stiffening in Soft Actuators by Triggered Phase Transition of Hydrogel-Filled Elastomers. *Advanced Functional Materials* **31.** ISSN: 16163028 (32 Aug. 2021).

94. Hu, Y. *et al.* Novel temperature/pH-responsive hydrogels based on succinoglycan/poly(N-isopropylacrylamide) with improved mechanical and swelling properties. *European Polymer Journal* **174.** ISSN: 00143057 (July 2022).

95. Luo, R. & Chen, C.-H. *Supporting Information One-step hydrothermal route to programmable stimuli-responsive hydrogels* 2015.

96. Adrus, N. & Ulbricht, M. Rheological studies on PNIPAAm hydrogel synthesis via in situ polymerization and on resulting viscoelastic properties. *Reactive and Functional Polymers* **73,** 141–148. ISSN: 13815148 (1 Jan. 2013).

97. Sasson, A., Patchornik, S., Eliasy, R., Robinson, D. & Haj-Ali, R. Hyperelastic mechanical behavior of chitosan hydrogels for nucleus pulposus replacement-Experimental testing and constitutive modeling. *Journal of the Mechanical Behavior of Biomedical Materials* **8,** 143–153. ISSN: 17516161 (Apr. 2012).

98. Kim, S. & Lee, J. Indentation and temperature response of liquid metal/hydrogel composites. *Journal of Industrial and Engineering Chemistry* **110,** 225–233. ISSN: 22345957 (June 2022).

99. Puleo, G. L. *et al.* Mechanical and rheological behavior of pNIPAAM crosslinked macrohydrogel. *Reactive and Functional Polymers* **73,** 1306–1318. ISSN: 13815148 (9 2013).

100. Esteki, M. H. *et al.* A new framework for characterization of poroelastic materials using indentation. *Acta Biomaterialia* **102,** 138–148. ISSN: 18787568 (Jan. 2020).

101. Ahearne, M., Yang, Y. & Liu, K.-K. *Mechanical Characterisation of Hydrogels for Tissue Engineering Applications Hydrogels for Tissue Engineering* 2008.

102. Czerner, M., Fellay, L. S., Suárez, M. P., Frontini, P. M. & Fasce, L. A. Determination of Elastic Modulus of Gelatin Gels by Indentation Experiments. *Procedia Materials Science* **8,** 287–296. ISSN: 22118128 (2015).

Smart Hydrogel Engineering for Soft Robotics: Synthesis, Characterization, and Mechanical Properties of PNIPAM Hydrogel

Srinivas Ajit Sagaram Radhakrishna [a], Jovana Jovanova [a], Q.(Aaron) Chen [a], Baris Kumru [a],

[a] *Department of Maritime and Transport Technology, Delft University of Technology, Mekelweg 2, 2628 CD, Delft, Zuid Holland, The Netherlands*

Abstract

The development of smart materials is critical for advancing technologies in soft robotics, where adaptability and environmental responsiveness are essential. This research investigates the synthesis, characterization, and mechanical properties of thermoresponsive Poly(N-isopropylacrylamide) (PNIPAM) hydrogels, which are capable of reversible volume changes in response to temperature variations. By varying the concentrations of monomers and crosslinkers, the study explores how these parameters influence the hydrogels' swelling behavior and mechanical properties. Through a combination of experimental techniques, including rheometry, indentation tests, and swelling-deswelling analysis, the results demonstrate that both stiffness and swelling capacity are directly affected by the synthesis conditions. The study also integrates simulation analysis to predict hydrogel behavior, highlighting both the potential and the limitations of current modeling techniques. The findings suggest that PNIPAM hydrogels are promising candidates for soft robotic applications, particularly in scenarios requiring precise control of mechanical properties and responsive actuation. Future research should focus on refining simulation models and exploring scalable production methods to enhance the practical application of these hydrogels in advanced robotics.

Key words: Poly (N-isopropylacrylamide) (PNIPAM), Smart hydrogels, Thermo-responsive hydrogel, PNIPAM hydrogel synthesis, Hydrogel characterization, LCST (Lower critical solution temperature).

1 Introduction

The fields of robotics and materials science have witnessed substantial progress in recent years, particularly through the advent of soft robotics and the development of smart materials. Traditional robotics, predominantly characterized by rigid, metal-based machines, has been pivotal in industrial automation, effectively performing repetitive and hazardous tasks in controlled environments [1]. However, the inherent rigidity of these systems limits their adaptability and safety in applications that require interaction with delicate objects or human tissues [2].

Soft robotics has emerged to address these limitations, focusing on the creation of robots composed of compliant materials such as elastomers and hydrogels [2]. These materials enable the robots to perform intricate and sensitive tasks, such as handling fragile items in fields like agriculture, healthcare, and logistics [1]. This shift towards softer, more adaptable robots has opened new possibilities, especially in healthcare, where soft robotic systems can be employed in minimally invasive surgeries or as prosthetic devices that closely mimic the natural movement of human limbs [2]. Central to the advancement of soft robotics is the development of smart materials—materials that can alter their properties in response to external stimuli [2]. Among these, hydrogels stand out due to their three-dimensional, hydrophilic polymer networks that can absorb and retain significant amounts of water [3], [4]. Their biocompatibility, flexibility, and ability to undergo substantial volume changes in response to environmental triggers make hydrogels particularly suitable for applications in soft robotics [3], [5]. These properties allow hydrogels to act as actuators, sensors, and even drug delivery systems, adapting their behavior according to temperature, pH, or electric fields.

This paper focuses specifically on the synthesis and characterization of thermoresponsive hydrogels, with an emphasis on Poly(N-isopropylacrylamide) (PNIPAM). PNIPAM is a well-studied polymer known for its lower

critical solution temperature (LCST) around 32°C, which enables reversible swelling and shrinking behavior in response to temperature changes [6], [7]. This unique property is particularly useful in applications requiring controlled actuation, such as in soft robotic grippers or in drug delivery systems where release can be triggered by body temperature.

The mechanical properties of PNIPAM hydrogels, such as elasticity and strength, are critical for their performance in real-world applications. These properties are significantly influenced by the synthesis parameters, including the concentrations of monomers and crosslinkers used during polymerization [7]. Tailoring these parameters is essential for optimizing the hydrogels for specific uses in soft robotics, ensuring a balance between flexibility and mechanical robustness.

This research aims to investigate the relationship between synthesis parameters and the resulting mechanical properties of PNIPAM hydrogels, contributing to the broader understanding and application of these materials in innovative fields like soft robotics.

2 Synthesis of Hydrogels

Hydrogels are three-dimensional polymeric networks capable of absorbing and retaining large amounts of water or biological fluids [8]. The network structure is formed through the cross-linking of hydrophilic polymer chains, which can be derived from both natural and synthetic polymers [5]. The unique ability of hydrogels to swell in the presence of water while maintaining their structure is due to the hydrophilic functional groups attached to the polymer backbone [3]. This characteristic makes hydrogels suitable for a wide range of applications, from drug delivery systems to tissue engineering and soft robotics.

The synthesis of hydrogels typically involves polymerization processes that create cross-linked structures [9]. The most common method is free-radical polymerization, where monomers with reactive vinyl groups are polymerized in the presence of a cross-linker [8], [10]. The cross-linker introduces covalent bonds between polymer chains, forming a stable network. The polymerization process can be initiated using thermal initiators, photoinitiators, or redox systems, depending on the desired properties of the hydrogel and the specific application [3].

Poly(N-isopropylacrylamide) (PNIPAM) hydrogels are a well-known class of thermoresponsive hydrogels, which undergo reversible volume changes in response to temperature variations [7]. PNIPAM hydrogels are synthesized through the free-radical polymerization of N-isopropylacrylamide (NIPAM) monomers, typically in the presence of a cross-linker like N,N'-methylenebis(acrylamide) (MBA) [6]. The unique feature of PNIPAM hydrogels is their lower critical solution temperature (LCST), around 32°C, above which the hydrogel transitions from a swollen state to a collapsed state [6], [7]. This thermoresponsive behavior is driven by the hydrophobic interactions of the isopropyl groups in the polymer backbone, which become more pronounced at temperatures above the LCST, causing the hydrogel to expel water and shrink.

The synthesis of PNIPAM hydrogels can be tailored to achieve specific mechanical and swelling properties by adjusting the concentrations of the monomer, cross-linker, and initiator [4]. The cross-linking density, which is controlled by the amount of cross-linker used, directly affects the hydrogel's stiffness and its ability to swell. A higher cross-linking density results in a stiffer and less swellable hydrogel, while a lower cross-linking density produces a softer, more swellable network.

3 Characterization of Hydrogels: Introduction

Characterizing hydrogels is crucial for understanding their mechanical properties, responsiveness to external stimuli, and suitability for various applications. Given their wide range of applications, from biomedical devices [11] to soft robotics [2], it is essential to thoroughly evaluate their behavior under different conditions. Characterization techniques provide insights into the elasticity, stiffness, viscoelastic properties, and swelling behavior of hydrogels, which are key factors in determining their performance [12]. This section explores the primary methods used to characterize hydrogels: indentation tests, rheometric tests, and swelling-deswelling tests.

3.1 Indentation tests

Indentation testing is a fundamental technique used to assess the mechanical properties of hydrogels, particularly their stiffness and elasticity [12]–[14]. The test involves pressing a probe of known geometry into the surface of the hydrogel and measuring the material's resistance to deformation [13]. The force applied and the resulting indentation depth are recorded to generate a force-displacement curve. This curve is then analyzed to determine key mechanical parameters such as the elastic modulus, which indicates the stiffness of the hydrogel [15].

For soft materials like hydrogels, indentation tests are especially valuable because they allow for localized measurements that reveal how the material responds to mechanical stress without causing significant damage. The elastic modulus derived from indentation tests helps in understanding how changes in the hydrogel's composition, such as varying the cross-linking density or the ratio of monomer to cross-linker, affect its overall mechanical behavior [13]–[18]. Additionally, by conducting indentation tests at different temperatures or hydration levels,

researchers can explore how environmental factors influence the hydrogel's mechanical properties, which is critical for applications in adaptive systems like soft robotics.

3.2 Rheological tests

Rheological tests are conducted to evaluate the viscoelastic properties of hydrogels, which describe the material's response to deformation under mechanical stress [12], [19]. Rheometry is used to measure two primary parameters: the storage modulus (G'), which represents the elastic or 'solid-like' behavior, and the loss modulus (G"), which represents the viscous or 'liquid-like' behavior [20]. Together, these parameters provide a comprehensive understanding of the hydrogel's mechanical stability and how it dissipates energy under stress.

In rheological tests, strain sweeps are performed to determine the linear viscoelastic region (LVR) of the hydrogel [12], [19]. This involves applying oscillatory shear with increasing strain amplitude while monitoring the material's response. The LVR is identified as the range where the storage modulus (G') remains constant, indicating that the hydrogel behaves elastically and its internal structure is intact [21]. Beyond this region, the material may enter a nonlinear viscoelastic regime where the structure begins to break down [12]. Frequency sweeps are another crucial test, where the strain is kept constant within the LVR, and the frequency of oscillation is varied [22]. This test provides insights into how the storage modulus (G') and loss modulus (G") vary with frequency, revealing the hydrogel's response to different deformation rates. Understanding these behaviors is vital for applications where the hydrogel is subjected to dynamic conditions, such as in soft robotics or biomedical devices.

3.3 Swelling-Deswelling tests

Swelling-deswelling tests are employed to study the ability of hydrogels to absorb and release water in response to environmental changes, such as temperature, pH, or ionic strength [12]. These tests are particularly relevant for thermoresponsive hydrogels like Poly(N-isopropylacrylamide) (PNIPAM), which exhibit significant changes in volume when exposed to temperatures above or below their lower critical solution temperature (LCST) [7].

During a swelling test, the hydrogel is immersed in water at a controlled temperature, and its weight is monitored over time as it absorbs water and swells. The swelling ratio, calculated as the ratio of the swollen weight to the dry weight, provides a measure of the hydrogel's capacity to absorb water [3], [12]. In deswelling tests, the swollen hydrogel is subjected to a temperature above its LCST, causing it to expel water and shrink [19]. The kinetics of the swelling and deswelling processes are analyzed to understand the rate at which these transitions occur, which is crucial for applications where rapid response times are needed, such as in drug delivery systems or soft actuators.

Swelling-deswelling behavior also offers insights into the network structure of the hydrogel. For example, a higher cross-linking density typically reduces the swelling capacity of the hydrogel because the tightly linked polymer chains restrict the expansion of the network [22]. Conversely, a lower cross-linking density results in a more open network structure, allowing greater water absorption and swelling [22]. These properties are critical for designing hydrogels that need to perform specific functions, such as in controlled release systems or as sensors that respond to environmental stimuli.

4 PNIPAM hydrogels

Poly(N-isopropylacrylamide) (PNIPAM) hydrogels are synthesized through free-radical polymerization, which involves the polymerization of N-isopropylacrylamide (NIPAM) monomers in the presence of a crosslinker like N,N'-methylenebis(acrylamide) (MBA) [7]. This process is typically initiated by thermal or chemical initiators, such as ammonium persulfate (APS), and this process is sped up by accelerators such as N,N,N',N'-Tetramethylethylenediamine (TEMED) in an aqueous environment [6]. The resulting three-dimensional polymeric network is capable of absorbing significant amounts of water. By adjusting the concentrations of monomers, crosslinkers, initiators and accelerators the mechanical properties and responsiveness of the hydrogels can be tailored to suit various applications [6], [7], [11].

Characterization of PNIPAM hydrogels is essential for understanding their mechanical properties and how they respond to environmental stimuli. Rheometry is a key technique used to measure the viscoelastic properties of these hydrogels, providing insights into their stiffness and durability under different conditions [7]. Indentation testing further helps in determining mechanical properties such as stiffness and elasticity by measuring the resistance of the hydrogel to deformation when a probe is pressed into it [13], [22]. Additionally, swelling-deswelling tests are conducted to evaluate the hydrogels' ability to absorb and release water in response to temperature changes, showcasing their thermoresponsive behavior.

The unique properties of PNIPAM hydrogels lend themselves to a wide range of applications [4]. In soft robotics, their reversible swelling and shrinking behavior is particularly valuable for actuators and sensors that need to respond to environmental changes [4], [14]. The ability of these hydrogels to change shape and stiffness with temperature variations allows for the development of adap-

tive robotic components that can delicately interact with various objects. This makes them ideal for applications requiring precise control and adaptability.

Beyond soft robotics, PNIPAM hydrogels find use in biomedical devices and tissue engineering [4], [7]. In biomedical applications, their temperature-sensitive swelling behavior enables controlled drug delivery, where the release of therapeutic agents can be triggered by the body's natural temperature fluctuations [6]. In tissue engineering, these hydrogels serve as scaffolds that support cell growth and tissue formation, thanks to their biocompatibility and ability to mimic the natural extracellular matrix [1], [4]. These versatile applications highlight the potential of PNIPAM hydrogels in both technological and biomedical fields.

5 Shapes of hydrogels

The shape and geometry of hydrogels are critical factors that influence their functionality in various applications, such as soft robotics, biomedical devices, and drug delivery systems. The ability to tailor hydrogels into specific shapes allows for their integration into devices where precise mechanical and responsive behaviors are required. Hydrogels can be synthesized in a wide range of forms, including sheets, slabs, disks, and more complex three-dimensional structures, depending on the application needs [3], [8], [11]. The process of shaping hydrogels typically involves using molds or templates during the polymerization process, which helps in achieving the desired geometry. The material used for molds, as well as the conditions under which polymerization occurs, play a significant role in determining the final shape and quality of the hydrogel.

6 Metholodgy

6.1 Materials and Equipment

In this research, a variety of materials and equipment were utilized to synthesize and characterize PNIPAM hydrogels. The primary materials included N-isopropylacrylamide (NIPAM) as the monomer, N,N'-Methylenebisacrylamide (MBA) as the cross-linker, ammonium persulfate (APS) as the initiator, and N,N,N',N'-Tetramethylethylenediamine (TEMED) as the accelerator. These chemicals, sourced from Sigma-Aldrich, were carefully selected for their reliability and effectiveness in hydrogel synthesis.

The equipment used for characterization included a Zwick Z010 Universal Testing Machine equipped with a Zwick 500N load cell for performing indentation tests to evaluate the mechanical properties of the hydrogels. A TA Instruments Discovery HR-3 Rheometer, known for its broad torque range and precise temperature control, was employed to conduct rheological tests and assess the viscoelastic properties of the samples. A Mettler Toledo Excellence XSR Analytical Balance was used for precise weighing of the hydrogel samples, ensuring accurate measurements throughout the experiments. Additionally, an IKA RET Basic Hotplate with Magnetic Stirrer was utilized during the synthesis process to ensure thorough mixing of the hydrogel components, while an Elix Essential 5 Water Purification System provided high-purity water to maintain consistency and reduce impurities during the experiments.

For the fabrication of custom-shaped hydrogels, a Prusa MK III 3D printer was used to create molds, which were then cast using Ecoflex-30 silicone. These molds allowed for the precise shaping of the hydrogels into specific geometries required for various testing and application purposes.

This combination of high-quality materials and advanced equipment ensured the reliability and precision of the experimental procedures, facilitating a thorough investigation into the properties and potential applications of PNIPAM hydrogels.

6.1.1 Synthesis of PNIPAM hydrogels

The synthesis of poly(N-isopropylacrylamide) (PNIPAM) hydrogels was conducted using free radical polymerization [6], [7]. The process involved dissolving varying amounts of N-isopropylacrylamide (NIPAM) as the monomer and N,N'-Methylenebisacrylamide (MBA) as the crosslinker, while maintaining a constant amount of ammonium persulfate (APS) at 0.01g as the initiator in 20 ml of deionized water. To ensure a homogeneous solution and to prevent oxygen inhibition, the mixture was thoroughly stirred and degassed by purging with nitrogen gas. N,N,N',N'-Tetramethylethylenediamine (TEMED) was then added as an accelerator, with 3 drops being introduced to the solution to initiate the polymerization process. The varying amount of monomer and crosslinker is as follows:

Table 1
Masses of monomer and crosslinker.

Monomer (g)	0.2g	0.5g	1g	1.5g	2g
Crosslinker (g)	0.01g	0.03g	0.05g	0.07g	0.09g

The wide range of monomer and crosslinker was used to check how their individual concentrations affect the opacity of the gel.

6.2 Indentation experiment

Indentation experiments were conducted to characterize the stiffness of the synthesized PNIPAM hydrogels.

These tests were performed using a Zwick Z010 Universal Testing Machine, which is equipped with a 500N load cell to ensure precise force measurements (see Fig. 1). The hydrogels, prepared as per the synthesis protocol mentioned earlier, were allowed to polymerize for 24 hours before being tested. The indentation test was performed on hydrogels in both their below LCST and above LCST states.

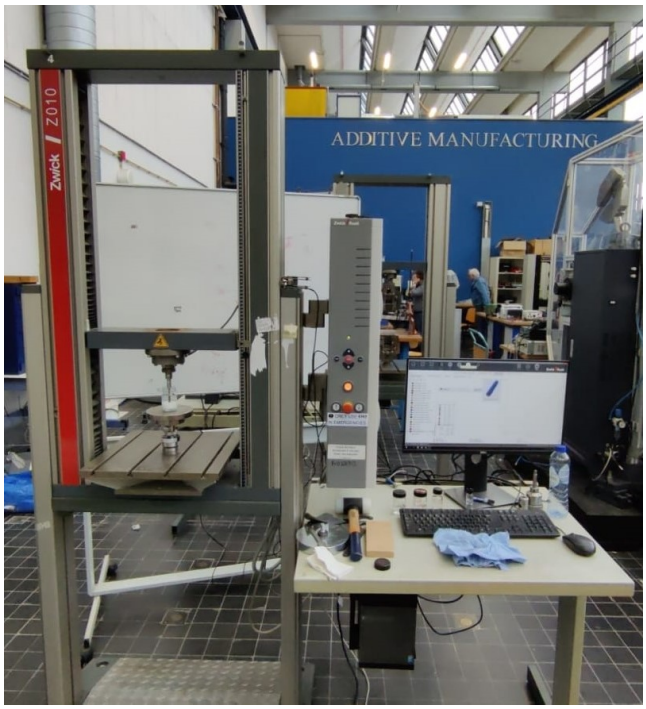

Fig. 1. Zwick Z010 indentation test setup.

For the indentation tests, a custom designed flat-ended cylindrical indenter was used, and the machine was configured to apply a controlled displacement rate of 0.5 mm/min. Each hydrogel sample was positioned under the indenter, which was then lowered to indent the surface to depths of 5mm and 10mm. The force required to achieve this indentation depth was recorded continuously, providing direct insights into the stiffness of the hydrogels [13]. The force-displacement data collected during the tests was used to determine the material's resistance to deformation, which directly relates to its stiffness.

6.3 Rhelogical experiments

Rheological measurements were conducted to evaluate the viscoelastic properties of PNIPAM hydrogels using a TA Instruments Discovery HR-3 Rheometer (see Fig. 2). The hydrogel samples were first synthesized and allowed to polymerize fully for 24 hours. After polymerization, the hydrogels were cut into uniform disks with a diameter of 20 mm and a thickness of 2-2.5 mm.

The rheological measurements were carried out on the hydrogels in three different states: equilibrium state (below LCST at 25°C), swollen state, and at 38°C (above LCST). To ensure consistent test conditions, the samples were soaked in water overnight to achieve full swelling. Each sample was placed between the sand-glazed parallel plates of the rheometer, with the gap adjusted to accommodate the sample's thickness. Strain sweep tests were performed, gradually increasing the strain amplitude from 0.001 to 10 (absolute strain) to observe the transition from the linear viscoelastic region (LVR) to the nonlinear region. During these tests, the storage modulus (G'), representing the elastic response, and the loss modulus (G"), representing the viscous response, were recorded to understand the hydrogel's behavior under different conditions. of 2-2.5 mm.

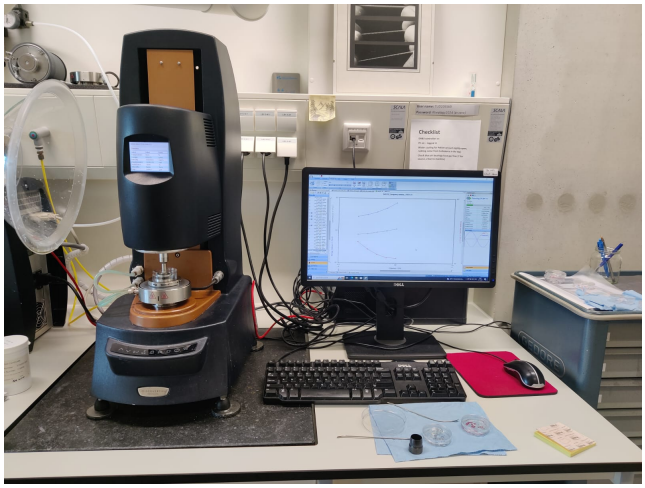

Fig. 2. TA Instruments Discovery HR-3 Rheometer test setup.

To prevent any form or evaporation during testing, solvent traps were employed. The data collected was analyzed to determine the linear viscoelastic region (LVR) across the different states, providing valuable insights into how the hydrogels' stiffness and flexibility change with temperature and swelling.

6.4 Swelling-Deswelling tests

The swelling and deswelling experiments were conducted to evaluate the hydrogels' capacity to absorb and release water under varying conditions. These tests provide insights into the hydrogels' responsiveness to environmental changes, which is crucial for their potential applications.

6.4.1 Swelling tests

The hydrogel samples, synthesized and left to polymerize for 24 hours, were prepared in uniform shapes and

sizes with different monomer and crosslinker ratios. The initial weights of the hydrogel samples were recorded using an analytical balance to record the weight before swelling (W_b). The samples were then submerged in distilled water at $20°C$, and ensuring they were fully immersed. The swelling process was monitored over periods of 24 hours and 48 hours, during which the samples absorbed water and increased in size and weight. After each swelling period, the hydrogels were gently removed from the water, blotted with filter paper to remove excess surface water, and weighed again (W_s) to calculate the swelling percentage using the formula:

$$Q = \frac{W_s - W_b}{W_b} \times 100\% \tag{1}$$

6.4.2 Deswelling tests

The deswelling tests utilized the swollen hydrogel samples from the previous experiment. These samples were exposed to temperatures above the hydrogel's Lower Critical Solution Temperature (LCST)($32°C$), to induce deswelling. For this research, the deswelling process was carried out by placing the swollen hydrogel samples in hot tap water maintained at approximately 60°C. After 30 minutes, the hydrogels were removed from the water, blotted to remove excess water, and then weighed to record the final weight (W_f). The deswelling percentage was calculated using the formula:

$$D = \frac{W_s - W_f}{W_s} \times 100\% \tag{2}$$

6.5 Shapes of hydrogels

The shaping of PNIPAM hydrogels began with the preparation of custom-designed molds, created using CAD software and 3D printed with PLA. After the molds were printed, flexible silicone (Eco-flex 30) was poured into the 3D printed molds and allowed to cure for 5 hours. This flexible material ensures easy removal of the hydrogels post-polymerization. The hydrogel solution, consisting of monomer (NIPAM), crosslinker (MBA), and initiator (APS) dissolved in deionized water, was thoroughly mixed to ensure homogeneity. To prevent oxygen inhibition during the polymerization process, the solution was purged with nitrogen gas for 30 minutes.

After purging, the solution was carefully poured into the prepared molds, which were then placed back into the nitrogen chamber to maintain an oxygen-free environment. The polymerization was initiated by adding N,N,N',N'-Tetramethylethylenediamine (TEMED) and allowed to proceed undisturbed for 24-36 hours to ensure complete gelation. Once cured, the hydrogels were gently removed from the molds and inspected for defects or irregularities, ensuring consistency in their final shapes. The samples were then allowed to swell in deionized water at $20°C$ for 24 hours. After swelling, the samples were blotted clean with parafilm paper, and their dimensions were measured. Following this, the samples were deswelled in a vacuum oven at $60°C$ for 4 hours, and the dimensions were measured again to determine the change in volume of the hydrogel.

6.6 Simulation Analysis

6.6.1 Simulation Setup and Model Development

Apart form the experiments, simulations of the swelling and deswelling behavior of PNIPAM hydrogels was carried out using the Finite Element Method (FEM) implemented in the ABAQUS software package. This simulation aimed to replicate the experimental conditions, particularly focusing on the hydrogels' response to temperature-induced swelling and shrinking.

6.6.2 Simulation setup and model development

The simulation of the swelling and deswelling behavior of PNIPAM hydrogels was conducted using the Finite Element Method (FEM) in ABAQUS. The goal was to replicate the experimental conditions and predict the hydrogel's dimensional changes in response to temperature-induced swelling and shrinking. A three-dimensional geometric model of the hydrogel shapes, such as cubes, cuboids, and cylinders, was developed. The simulations utilized a UHYPER (User-defined Hyperelastic) material model, which incorporates a free energy function accounting for polymer network stretching and polymer-fluid mixing interactions. The free energy model for hydrogels, expressed in its transformed form, is:

$$\hat{W} = W(\mathbf{F}, C) - \mu C \tag{3}$$

where F is the deformation gradient tensor, C is the solvent concentration, and μ is the chemical potential. The model also considers the incompressibility condition:

$$\det(\mathbf{F}) = 1 + vC \tag{4}$$

6.6.3 Meshing and boundary contidions

The hydrogel models were discretized using a 3D mesh with finer mesh density in areas expected to experience significant deformation. Boundary conditions were applied to simulate the physical constraints encountered during experimental testing. To simulate the swelling process, temperature changes were applied across the model, triggering the hydrogel to swell or shrink depending on the thermal conditions. The Flory-Huggins interaction parameter (χ) was incorporated into the free energy function to quantify the interactions between the

polymer and the solvent, refining the accuracy of the model. The free energy density in the finite element solver was expressed as:

$$W(\mathbf{F},\mu) = \frac{1}{2}NkT\left(I_1 - 3 - 2\log(J)\right) + \frac{kT}{v}\left(J\log\left(\frac{J}{\lambda}\right) + \chi J\left(1 - \frac{1}{\lambda}\right)\right) \quad (5)$$

where N is the number of polymer chains per unit volume, k is the Boltzmann constant, T is the temperature, I_1 is the first invariant of $\mathbf{F}$, and J is the determinant of $\mathbf{F}$.

6.6.4 Swelling simulations and Assumptions

The simulations assumed a homogeneous free-swelling state, meaning the hydrogel swelled uniformly in all directions. The contact between the hydrogel and surrounding structures was modeled using isotropic friction and a hard contact model to prevent surface penetration and ensure consistent stress transfer during deformation. The swelling behavior was modeled by adjusting the free energy function within the UHYPER model, enabling accurate predictions of how the hydrogel would respond to temperature changes. The Flory-Huggins interaction parameter (χ) was temperature-dependent, and its values were adjusted based on empirical data to reflect the hydrogel's behavior at different temperatures.

6.6.5 Execution and data analysis

The simulation was executed under controlled temperature conditions that replicated the experimental swelling and deswelling cycles. The key focus was on comparing the dimensions of the hydrogel in its swollen state (after soaking in water) and deswollen state (after exposure to high temperatures). The simulated results, including deformation patterns and final dimensions, were compared with the experimental measurements to validate the accuracy of the model. The comparison of these dimensions provided insights into the reliability of the simulation in predicting the hydrogel's behavior, with any discrepancies highlighting areas for refinement in future models.

7 Results and discussion

7.1 Synthesis experiments

The synthesis experiments focused on evaluating the effectiveness of TEMED as an accelerator and investigating the impact of crosslinker concentration on the opacity of the resulting hydrogels. Refer to the table 1 for the masses of monomer and crosslinker investigated.

7.1.1 TEMED as an Accelerator

The results demonstrated that TEMED is a highly effective accelerator for the synthesis of PNIPAM hydrogels. When TEMED was used, the polymerization process occurred almost instantly at room temperature across various monomer concentrations. For instance, at higher monomer concentrations (1g, 1.5g, 2g), solid gels were successfully formed, indicating the rapid and effective gelation facilitated by TEMED. However, at the lowest monomer concentration of 0.2g, although polymerization initiated, the gel remained a white viscous liquid, suggesting that higher monomer concentrations are necessary for forming a solid gel structure under these conditions. This rapid gelation process makes TEMED an optimal choice for scenarios where quick hydrogel formation is required.

7.1.2 Impact of crosslinker concentration on Opacity of the gel

The experiments also revealed a clear relationship between the crosslinker concentration and the opacity of the hydrogels. At low crosslinker concentrations (0.01g, 0.03g), the hydrogels remained transparent, suggesting a homogeneous network with minimal aggregation of polymer chains. As the concentration of the crosslinker increased to moderate levels (0.05g), the gels began to turn slightly turbid, indicating the onset of polymer chain aggregation. Further increasing the crosslinker concentration to 0.07g resulted in gels with an off-white appearance, and at the highest concentration (0.09g), the gels turned pearl white, indicating substantial polymer chain aggregation. This increased aggregation at higher crosslinker concentrations likely leads to the formation of a denser and less homogeneous network, which can impact the mechanical properties and potentially increase the brittleness of the gels.

These findings underscore the importance of selecting the appropriate crosslinker concentration to control the optical and potentially even the mechanical properties of PNIPAM hydrogels, depending on their intended application.

7.2 Indentation tests

7.2.1 Selection tests

The initial phase of the indentation experiments involved selection tests to determine the impact of varying monomer and crosslinker concentrations on the stiffness of the hydrogels. The indentation tests were carried out at a depth of 5 mm with an indentation speed of 0.5 mm/sec. For the monomer variation tests, the crosslinker concentration was kept constant at 0.01g while the monomer concentrations were varied. The

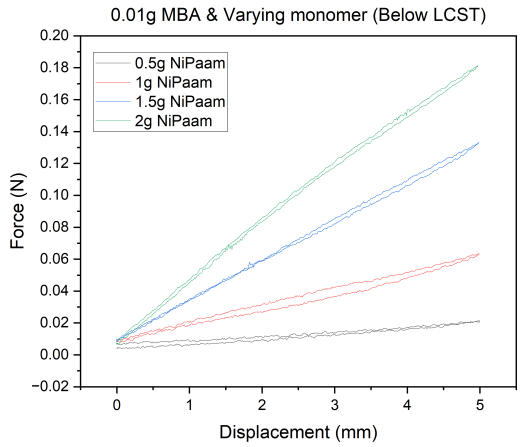

Fig. 3. Force-displacement curves for the varying monomer test (Below LCST).

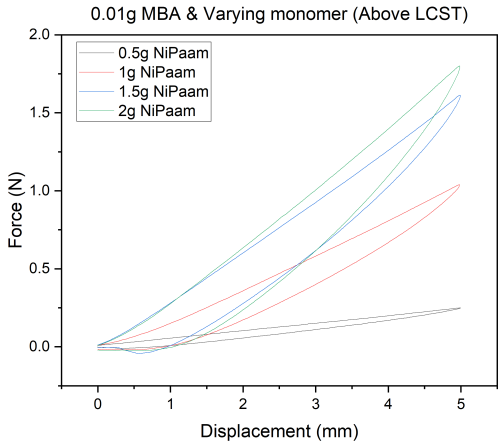

Fig. 4. Force-displacement curves for the varying monomer test (Above LCST).

force vs. displacement curves were generated for different monomer concentrations, and the corresponding stiffness values were calculated both below and above the Lower Critical Solution Temperature (LCST).

The results indicated that as the monomer concentration increased from 0.5g to 2g, there was a significant increase in stiffness both below and above the LCST (see Fig. 3 & Fig. 4). Specifically, at a monomer concentration of 2g, the stiffness reached 35.16 N/m below LCST and 365.96 N/m above LCST. This trend highlights the influence of monomer concentration on the mechanical properties of the hydrogel, with higher concentrations leading to denser and stiffer gel networks.

Following the monomer tests, the crosslinker concentration was varied while keeping the monomer mass constant at 1.5g. The results from these tests revealed a positive correlation between crosslinker concentration and stiffness (see Fig. 5 & Fig. 6). However, the increase in stiffness plateaued and eventually decreased at higher crosslinker concentrations (0.07g and 0.09g), suggesting that excessive crosslinking may lead to brittleness in the hydrogel. Based on these observations, certain monomer and crosslinker concentrations were eliminated from further testing to focus on the most promising combinations.

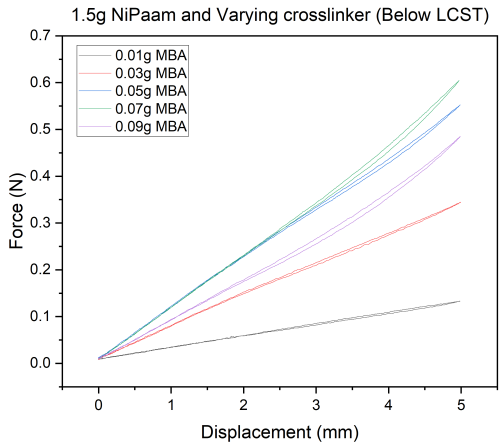

Fig. 5. Force-displacement curves for the varying crosslinker test (Below LCST).

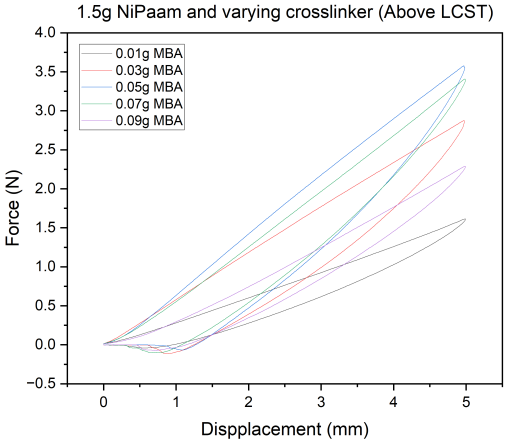

Fig. 6. Force-displacement curves for the varying crosslinker test (Above LCST).

7.2.2 Final indentation tests

The final indentation tests were conducted on a narrowed selection of hydrogel samples with monomer masses of 1g and 2g, and crosslinker masses of 0.03g, 0.05g, and 0.07g. These tests were performed at a 10mm indentation depth to evaluate the failure point and maximum stiffness of the hydrogels. The results showed that

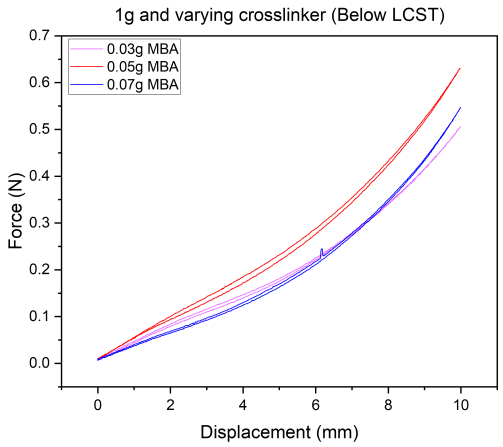

Fig. 7. Force-displacement curves of 1g monomer with varying crosslinker test (Below LCST).

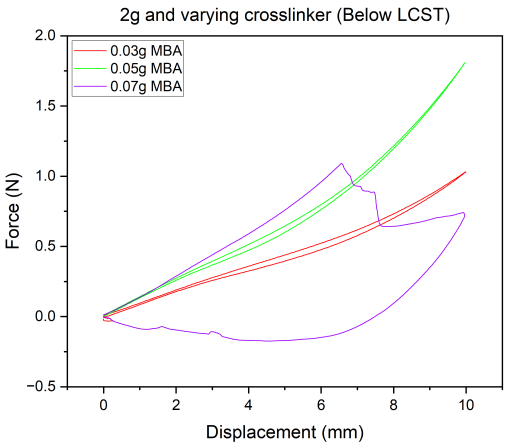

Fig. 9. Force-displacement curves of 2g monomer with varying crosslinker test (Below LCST).

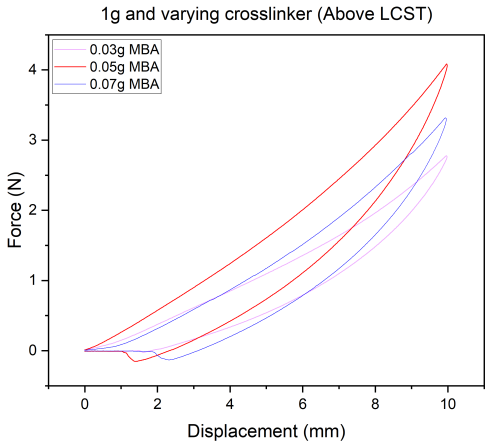

Fig. 8. Force-displacement curves of 1g monomer with varying crosslinkertest (Above LCST).

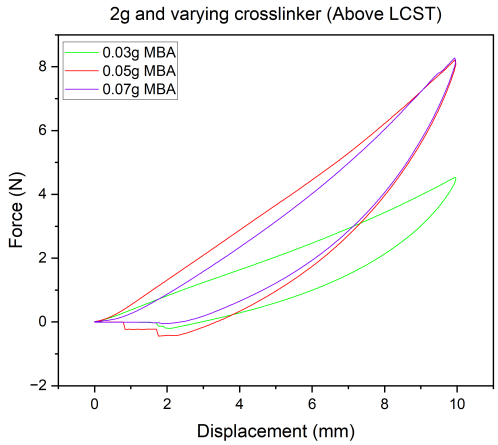

Fig. 10. Force-displacement curves of 2g monomer with varying crosslinkertest (Above LCST).

below LCST, the sample with 2g monomer and 0.05g crosslinker exhibited the highest stiffness (167 N/m) (see Fig. 9). However, the sample with 2g monomer and 0.07g crosslinker failed around a 6mm indentation depth, likely due to the increased crosslinking density leading to brittleness (see Fig. 9).

Above LCST (see Fig. 10), all samples displayed a significant increase in stiffness compared to their below LCST states, demonstrating the thermoresponsive nature of PNIPAM hydrogels. The stiffness increased by almost four times in some cases, with the 2g monomer and 0.05g crosslinker sample reaching 825 N/m. This drastic change in stiffness above LCST highlights the property of these hydrogels to stiffen up above LCST (due to the collapse of polymer chains and shrinking).

These findings confirm that both monomer and crosslinker concentrations significantly influence the stiffness of PNIPAM hydrogels. Increasing the monomer concentration consistently enhances the stiffness of the hydrogels. However, the impact of crosslinker concentration is more complex. Initially, as the concentration of crosslinker increases, the stiffness also increases. Yet, beyond a certain point, excessive crosslinking leads to brittleness, reducing the overall stiffness. This effect was particularly evident with the 0.07g crosslinker concentration, where the hydrogel became brittle and failed under stress (see Fig. 10.

7.3 Rheological tests

Strain sweeps were conducted on PNIPAM hydrogel samples to evaluate their viscoelastic properties under varying strain levels. The strain range was set from 0.001 to 10 (absolute strain), and the tests were per-

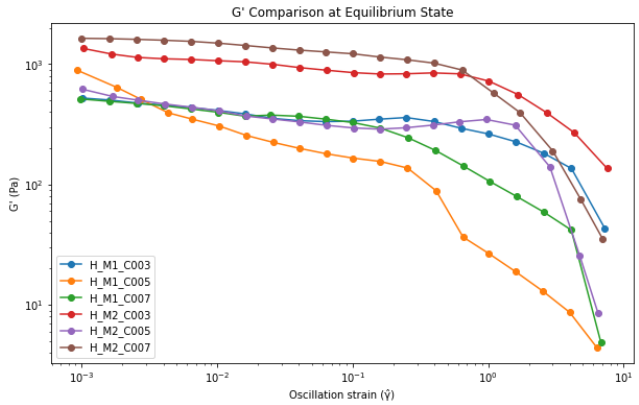

Fig. 11. G' comparison of samples at equilibirum state.

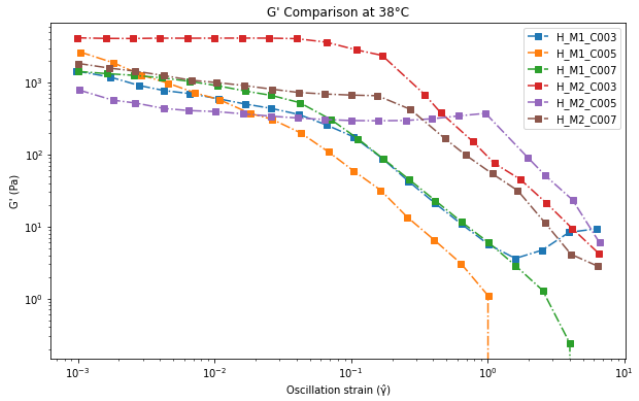

Fig. 12. G' comparison of samples at 38 Deg C.

formed in three different states: equilibrium state (below LCST), swollen state, and at 38°C (above LCST). The large strain range was selected to see if failure of gels is encountered. The primary focus was on determining the storage modulus (G') and loss modulus (G") of the hydrogels, which indicate the elastic and viscous properties, respectively.

The hydrogel samples tested were named H_M1_C003, H_M1_C005, H_M1_C007, H_M2_C003, H_M2_C005, and H_M2_C007, representing different formulations with 1g and 2g monomer concentrations, and varying crosslinker concentrations (0.03g, 0.05g, 0.07g).

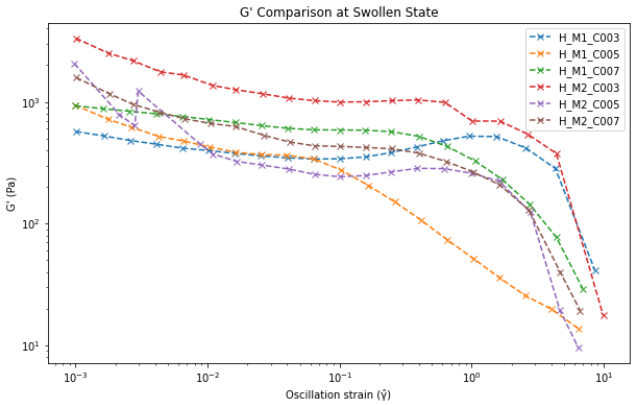

Fig. 13. G' comparison of samples at swollen state.

The results showed that hydrogels with a higher monomer content (2g) consistently exhibited higher storage modulus (G') values compared to those with 1g monomer (see Fig. 11). Among the samples, the one with 2g monomer and 0.07g crosslinker displayed the highest G' in the equilibrium state, indicating a stiffer and more robust network structure (see Fig. 11). The data also indicated that the G' values remained relatively stable across lower strain levels, indicating the hydrogels were within their Linear Viscoelastic Region (LVR). However, as strain increased beyond the LVR, a noticeable decrease in G' was observed, reflecting the strain-softening behavior typical of soft hydrogels.

7.3.1 Analysis of the results

In the equilibrium state (see Fig. 11), the hydrogels exhibited varying degrees of stiffness, as indicated by their storage modulus (G') values. The H_M2_C007 hydrogel, with the highest monomer content, showed the highest stiffness (1072.37 Pa), followed by the H_M2_C003 hydrogel, which had a slightly lower crosslinker concentration. Hydrogels with lower monomer content, such as H_M1_C005 and H_M1_C003, demonstrated lower G' values, reflecting a less densely crosslinked network and reduced stiffness.

When swollen (see Fig. 13), the hydrogels absorbed water, which influenced their mechanical properties. The H_M2_C003 hydrogel maintained the highest G' (1232.62 Pa) in the swollen state, indicating its ability to retain stiffness even after absorbing water. This suggests that higher initial stiffness from greater monomer content leads to better performance post-swelling. The changes in G' across samples in the swollen state compared to equilibrium highlight the balance between network expansion due to water uptake and the inherent stiffness of the polymer structure.

At 38°C (see Fig. 12), above the LCST, the hydrogels underwent significant phase transitions that altered their

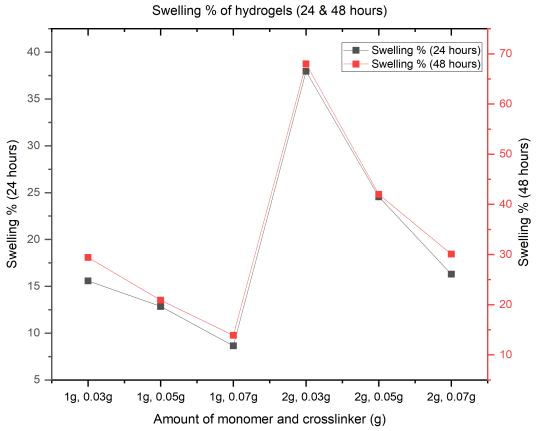

Fig. 14. Swelling percentages at 24 and 48 hours.

mechanical properties. The H_M2_C003 hydrogel displayed the highest G' (2355.10 Pa), retaining significant stiffness at elevated temperatures, likely due to its higher initial stiffness and thermally stable network. The H_M2_C007 hydrogel also showed considerable stiffness (670.04 Pa), though lower than H_M2_C003, possibly due to the higher crosslinker concentration, which may be more susceptible to thermal effects. It is important to note that the steep drop in G' observed at $38°C$ for some samples may be partly due to experimental artifacts. As the hydrogels shrink and release water at this elevated temperature, slippage can occur between the top plate of the rheometer and the gel surface. This slippage could lead to an artificial increase in the measured loss modulus (G") and a corresponding decrease in the measured storage modulus (G'), possibly affecting the accuracy of the measurements.

7.4 Swelling-Deswelling tests

7.4.1 Swelling tests

The swelling experiments were conducted to evaluate how varying amounts of monomer and crosslinker influence the hydrogels' ability to absorb water. The results showed that increasing monomer content had a positive impact on swelling capacity, while increasing crosslinker content had the opposite effect (see Fig. 14). Hydrogels with higher monomer content exhibited greater swelling percentages, likely due to the increased number and length of polymer chains within the gel network, which provided more space for water molecules to occupy. For instance, samples with 2g of monomer showed significantly higher swelling percentages compared to those with 1g, with a peak swelling of 68% observed after 48 hours. In contrast, increasing the crosslinker concentration led to a denser network structure, which restricted the hydrogel's ability to absorb water. This is because the tightly connected polymer chains within the network limited the expansion of the gel, thereby reducing its swelling capacity. For example, hydrogels with 0.03g of crosslinker swelled more than those with 0.07g. This trend illustrates the delicate balance between monomer and crosslinker concentrations necessary to optimize the swelling behavior of PNIPAM hydrogels.

7.4.2 Deswelling tests

Deswelling experiments were conducted to evaluate the ability of the hydrogels to release absorbed water when subjected to elevated temperatures. The swollen hydrogels were exposed to a temperature above their Lower Critical Solution Temperature (LCST), specifically at 60°C. The hydrogels were weighed before and after the deswelling process, which lasted for 30 minutes.

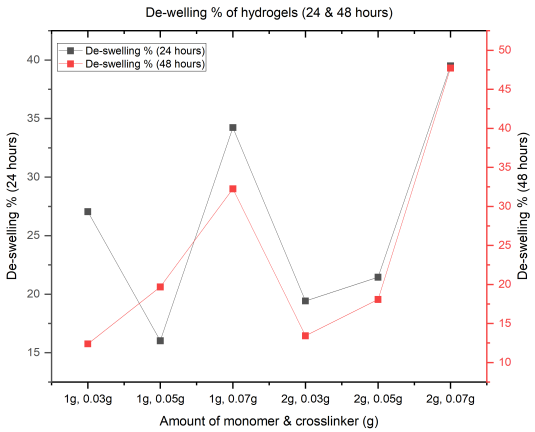

Fig. 15. Deswelling percentages at 24 and 48 hours.

The results showed that hydrogels with higher crosslinker concentrations exhibited more pronounced deswelling behavior (see Fig. 15). This effect can be explained by the denser network structure, which promotes stronger hydrophobic interactions within the hydrogel, leading to a more effective expulsion of water when exposed to heat. Although these denser networks hold less water initially, they are more efficient at releasing the water they contain during deswelling. This behavior underscores the complex interplay between the network structure and the hydrogel's responsiveness to thermal stimuli.

Overall, the swelling and deswelling experiments demonstrate that by manipulating the monomer and crosslinker concentrations, it is possible to tailor the water absorption and release properties of PNIPAM hydrogels for specific applications.

7.5 Shapes and sizes of hydrogels

The study involved fabricating hydrogels in various shapes, including square slabs, rectangular slabs, and

circular disks, with two different sizes for each shape. The primary goal was to overcome the issue of dissolved oxygen, which can interfere with the polymerization and gelation of hydrogels. A custom-made enclosure was used, built from PMMA sheets and sealed with silicone to ensure it was air and water tight. Nitrogen gas was used to fill the enclosure, minimizing oxygen exposure during the polymerization process (see Fig. 16).

The shapes fabricated were square slabs of 20x20 mm and 40x40 mm, rectangular slabs of 20x10 mm and 40x20 mm, and circular disks with diameters of 20 mm. This experiment demonstrated the ability to successfully create hydrogels in specific shapes and sizes under controlled conditions.

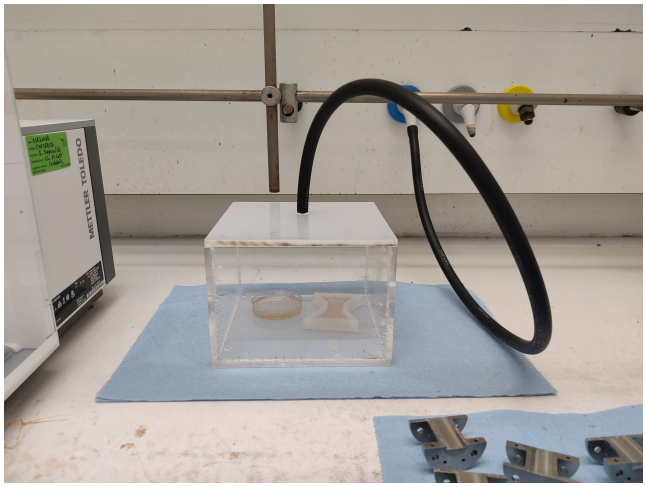

Fig. 16. Nitrogen ecnlosure built for making shapes of hydrogels.

7.5.1 Observations and findings

(1) Nitrogen Gas Influence: The continuous flow of nitrogen gas led to the drying of the hydrogels, causing them to lose volume due to moisture removal. Hydrogels, typically composed of around 85% water, started to dry up, leading to a reduction in their size.
(2) Optimization of Nitrogen Flow: Initially, the nitrogen was applied for 24 hours, which was then reduced to 4 hours and eventually to 1 hour, with 30 minutes of solution degassing. This adjustment minimized the drying effect while still effectively reducing oxygen levels, proving to be a better approach for maintaining hydrogel integrity.
(3) Dimensional Changes: The thickness of all hydrogel models, except for the 20 mm diameter circular plate, was reduced to 8 mm after gelation. This reduction in thickness was likely due to the prolonged exposure to nitrogen gas, which removed moisture from the gels during polymerization.
(4) Swelling and Shrunken States: The fabricated hydrogels exhibited notable differences in dimensions when comparing their shrunken and swollen states. For example, a 40x20 mm rectangular slab showed significant size reduction in its shrunken state compared to its swollen state after rehydration.

In conclusion, The shapes of hydrogels were successfully fabricated and showed predictable behavior in response to nitrogen exposure and swelling conditions. The experiment highlighted the importance of optimizing the nitrogen gas flow to balance between minimizing oxygen interference and maintaining the structural integrity of the hydrogels.

Table 2
Experimental dimensions of the hydrogels

Shrunken dimensions			
Shape	Length/diameter (mm)	Width (mm)	Thickness (mm)
Cube	18.32	18.34	6.79
Cube	39.99	39.99	7.15
Cuboid	18.34	7.65	6.52
Cuboid	40.26	18	6.42
Circular plate	18.19 (dia)		9.47
Swollen dimensions			
Shape	Length (mm)	Width (mm)	Thickness (mm)
Cube	22.13	22.13	9.34
Cube	46.69	46.69	10.02
Cuboid	21.7	9.51	10.3
Cuboid	43.04	21.42	9.33
Cylinder	22.47 (dia)		12.08

Table 3
Swollen dimensions of the hydrogels (Simulations).

Swollen dimensions (Simulations)			
Shape	Length (mm)/diameter (mm)	Width (mm)	Final thickness (mm)
Cube	23.93	23.93	9.51
Cube	52.1	52.1	10.02
Cuboid	23.93	9.14	10.7
Cuboid	52.2	23.49	9.01
Cylinder	23.74 (dia)		12.3

7.5.2 Comparison with simulation

The simulation analysis of the hydrogel shapes revealed that while the simulations provided a good approximation of the swelling behavior, there were notable discrepancies when compared to the experimental results (see table. 2 & table 3).

(1) Thickness Accuracy: The thickness values predicted by the simulations were close to the actual experimental values but not entirely accurate. The simulation predicted thicknesses that were generally consistent across different hydrogel shapes, but slight deviations were observed. For example, while the experimental thickness for a cube-shaped hydrogel was 9.34 mm, the simulation predicted

9.51 mm. Although this difference is minor, it highlights the limitations of the simulation model in perfectly capturing the experimental behavior of the hydrogels.

(2) Dimensional Discrepancies: The simulation results showed larger discrepancies in dimensions such as length, width, and diameter compared to the thickness. For instance, the final swollen length of a cube was predicted to be 23.93 mm by the simulation, whereas the experimental result was 22.13 mm. These variations suggest that while the simulation model captures the general trend of swelling, it does not fully account for the complexities of real-world swelling behavior.

(3) Shape Retention: Despite the discrepancies, the simulations were successful in predicting that the hydrogels would generally retain their shape during the swelling and shrinking processes. However, minor deviations in the edges and corners were observed experimentally, which were not fully captured by the simulation. These could be due to inhomogeneous swelling or slight material inconsistencies not modeled in the simulation.

(4) Impact of Simplifications: The differences between the simulated and experimental results are attributed to the assumptions made in the simulation model, such as assuming homogeneous swelling and a simplified material model. These assumptions likely led to the overestimation or underestimation of the final dimensions of the hydrogels, particularly for more complex or larger geometries.

In conclusion, The simulation provided a useful predictive framework for understanding the swelling behavior of hydrogels in different shapes, but it also underscored the need for more refined models. Future simulations could benefit from incorporating more complex material behaviors and accounting for environmental variables to achieve closer alignment with experimental results.

8 Potential application

The research into PNIPAM hydrogels, particularly in relation to their thermoresponsive properties, opens up significant potential applications in the field of soft robotics. Two key applications have been identified: actuation and stiffness enhancement in soft grippers.

8.1 Soft Gripper Actuation

The ability of PNIPAM hydrogels to undergo reversible swelling and shrinking in response to temperature changes makes them ideal for actuation purposes in soft robotic grippers. When used as actuators, these hydrogels can change shape or volume upon exposure to specific temperature conditions. For instance, a hydrogel can be pre-dried to a shrunken state, making it rigid like plastic. When rehydrated inside a silicone chamber with dimensions smaller than its original size, the hydrogel swells and expands, exerting sufficient force to bend the gripper's fingers. This bending motion can be precisely controlled by adjusting the amount of water introduced, making it a powerful tool for soft robotic applications where delicate and controlled movement is required.

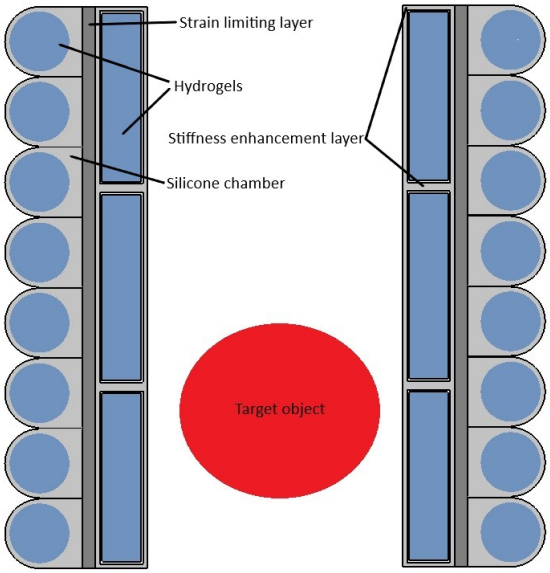

Fig. 17. Potential application of PNIPAM hydrogels in a soft robotic gripper.

8.2 Stiffness Enhancement

The mechanical properties of PNIPAM hydrogels, such as stiffness, can be tuned by altering the concentration of monomers and crosslinkers during synthesis. This tunability allows these hydrogels to be used as stiffness enhancement layers in soft grippers. For example, when the hydrogel is in its swollen state, it can provide significant support, increasing the gripping force of the soft robotic gripper. The research showed that at temperatures above the lower critical solution temperature (LCST), the hydrogel's stiffness increased, leading to a higher block force during indentation tests. This property is particularly useful for applications requiring a gripper that can adapt its stiffness to handle objects with varying degrees of fragility or irregular shapes.

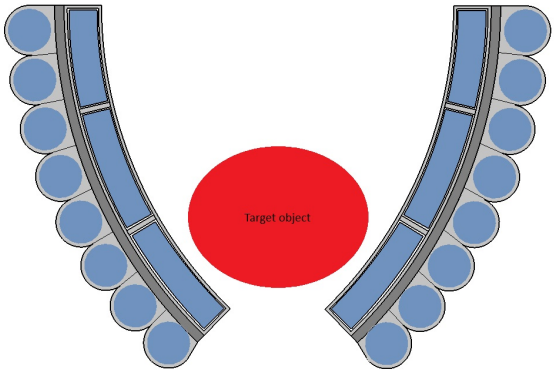

Fig. 18. Bent hydrogel gripper.

8.3 Deformable shapes

Another promising application of PNIPAM hydrogels in soft robotics is the use of deformable hydrogel shapes. These hydrogels can be fabricated into various shapes that deform predictably when exposed to thermal stimuli. For instance, a bowtie-shaped hydrogel was successfully synthesized and observed to undergo significant deformation during deswelling processes. This shape was selected to explore how specific geometries can be tailored to achieve desired mechanical responses in soft robotic applications.

Fig. 19. Swollen bow-tie shaped hydrogel.

The bowtie-shaped hydrogel demonstrated the ability to deform (see Fig. 20), making it suitable for applications that require adaptable components capable of gripping, manipulating, or interacting with objects of varying geometries. The ability to engineer hydrogels into specific, responsive shapes allows for the development of custom-designed soft robotic parts that can perform complex tasks with a high degree of precision. This application

Fig. 20. Shrunken and deformed bow-tie shaped hydrogel.

is particularly advantageous in environments where the robotic system needs to adapt quickly to different shapes and sizes of objects, enhancing the versatility and functionality of soft robotic systems.

These applications not only demonstrate the adaptability and functionality of PNIPAM hydrogels but also highlight their relevance in advancing soft robotics technology, particularly in environments that demand gentle handling or adaptive stiffness control.

9 Conclusion

The comprehensive study of PNIPAM hydrogels, focusing on their synthesis, mechanical properties, and thermoresponsive behavior, has led to several important findings that contribute to the understanding and application of these materials in soft robotics.

Influence of Synthesis Parameters

The research established a clear link between the concentrations of monomers and crosslinkers and the resulting properties of the hydrogels. Specifically, it was found that higher concentrations generally enhance the stiffness and mechanical strength of the hydrogels but

reduce their swelling capacity. This finding is crucial for applications where a balance between flexibility and mechanical robustness is required.

Mechanical Properties

The mechanical testing through indentation and rheometer experiments demonstrated that PNIPAM hydrogels could be tailored for specific mechanical properties by adjusting the synthesis parameters. Higher crosslinker concentrations led to increased stiffness, which is beneficial for applications requiring a rigid response. However, this also resulted in brittleness and potential aggregation likely due to excessive crosslinking, indicating a trade-off between stiffness and durability.

Sweilling-Deswelling behaviors

The swelling and deswelling experiments highlighted the unique thermoresponsive behavior of PNIPAM hydrogels. It was observed that increasing the crosslinker content reduced the hydrogels' swelling capacity, as the denser network structure limited the amount of water that could be absorbed. However, this same increase in crosslinker content enhanced the deswelling ability, allowing the hydrogels to release absorbed water more rapidly. Hydrogels with higher monomer content showed a greater initial swelling capacity, but the rate of deswelling was more efficient in those with higher crosslinker content. This behavior is particularly useful in applications that require materials to adapt their volume and shape in response to temperature changes.

Simualtion accuracy

The simulation analysis provided valuable insights into the swelling behavior of PNIPAM hydrogels. While the simulations were generally accurate in predicting thickness changes, there were discrepancies in the predicted lengths and widths of the hydrogel shapes compared to experimental data. These differences underscore the complexity of accurately modeling hydrogel behavior and suggest that further refinement of simulation models is needed to account for inhomogeneities and environmental factors.

Potential applications

The study identified significant potential applications for PNIPAM hydrogels in soft robotics, particularly in the development of soft grippers. The ability to control the swelling and mechanical properties of these hydrogels through synthesis makes them ideal candidates for actuators and stiffness enhancement layers in soft robotic devices. These applications demonstrate the versatility and adaptability of PNIPAM hydrogels in advanced technological applications.

In conclusion, this research advances the understanding of PNIPAM hydrogels, particularly in how their synthesis parameters influence their mechanical and responsive properties. The findings lay the groundwork for further exploration and optimization of these materials for use in soft robotics and other emerging fields. The study also emphasizes the importance of integrating experimental data with simulation models to enhance the predictability and performance of hydrogels in real-world applications.

9.1 Future recommendations

This comprehensive study of PNIPAM hydrogels only focused on the effect of monomer and crosslinker concentrations on the final hydrogel's behavior and mechanical properties. Further experimentation with varying concentrations of initiators and accelerators could yield deeper insights into the optimal synthesis conditions for PNIPAM hydrogels, potentially enhancing their mechanical properties and responsiveness.

Another promising area for future research is predicting (Simulating) the behavior of hydrogels under different monomer and crosslinker concentrations or varying crosslinking densities, and then comparing these predictions with the experimental behavior of gels. This would help assess the accuracy of simulations and identify ways to improve the models used, ultimately enabling the design of hydrogels with tailored mechanical and responsive properties for specific applications.

Furthermore, conducting frequency sweeps using a rheometer would provide valuable insights into the gel's recovery behavior, helping to understand its performance under repeated actuation cycles with varying environmental conditions. Such a study could offer essential data to improve the reliability of hydrogels and expand their applications in industrial and biomedical fields.

Finally, further exploration into creating and testing deformable shapes of hydrogels could open up new avenues in soft robotics, providing customized solutions for unique challenges in actuation and stiffness enhancement.

References

[1] N. El-Atab, R. B. Mishra, F. Al-Modaf, *et al.*, "Soft actuators for soft robotic applications: A review," *Advanced Intelligent Systems*, vol. 2, 10 Oct. 2020, ISSN: 2640-4567. DOI: 10.1002/aisy.202000128.

[2] J. Shintake, V. Cacucciolo, D. Floreano, and H. Shea, *Soft robotic grippers*, Jul. 2018. DOI: 10.1002/adma.201707035.

[3] "Hydrogels review 2015,"

[4] M. J. Ansari, R. R. Rajendran, S. Mohanto, *et al.*, *Poly(n-isopropylacrylamide)-based hydrogels for biomedical applications: A review of the state-of-the-art*, Jul. 2022. DOI: 10.3390/gels8070454.

[5] "Hydrogels review 2015,"

[6] M. A. Haq, Y. Su, and D. Wang, *Mechanical properties of pnipam based hydrogels: A review*, Jan. 2017. DOI: 10.1016/j.msec.2016.09.081.

[7] L. Tang, L. Wang, X. Yang, Y. Feng, Y. Li, and W. Feng, *Poly(n-isopropylacrylamide)-based smart hydrogels: Design, properties and applications*, Jan. 2021. DOI: 10.1016/j.pmatsci.2020.100702.

[8] Y. Lee, W. J. Song, and J. Y. Sun, *Hydrogel soft robotics*, Dec. 2020. DOI: 10.1016/j.mtphys.2020.100258.

[9] M. F. Akhtar, M. Hanif, and N. M. Ranjha, *Methods of synthesis of hydrogels ... a review*, Sep. 2016. DOI: 10.1016/j.jsps.2015.03.022.

[10] P. ; Jiménez-Rosado and M. ; Romero, "Citation: Sánchez-cid," *Polymers*, vol. 2022, p. 3023, 2022. DOI: 10.3390/polym. [Online]. Available: https://doi.org/10.3390/polym.

[11] M. Ding, L. Jing, H. Yang, *et al.*, *Multifunctional soft machines based on stimuli-responsive hydrogels: From freestanding hydrogels to smart integrated systems*, Dec. 2020. DOI: 10.1016/j.mtadv.2020.100088.

[12] Z. Ahmad, S. Salman, S. A. Khan, *et al.*, *Versatility of hydrogels: From synthetic strategies, classification, and properties to biomedical applications*, Mar. 2022. DOI: 10.3390/gels8030167.

[13] A. Sasson, S. Patchornik, R. Eliasy, D. Robinson, and R. Haj-Ali, "Hyperelastic mechanical behavior of chitosan hydrogels for nucleus pulposus replacement-experimental testing and constitutive modeling," *Journal of the Mechanical Behavior of Biomedical Materials*, vol. 8, pp. 143–153, Apr. 2012, ISSN: 17516161. DOI: 10.1016/j.jmbbm.2011.12.008.

[14] S. Kim and J. Lee, "Indentation and temperature response of liquid metal/hydrogel composites," *Journal of Industrial and Engineering Chemistry*, vol. 110, pp. 225–233, Jun. 2022, ISSN: 22345957. DOI: 10.1016/j.jiec.2022.02.059.

[15] G. L. Puleo, F. Zulli, M. Piovanelli, *et al.*, "Mechanical and rheological behavior of pnipaam crosslinked macrohydrogel," *Reactive and Functional Polymers*, vol. 73, pp. 1306–1318, 9 2013, ISSN: 13815148. DOI: 10.1016/j.reactfunctpolym.2013.07.004.

[16] M. H. Esteki, A. A. Alemrajabi, C. M. Hall, G. K. Sheridan, M. Azadi, and E. Moeendarbary, "A new framework for characterization of poroelastic materials using indentation," *Acta Biomaterialia*, vol. 102, pp. 138–148, Jan. 2020, ISSN: 18787568. DOI: 10.1016/j.actbio.2019.11.010.

[17] M. Ahearne, Y. Yang, and K.-K. Liu, *Mechanical characterisation of hydrogels for tissue engineering applications hydrogels for tissue engineering*, 2008.

[18] M. Czerner, L. S. Fellay, M. P. Suárez, P. M. Frontini, and L. A. Fasce, "Determination of elastic modulus of gelatin gels by indentation experiments," *Procedia Materials Science*, vol. 8, pp. 287–296, 2015, ISSN: 22118128. DOI: 10.1016/j.mspro.2015.04.075.

[19] M. L. Oyen, *Mechanical characterisation of hydrogel materials*, 2014. DOI: 10.1179/1743280413Y.0000000022.

[20] G. Stojkov, Z. Niyazov, F. Picchioni, and R. K. Bose, *Relationship between structure and rheology of hydrogels for various applications*, Dec. 2021. DOI: 10.3390/gels7040255.

[21] J. H. Choi, J. S. Lee, D. H. Yang, *et al.*, "Development of a temperature-responsive hydrogel incorporating pva into nipaam for controllable drug release in skin regeneration," *ACS Omega*, vol. 8, pp. 44 076–44 085, 46 Nov. 2023, ISSN: 24701343. DOI: 10.1021/acsomega.3c06291.

[22] F. Visentin, S. P. M. Babu, F. Meder, and B. Mazzolai, "Selective stiffening in soft actuators by triggered phase transition of hydrogel-filled elastomers," *Advanced Functional Materials*, vol. 31, 32 Aug. 2021, ISSN: 16163028. DOI: 10.1002/adfm.202101121.

[23] J. Jovanova and Q. Chen, *Graduation project modelling a novel design of soft grippers actuated by smart hydrogel*, 2023.

[24] T. Iizawa, H. Taketa, M. Maruta, T. Ishido, T. Gotoh, and S. Sakohara, "Synthesis of porous poly (n-isopropylacrylamide) gel beads by sedimentation polymerization and their morphology," *Journal of applied polymer science*, vol. 104, no. 2, pp. 842–850, 2007.

[25] L. Yang, J. S. Chu, and J. A. Fix, "Colon-specific drug delivery: New approaches and in vitro/in vivo evaluation," *International journal of pharmaceutics*, vol. 235, no. 1-2, pp. 1–15, 2002.

[26] Z. Maolin, L. Jun, Y. Min, and H. Hongfei, "The swelling behavior of radiation prepared semi-interpenetrating polymer networks composed of polynipaam and hydrophilic polymers," *Radiation Physics and Chemistry*, vol. 58, no. 4, pp. 397–400, 2000.

[27] M. C. Hacker, J. Krieghoff, and A. G. Mikos, "Synthetic polymers," in *Principles of regenerative medicine*, Elsevier, 2019, pp. 559–590.

[28] S. Boral, A. N. Gupta, and H. B. Bohidar, "Swelling and de-swelling kinetics of gelatin hydrogels in ethanol-water marginal solvent," *International Journal of Biological Macromolecules*, vol. 39, pp. 240–249, 4-5 Nov. 2006, ISSN: 01418130. DOI: 10.1016/j.ijbiomac.2006.03.028.

[29] A. Vedadghavami, F. Minooei, M. H. Mohammadi, *et al.*, *Manufacturing of hydrogel biomaterials with controlled mechanical properties for tissue engineering applications*, Oct. 2017. DOI: 10.1016/j.actbio.2017.07.028.

[30] S. Y. Kim, H. S. Shin, Y. M. Lee, and C. N. Jeong, "Properties of electroresponsive poly (vinyl alcohol)/poly (acrylic acid) ipn hydrogels under an electric stimulus," *Journal of applied polymer science*, vol. 73, no. 9, pp. 1675–1683, 1999.

[31] Q. Shi, H. Liu, D. Tang, Y. Li, X. J. Li, and F. Xu, *Bioactuators based on stimulus-responsive hydrogels and their emerging biomedical applications*, Dec. 2019. DOI: 10.1038/s41427-019-0165-3.

[32] S. Bashir, M. Hina, J. Iqbal, *et al.*, *Fundamental concepts of hydrogels: Synthesis, properties, and their applications*, Nov. 2020. DOI: 10.3390/polym12112702.

[33] E. M. Ahmed, *Hydrogel: Preparation, characterization, and applications: A review*, 2015. DOI: 10.1016/j.jare.2013.07.006.

[34] W. Zhao, X. Jin, Y. Cong, Y. Liu, and J. Fu, "Degradable natural polymer hydrogels for articular cartilage tissue engineering," *Journal of Chemical Technology Biotechnology*, vol. 88, no. 3, pp. 327–339, 2013.

[35] G. Gao, Z. Wang, D. Xu, *et al.*, "Snap-buckling motivated controllable jumping of thermoresponsive hydrogel bilayers," *ACS applied materials & interfaces*, vol. 10, no. 48, pp. 41 724–41 731, 2018.

[36] L.-W. Xia, R. Xie, X.-J. Ju, W. Wang, Q. Chen, and L.-Y. Chu, "Nano-structured smart hydrogels with rapid response and high elasticity," *Nature communications*, vol. 4, no. 1, p. 2226, 2013.

[37] M. I. Din, R. Khalid, F. Akbar, G. Ahmad, J. Najeeb, and Z. U. Nisa Hussain, "Recent progress of poly (n-isopropylacrylamide) hybrid hydrogels: Synthesis, fundamentals and applications–review," *Soft Materials*, vol. 16, no. 3, pp. 228–247, 2018.

[38] X. Wang and C. Wu, "Light-scattering study of coil-to-globule transition of a poly (n-isopropylacrylamide) chain in deuterated water," *Macromolecules*, vol. 32, no. 13, pp. 4299–4301, 1999.

[39] K. Nagase, M. Yamato, H. Kanazawa, and T. Okano, "Poly (n-isopropylacrylamide)-based thermoresponsive surfaces provide new types of biomedical applications," *Biomaterials*, vol. 153, pp. 27–48, 2018.

[40] J. S. Scarpa, D. D. Mueller, and I. M. Klotz, "Slow hydrogen-deuterium exchange in a non-. alpha.-helical polyamide," *Journal of the American Chemical Society*, vol. 89, no. 24, pp. 6024–6030, 1967.

[41] T. Sun, W. Song, and L. Jiang, "Control over the responsive wettability of poly (n-isopropylacrylamide) film in a large extent by introducing an irresponsive molecule," *Chemical communications*, no. 13, pp. 1723–1725, 2005.

[42] M. Wang, Y. Gao, C. Cao, *et al.*, "Binary solvent colloids of thermosensitive poly (n-isopropylacrylamide) microgel for smart windows," *Industrial & Engineering Chemistry Research*, vol. 53, no. 48, pp. 18 462–18 472, 2014.

[43] Y. Hirokawa and T. Tanaka, "Volume phase transition in a nonionic gel," *The Journal of chemical physics*, vol. 81, no. 12, pp. 6379–6380, 1984.

[44] O. Erol, A. Pantula, W. Liu, and D. H. Gracias, "Transformer hydrogels: A review," *Advanced Materials Technologies*, vol. 4, no. 4, p. 1 900 043, 2019.

[45] M. Heskins and J. E. Guillet, "Solution properties of poly (n-isopropylacrylamide)," *Journal of Macromolecular Science—Chemistry*, vol. 2, no. 8, pp. 1441–1455, 1968.

[46] M. Keerl and W. Richtering, "Synergistic depression of volume phase transition temperature in copolymer microgels," *Colloid and Polymer Science*, vol. 285, pp. 471–474, 2007.

[47] R. Pelton and P. Chibante, "Preparation of aqueous latices with n-isopropylacrylamide," *Colloids and surfaces*, vol. 20, no. 3, pp. 247–256, 1986.

[48] M. Füllbrandt, E. Ermilova, A. Asadujjaman, *et al.*, "Dynamics of linear poly (n-isopropylacrylamide) in water around the phase transition investigated by dielectric relaxation spectroscopy," *The Journal of Physical Chemistry B*, vol. 118, no. 13, pp. 3750–3759, 2014.

[49] Y. Hu, Y. Kim, J. pil Jeong, *et al.*, "Novel temperature/ph-responsive hydrogels based on succinoglycan/poly(n-isopropylacrylamide) with improved mechanical and swelling properties," *European Polymer Journal*, vol. 174, Jul. 2022, ISSN: 00143057. DOI: 10.1016/j.eurpolymj.2022.111308.

[50] R. Luo and C.-H. Chen, *Supporting information one-step hydrothermal route to programmable stimuli-responsive hydrogels*, 2015.

[51] N. Adrus and M. Ulbricht, "Rheological studies on pnipaam hydrogel synthesis via in situ polymerization and on resulting viscoelastic properties," *Reactive and Functional Polymers*, vol. 73, pp. 141–148, 1 Jan. 2013, ISSN: 13815148. DOI: 10.1016/j.reactfunctpolym.2012.08.015.

A

Rheometer test graphs

This section contains the strain sweep graphs (Both G' & G" vs Oscillation strain) of each sample in 3 different states. These graphs have been included to showcase the G' and G" vs strain in a single graph.

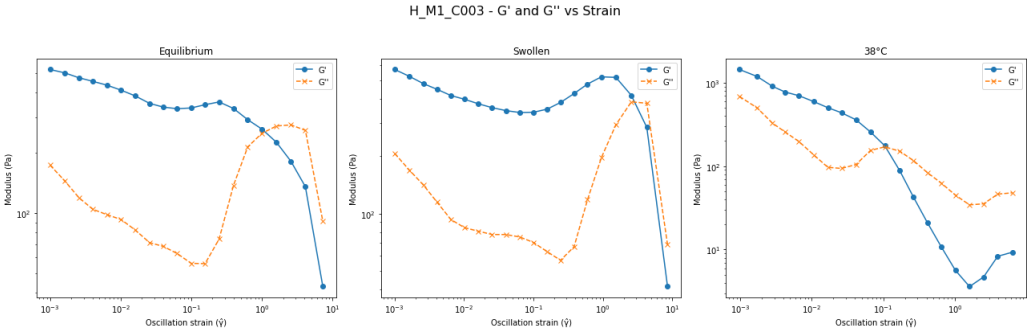

Figure A.1: Strain sweep of H_M1_C003 sample.

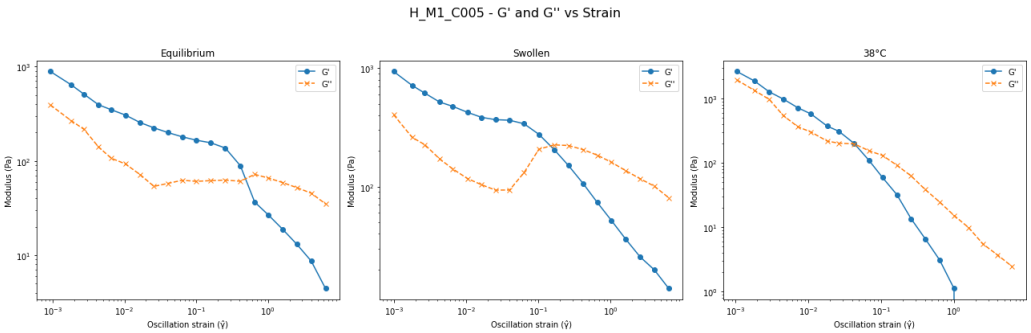

Figure A.2: Strain sweep of H_M1_C005 sample.

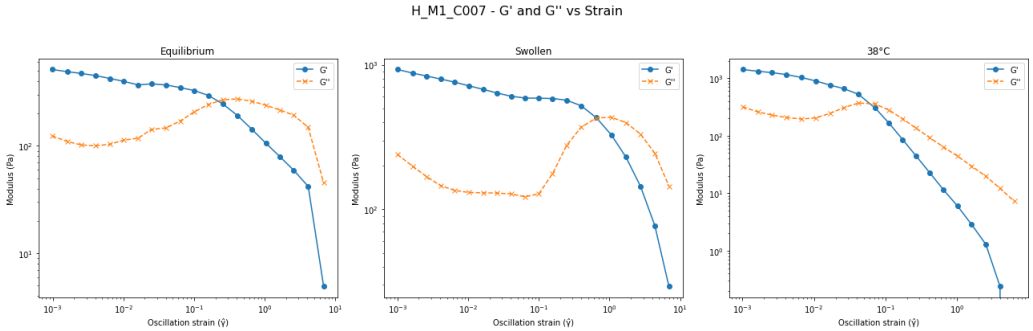

Figure A.3: Strain sweep of H_M1_C007 sample.

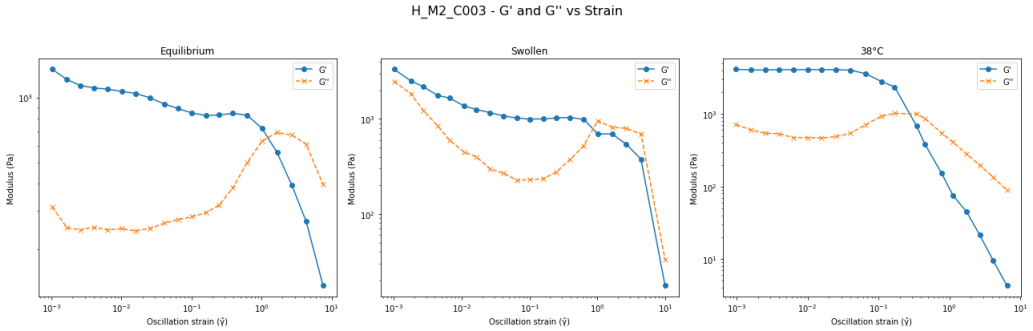

Figure A.4: Strain sweep of H_M2_C003 sample.

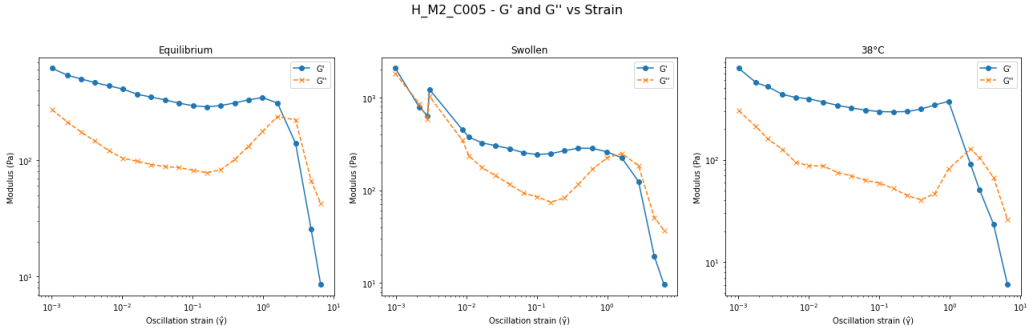

Figure A.5: Strain sweep of H_M2_C005 sample.

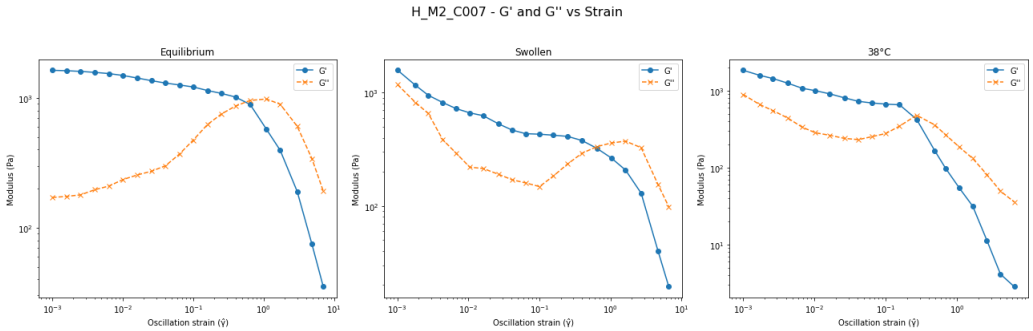

Figure A.6: Strain sweep of H_M2_C007 sample.

B

Synthesis experiment photos

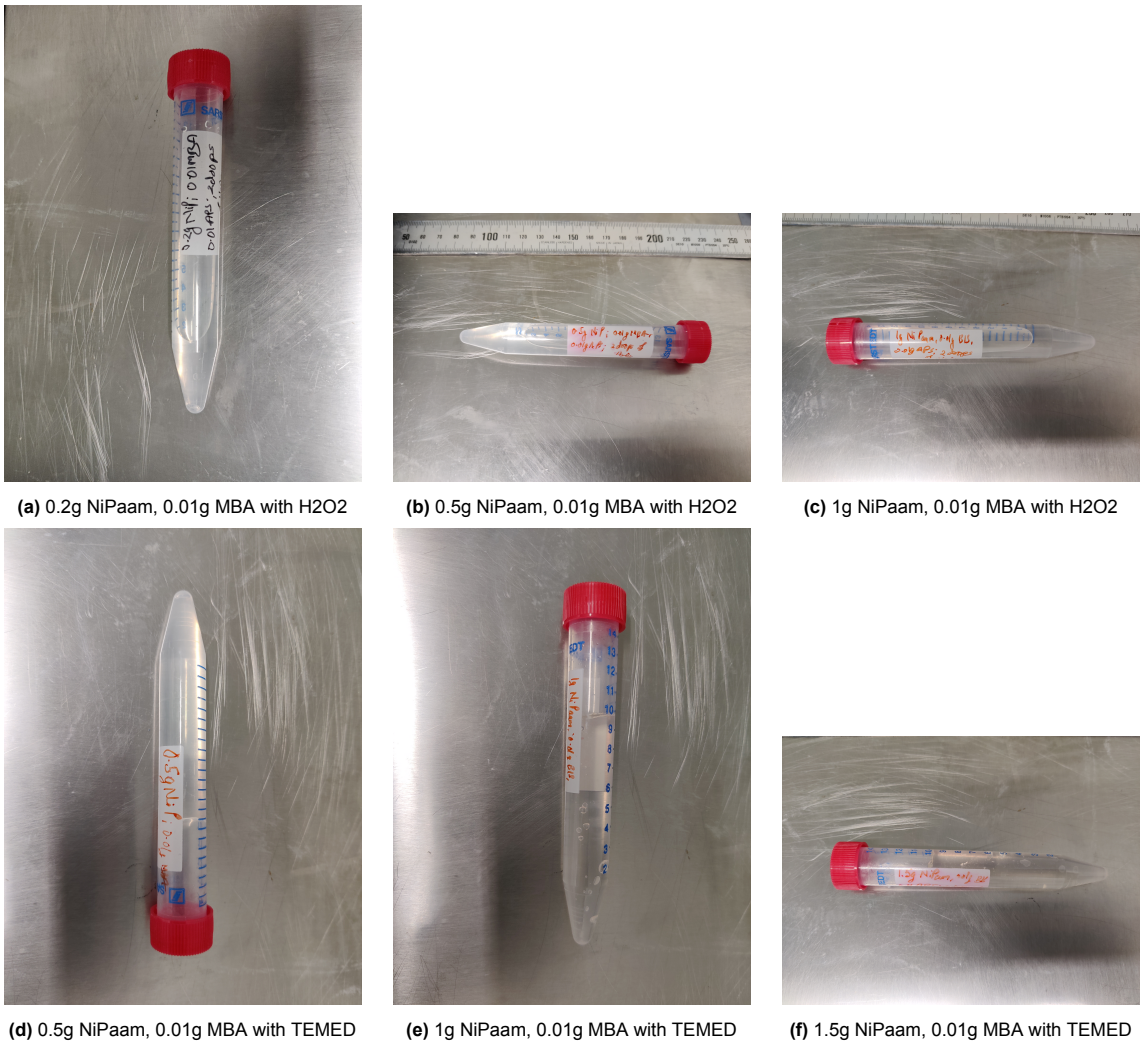

(a) 0.2g NiPaam, 0.01g MBA with H2O2

(b) 0.5g NiPaam, 0.01g MBA with H2O2

(c) 1g NiPaam, 0.01g MBA with H2O2

(d) 0.5g NiPaam, 0.01g MBA with TEMED

(e) 1g NiPaam, 0.01g MBA with TEMED

(f) 1.5g NiPaam, 0.01g MBA with TEMED

Figure B.1: Comparison of H2O2 and TEMED Samples

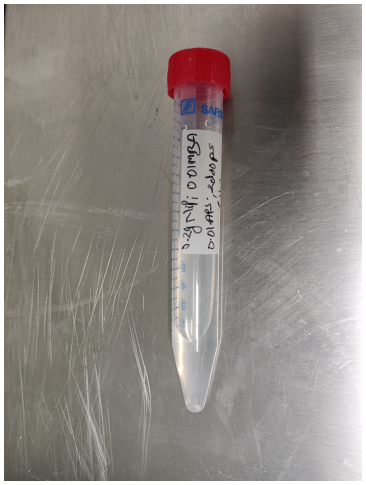

(a) 0.2g NiPaam, 0.01g MBA and H2O2.

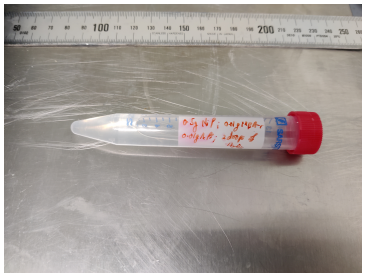

(b) 0.5g NiPaam, 0.01g MBA and H2O2.

(c) 1g NiPaam, 0.01g MBA and H2O2.

Figure B.2: Photos of samples with H2O2 accelerator (0.01g crosslinker).

(a) 0.5g NiPaam, 0.01g MBA and TEMED.

(b) 1g NiPaam, 0.01g MBA and TEMED.

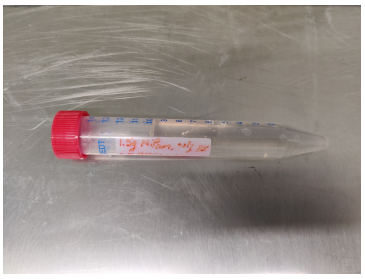

(c) 1.5g NiPaam, 0.01g MBA and TEMED.

Figure B.3: Photos of samples with TEMED accelerator (0.01g crosslinker).

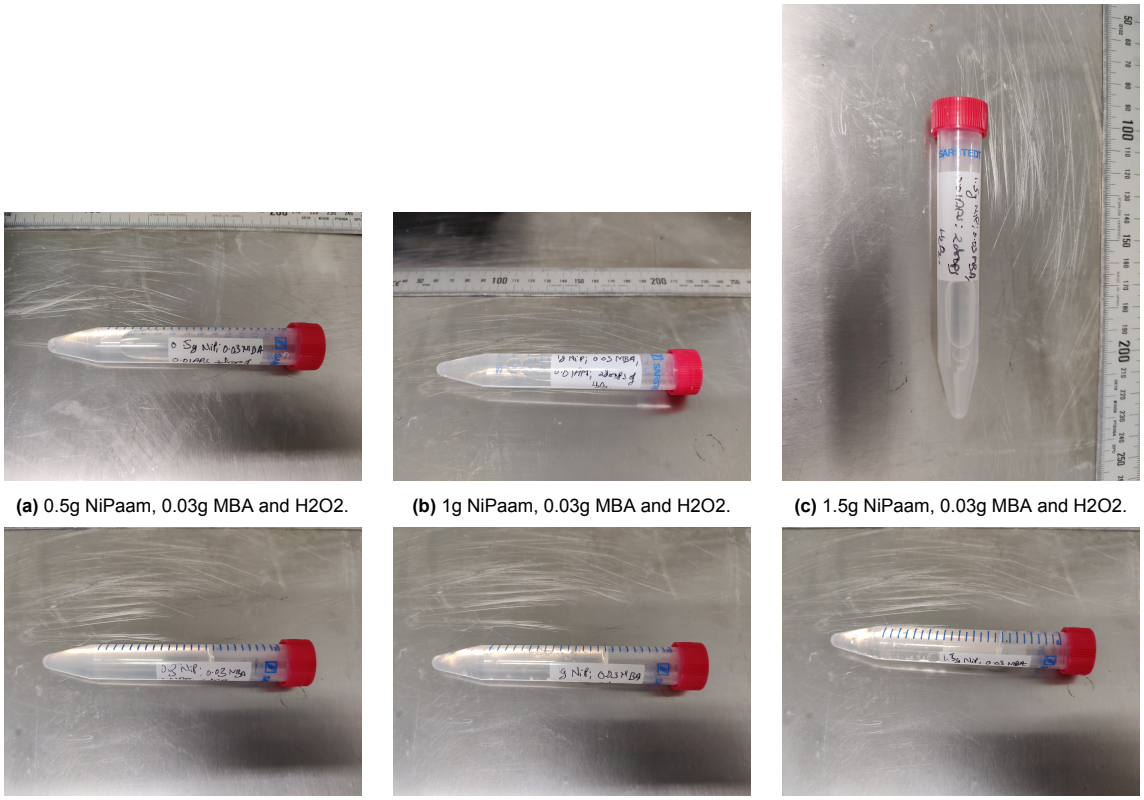

(a) 0.5g NiPaam, 0.03g MBA and H2O2.

(b) 1g NiPaam, 0.03g MBA and H2O2.

(c) 1.5g NiPaam, 0.03g MBA and H2O2.

(d) 0.5g NiPaam, 0.03g MBA and TEMED.

(e) 1g NiPaam, 0.03g MBA and TEMED.

(f) 1.5g NiPaam, 0.03g MBA and TEMED.

Figure B.4: Photos of H2O2 and TEMED Samples with 0.03g crosslinker.

(a) 0.2g NiPaam, 0.05g MBA and H2O2.

(b) 0.5g NiPaam, 0.05g MBA and H2O2.

(c) 1g NiPaam, 0.05g MBA and H2O2.

(d) 1.5g NiPaam, 0.05g MBA and H2O2.

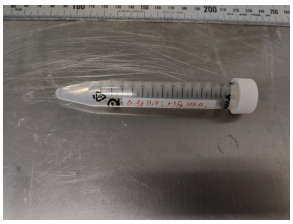

(e) 0.2g NiPaam, 0.05g MBA and TEMED.

(f) 0.5g NiPaam, 0.05g MBA and TEMED.

(g) 1g NiPaam, 0.05g MBA and TEMED.

(h) 1.5g NiPaam, 0.05g MBA and TEMED.

Figure B.5: Photos of H2O2 and TEMED samples with 0.05g crosslinker and varying monomer.

(a) 0.2g NiPaam, 0.07g MBA and TEMED.

(b) 1g NiPaam, 0.07g MBA and TEMED.

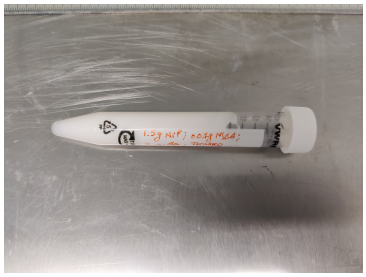

(c) 1.5g NiPaam, 0.07g MBA and TEMED.

Figure B.6: Photos of TEMED samples with 0.07g crosslinker and varying monomer.

(a) 0.2g NiPaam, 0.09g MBA and TEMED.

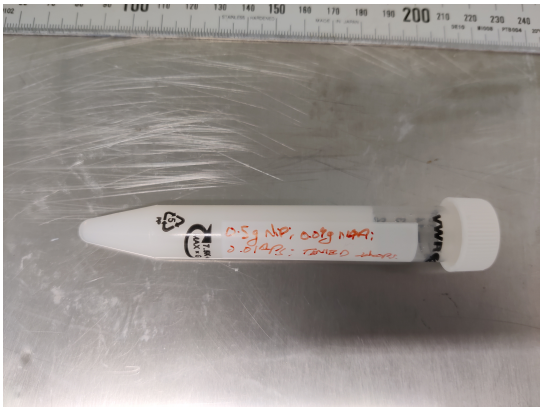

(b) 0.5g NiPaam, 0.09g MBA and TEMED.

(c) 1g NiPaam, 0.09g MBA and TEMED.

(d) 1.5g NiPaam, 0.09g MBA and TEMED.

Figure B.7: Photos of TEMED samples with 0.09g crosslinker with varying monomer.

C

Shapes and sizes of hydrogel photos

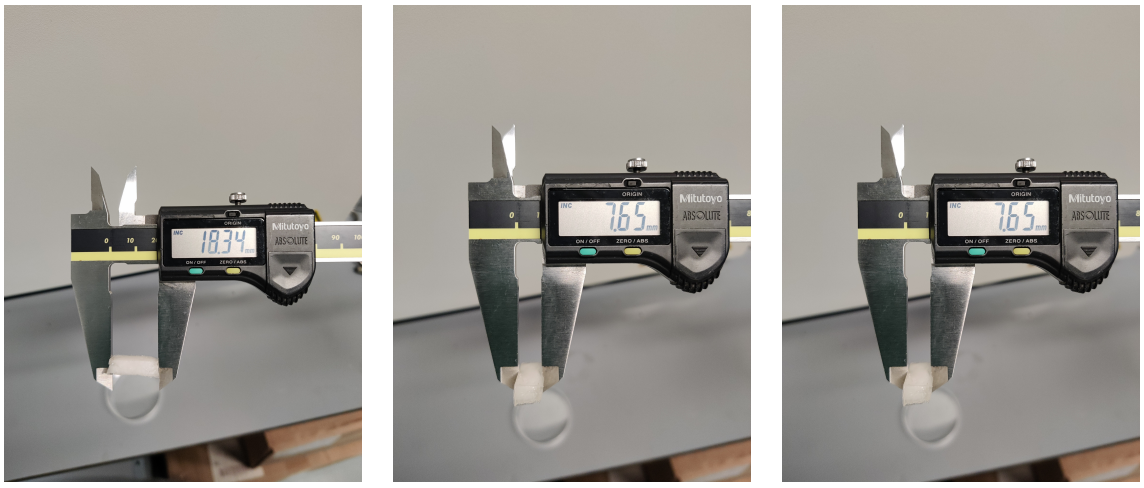

(a) Shrunken 20mm rectangle length. **(b)** Shrunken 20mm rectangle width. **(c)** Shrunken 20mm rectangle thickness.

(d) Swollen 20mm rectangle length. **(e)** Swollen 20mm rectangle width. **(f)** Swollen 20mm rectangle thickness.

Figure C.1: Comparison of Shrunken and Swollen 20mm rectangle sample.

(a) Shunken 20mm square.

(b) Shrunken 20mm square thickness.

(c) Swollen 20mm sqaure.

(d) Swollen 20mm sqaure thickness.

Figure C.2: Comparison of Shrunken and Swollen 20mm square samples.

(a) Shunken 40mm square.

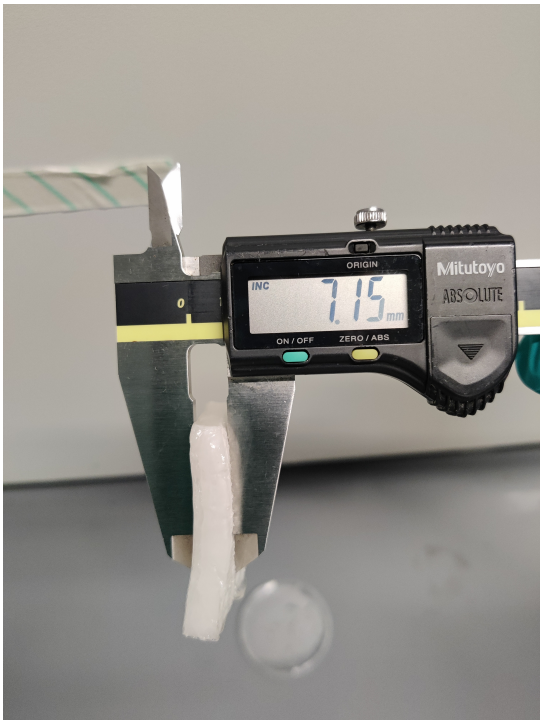

(b) Shrunken 40mm square thickness.

(c) Swollen 40mm sqaure.

(d) Swollen 40mm sqaure thickness.

Figure C.3: Comparison of Shrunken and Swollen 40mm square samples.

(a) Shunken 20mm circle dia.

(b) Shrunken 20mm circle thickness.

(c) Swollen 20mm circle dia.

(d) Swollen 20mm circle thickness.

Figure C.4: Comparison of Shrunken and Swollen 20mm circular samples.

C.1. Simulation photos

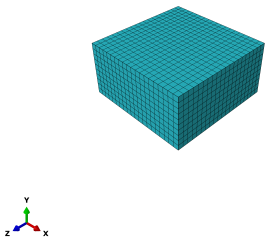

Figure C.5: Shrunken state 20x20 square plate.

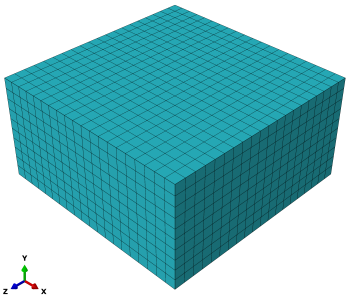

Figure C.6: Swollen state 20x20 sqaure plate.

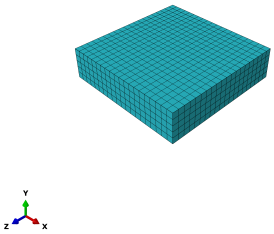

Figure C.7: Shrunken state 40x40 square plate.

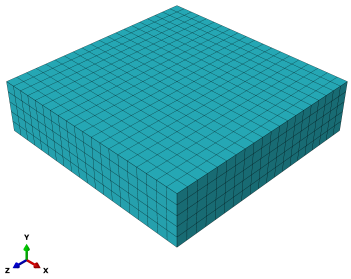

Figure C.8: Swollen state 40x40 square plate.

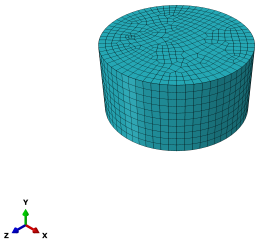

Figure C.9: Shrunken state 20 dia circular plate.

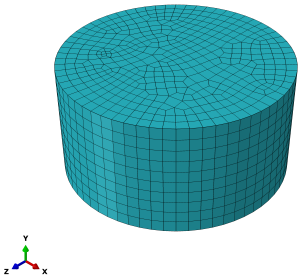

Figure C.10: Swollen state 20 dia circular plate.

Figure C.11: Comparison of Initial and Swollen States of Different Shapes